THE INITIAL REGION OF A PLANE TURBULENT MIXING LAYER

by

Gazi Md. Khalil

A Thesis

submitted to the

Department of Mechanical Engineering

in partial fulfilment of

the requirements for the Degree of

Doctor of Philosophy

Bangladesh University of Engineering & Technology,

DHAKA

1982

C E R T I F I C A T E

This is to certify that this work has been done by me and has not been submitted anywhere for the award of any Degree or Diploma or for publication.

Gazi Md. Khalil

(GAZI MD. KHALIL)

THE INITIAL REGION OF A PLANE TURBULENT MIXING LAYER

A Thesis

by

Gazi Md. Khalil

Approved as to style and content

Dr. Musharrif Hussain Khan
Chairman & Supervisor

Dr. Md. Anwar Hossain
Head & Member

Dr. S. M. Nazrul Islam
Member & Co-supervisor

Dr. A. M. Aziz-ul Huq
Member

Dr. A. K. M. Fazle Hussain
External Member

Dr. S. Ali Afzal
Member

Dr. M. Fazli Ilahi
Member

December 1982

ABSTRACT

The interaction of two incompressible turbulent streams was investigated experimentally in the present work. For this purpose a low subsonic wind tunnel of test section, 1.5 ft x 1.5 ft x 10 ft 8 inches (45.72 cm x 45.72 cm x 325.12 cm) was designed, constructed, installed and calibrated. Nozzles of aspect ratios 4.5 and 3 were set up within the test section to produce jets. The initial region of the plane turbulent mixing layer was studied indentifying the exit conditions which play a vital role in the development of jets.

Two different turbulent boundary layer velocity profiles at the nozzle exit were generated to investigate the influence of the initial conditions on the flow. The displacement thicknesses of the velocity profile at the exit planes of the two nozzles were δ^*/δ = 0.128 and 0.137 respectively with corresponding Reynolds numbers, $Re_D = 1.65 \times 10^5$ and 2.27×10^5. The measured velocity profile within the boundary layer at the exit plane indicated that the flow at the exit was turbulent.

For each case the mean axial velocity and the mean static pressure were measured across the jets, and the experimental results were compared with those of other investigators. The mean velocity profile within the mixing region of two streams was found to show a high shear due to the presence of a steep velocity gradient. This

velocity gradient gradually decreased with the increase of axial distance. The velocity profile in the mixing region did not show self-preserving characteristics.

The maximum mean axial velocity was observed to decay linearly except close to the outlet for both the lower jet and the upper stream. The rate of decay of the maximum mean axial velocity was higher for the faster moving jet compared to that for the slower moving upper stream.

The pressure distribution was found to be uniform across the streams except for a small suction in the region of wake ahead of the thin plate which separated the two streams.

The width for the maximum velocity, y_m, increased linearly along the axial direction. The wake formed between the two interacting streams disappeared approximately at the same axial distance, viz $x/D = 7$ for both the nozzles.

The centre of the uniform portion of the velocity profile in the jets deviated from the geometric centre-line of the nozzle. This may be due to the presence of a small step at the bottom of the nozzle.

Experiments were also conducted with a knife edged splitter in the middle of the inlet duct to study the mixing in absence of the wake in the shear layer. Measurements of pressure and velocity were taken. The flow characteristics in the mixing region was found to be similar to those with wakes but the mixing process was comparatively slow. Therefore, the mean velocity development was more gradual.

To My Parents

ACKNOWLEDGEMENTS

The author acknowledges profound indebtedness to Professor Dr. Wahiduddin Ahmed, an eminent educationist and the Vice-Chancellor of Bangladesh University of Engineering & Technology, Dhaka for his constant inspiration and encouragement throughout this work.

The author is highly grateful to his supervisor Dr. M.H. Khan, Professor & Dean, Faculty of Mechanical Engineering, BUET, without whose guidance, encouragement and invaluable suggestions, this work would not have been possible.

The author is also grateful to Dr. S.M.N. Islam who supervised and assisted him in various ways at all phases of the work.

The author also expresses his gratitude to Professor A.K.M.F. Hussain, Director, Turbulence and Aerodynamics Laboratory, University of Houston, Texas, who contributed to the improvement of this work.

He is also indebted to Prof. M.A. Hossain, Prof. A.M. Azizul Huq, Prof. S.A. Afzal, Dr. M.F. Ilahi for their constructive criticism and invaluable suggestions which have definitely raised the quality of the work.

The author is indebted to Professor A.M. Patwari, the Director, and Professor J.R. Chowdhury, the former Director of the Computer Centre for the permission to use the computer

without which it would have been impossible to process the data. He also appreciates the co-operation obtained from the Computer Centre staff during the entire period of research.

The author gratefully acknowledges the inspiration received from Dr. Mahiuddin Chowdhury, during the lengthy period of this research.

Thanks are also due to many people of the various workshops of BUET for their assistance in constructing the wind tunnel and also fabricating the experimental set-up.

His expression of gratitude is offered to Mr. A.B.Siddiqui, the Librarian, BUET Library for supplying numerous technical papers related to the present work.

And finally, the author wishes to thank Messrs. Md. Nizamuddin and Md. Abdullah for typing the thesis, and Md. Rafiqur Rahman for drawing the figures with patience and care.

TABLE OF CONTENTS

LIST OF FIGURES

LIST OF TABLES

LIST OF APPENDICES

NOMENCLATURE

a	exponent for the maximum mean axial velocity distribution of a wall jet along the axial direction ($U_{Jmax} \propto x^{a}$).
A	aspect ratio of the rectangular nozzle (= b/D)
b	width of the rectangular nozzle
c	a constant
C_f	skin friction coefficient
C_p	pressure coefficient
D	depth of the rectangular nozzle; diameter of the circular nozzle
D_s	depth of the upper nozzle
D_T	depth of the test section of the wind tunnel
e	eccentricity of the nozzle (= D/b)
h	thickness of the splitter
H	shape factor of the boundary layer velocity profile

L	length scale ($= h + \theta_N + \theta_s$)
L_o	length scale for jets in the normal direction ($= y_{m/2} - y_m$)
m_G	entrainment function
M_J	the total momentum flux
n	exponent for velocity distribution in the boundary layer of a wall jet.
p	static pressure in the wall jet.
P_a	static atmospheric pressure
q	rms value of the turbulent fluctuations ($\overline{q^2} = \overline{u'^2} + \overline{v'^2} + \overline{w'^2}$)
R	ratio of jet velocity to free-stream velocity ($= U_{Jmax}/U_{smax}$)
Re	Reynolds number of the flow
Re_D	Reynolds number based on the mean axial velocity and the depth of the nozzle.
Re_θ	Reynolds number based on the mean axial velocity and the momentum thickness of the boundary layer at the nozzle exit.
u'	fluctuating component of velocity in the x-direction

U^*	shear velocity
U_o	maximum mean axial velocity in a jet in still surroundings
U_J	local mean axial velocity of the lower jet
U_N	mean axial velocity of the lower jet at the nozzle exit
U_S	local mean axial velocity of the upper stream
U_{SN}	mean axial velocity in the upper stream at the nozzle exit
U_T	mean axial velocity in the test section
U_{Tmid}	mean axial velocity in the test section at the middle of the test for reproducibility of results
$U_{\infty C}$	mean axial velocity of the free stream
v'	fluctuating component of velocity in the y - direction
V	mean velocity in the y - direction
w'	fluctuating component of velocity in the z - direction

W	mean velocity in the z - direction
x	axial distance measured from the nozzle exit
x_o	distance of hypothetical origin from slot exit
y	cross stream ordinate measured from the test section floor
y_m	minimum value of y where $U_J = U_{Jmax}$
$y_{m/2}$	value of y at which $U_J = \frac{1}{2} U_o$ for a wall jet in still surroundings, or, value of y at which $U_J = \frac{1}{2} (U_{Jmax} + U_{Smax})$ for a wall jet in streaming flow.
Y	co-ordinate normal to the wall measured from the lower surface of the nozzle.
Y_s	cross stream ordinate measured from the top surface of the splitter.
Z	transverse co-ordinate measured normal to the jet axis and parallel to the wall
Z_E	ratio of the law-of-the-wall velocity at the outer edge of the boundary layer to the mainstream velocity

Z_m the minimum value of Z at which $U_J = U_{Jmax}$

$Z_{m/2}$ the value of Z at which $U_J/U_{Jmax} = 0.5$

Greek Symbols

α the wave number

δ the boundary layer thickness

δ^* the displacement thickness at the nozzle exit

ΔU difference of mean axial velocity between the jet and the upper stream ($= U_J - U_{Smax}$)

ΔU_{max} maximum local excess mean axial velocity ($= U_{Jmax} - U_{Smax}$)

ΔU_{Nmax} maximum excess mean axial velocity at the nozzle exit ($= U_{Nmax} - U_{SNmax}$)

ϵ eddy viscosity

θ momentum thickness of the boundary layer

θ_N momentum thickness at the nozzle exit

θ_s momentum thickness at the exit of the upper channel

η	non-dimensional co-ordinate perpendicular to the wall ($= y/l_o$, y/δ)
ν	kinematic viscosity of fluid
ν_T	turbulent eddy viscosity of fluid
ρ	density of the fluid
σ	jet growth parameter
τ	turbulent shear stress ($= -\rho\overline{u'v'}$)
τ_w	shear stress at the wall
ϕ	the slope of the mixing profile

Subscripts

Max	maximum value
Mean	average value
RMS	root mean square

CHAPTER - I

INTRODUCTION AND LITERATURE REVIEW

1.1 Preview

Most flows which occur in practical applications are turbulent. Turbulence is a three-dimensional, time-dependent, vortical motion in which vortex stretching causes velocity fluctuation to spread to all wavelengths between a minimum (i.e. Kolmogoroff scale) determined by viscous forces and a maximum (i.e. integral scale) determined by the geometry of flow. These motions are so complex that it seems to be inaccessible to mathematical treatment. Despite efforts of many scientists over the decades, turbulence continues to persist as one of the least understood arenas of the natural sciences. The Reynolds decomposition, which treats a turbulent flow as a superposition of a time-mean (i.e. constant) component and a time-dependent component, produces the well-known 'turbulence closure problem', arising from the nonlinearity of the governing (Navier-Stokes) equations, to which no universal solution has either been found or appears likely. The gradient transport hypotheses, which are tolerably acceptable for some crude engineering predictions of simple flows, are both conceptually incorrect and incapable of producing acceptable predictions in complex situations. These serve as reminders of the inherent complexity of turbulent flows even in the simplest possible configurations and emphasize the pressing need for continued and vigorous basic investigations of turbulent flows. Unfortunately, the nonlinearity of the governing partial differential equations have stifled any breakthrough on the theoretical front. In fact, most significant advances in turbulence have been made via experimental investigations, and the primary limitation in the progress of this field continues to be the physics of turbulence. As such, experi-

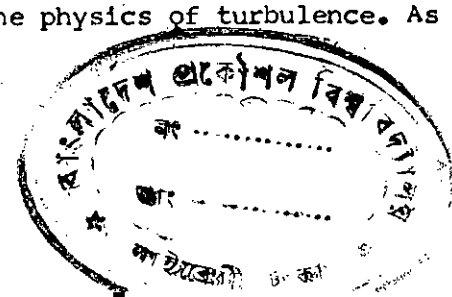

mental studies will continue to play a pivotal role in the advancement of knowledge in turbulence.

Turbulence research has experienced two revolutions in the past decade. The first, rather profound, is the discovery of large-scale coherent structures. The second is the integration of the digital computer as an active (even interactive) component of the turbulence research arsenal (1).

A coherent structure is a connected turbulent fluid mass with a phase-correlated vorticity over its spatial extent. That is, underlying the three-dimensional random vorticity fluctuations, there is an organized component of the vorticity which is phase-correlated (i.e. coherent) over the extent of the structure. This is called coherent vorticity (1). The profound impact of the coherent structure approach should be evident from the fact that it is being pursued by essentially every turbulence researcher in one form or another. While rise and fall of ideas is not new to turbulence, it must be admitted that the advancement continues. But the closure problem still persists, and obviously more studies are required for a complete understanding of the problem.

1.2 Wall Jets

When a fluid is discharged through a nozzle or an orifice from a container under higher pressure into a region of lower pressure, a jet is formed. When the jet impinges onto a rigid wall, it is called a wall jet. The spread of the wall jet is inhibited on one side by the presence of a solid surface, where the velocity is zero. In most practical examples, the wall jet will be turbulent. The wall jet comprises of a boundary layer flow near the wall and a free mixing flow in the outer part.

1.2a Review of Experimental Investigations

i) Wall Jet in a Stagnant Environment

The earliest known work on the plane wall jet was by Forthman (2) who observed that the wall jet was self-preserving, the boundary layer thickness varied linearly with x, and the maximum velocity, U_{Jmax}, varied inversely as the half power of x. The velocity in the inner layer followed the 1/7th power law, and the angle of the jet spread was 4.7°.

Sigalla (3) studied a tangential plane wall jet and correlated the existing data on wall jets. In the developed part of the wall jet the maximum velocity, U_{Jmax}, could be expressed as

$$U_{Jmax} / U_{Nmax} = 3.45 \ (x/D)^{-0.5}$$

Schwarz and Cosart (4) measured the mean velocity distribution of an incompressible, turbulent, plane wall jet with a hot-wire. Over the entire range of the experiment a single velocity scale, U_{Jmax}, and a single length scale, δ, seemed to correlate all the velocity data except very close to the wall. Scatter in the data was appreciable near the wall (a distance of the order of 0.2 mm, $\eta < 0.005$). Hence the flow very close to the wall cannot be treated like a turbulent boundary layer. In fact, there are certain important dissimilarities between the turbulent boundary layer and the inner layer of the wall jet. The most important difference is in the intermittent nature of the outer part of the turbulent boundary layer. Another point of difference lies in the modification of the structure of the inner layer of the wall jet by the turbulence in the outer layer. The square of

the hyperbolic secant, which satisfactorily represents the mean velocity profile of a free mixing layer, does not accurately represent the outer layer of the wall jet.

Myers et al.'s (5) data on a two-dimensional plane tangential wall jet agreed well with the findings of previous investigators (3,4,6). The velocity profiles exhibited similarity for $24 < x/D < 180$, and were independent of the Reynolds number. The maximum mean axial velocity varied as $x^{-0.50}$ as against $x^{-0.555}$ of Schwarz and Cosart (4).

Sforza and Herbst (7) carried out an experimental investigation of the mean properties of turbulent, three-dimensional, incompressible jets of air issuing into a quiescent ambient air tangent to a flat plate. Subsequent mean flow measurements with a constant current hot-wire agreed very well with earlier pitot probe measurements.

ii) Wall Jet in a Free Stream

Kruka and Eskinazi (8) conducted experimental investigation in a plane wall jet blowing tangentially to a semi-infinite, rigid wall and under a uniform moving stream with different velocity ratios R. Similarity was found to exist in both the inner and the outer layers for mean as well as turbulent quantities; however, the same scales do not apply to both the layers. The flow was divided into two regions: at the U_{Jmax} location for mean measurements and at $\overline{v' u'} = 0$ location for turbulence quantities; separation between these two points is small. In the inner

layer, the maximum velocity and its location were found to reduce the mean velocity to a similarity form independent of x. The width scale was found to vary as x^1 for all values of R. The corresponding boundary layer width was proportional to $x^{4/5}$. In the immediate vicinity of the wall, a universal boundary layer type similarity exists, though the coefficients have different values. In the outer layer a reduced longitudinal distance, x_s, was necessary for comparing the results. The characteristic width is linear with x_s for all values of R. In both the inner and outer layers, the velocity scale varies as x_s^a where 'a' is a function of R.

Irwin (9) studied a wall jet in a pressure gradient in the presence of a free stream. The quantities measured with a linearized hot-wire anemometer were the mean and turbulent velocities which reached self-preservation. The mean velocity profile close to the wall was found to be similar to those in boundary layers and pipe flows.

iii) Wall Jet on a Curved Surface

When a wall jet flows over a surface which is curved the rate of entrainment of surrounding fluid is modified by the curvature. The large eddy length scale and the lateral turbulence intensity are increased over a convex surface and thus the entrainment is increased. The reverse applies to a concave surface (10).

1.2b Review of Theoretical Investigations

i) Wall Jet in a Stagnant Environment

The first theory of the wall jet was developed by Glauert (11) on the basis of a model of flow (as shown in Figure 1.1) involving two regions divided by the line of maximum velocity. The flow was assumed to behave rather like a boundary layer in the inner region and a free jet in the outer region. He took a constant eddy viscosity, $\epsilon \propto U_J \delta$ in the outer region and a variable eddy viscosity $\epsilon \propto U_J^6$ in the inner region. It is only the matching of the inner to the outer flows at the point of maximum velocity that gave rise to some difficulty since the appropriate similarity forms were in conflict there.

Integral methods for calculating the growth of a two-dimensional, incompressible, turbulent wall jet in still surroundings have been developed by Myers et al (5). The problem was solved in two parts: (a) the 'starting length' close to the nozzle exit where the maximum jet velocity has not yet begun to decay, and (b) the region downstream where the maximum velocity decays. The solution for the first part was used as the initial condition for the second part. They followed the two-layer concept of Glauert (11) for analysing each of these two parts, in addition to a potential core for the first part. They assumed that the velocity profile and shear stress in the inner and outer layers, considered separately, are the same for the two parts.

ii) Wall Jet in a Free Stream

A theory for wall jets in streaming flow in zero pressure gradient

was developed by Eichelbrenner and Dumargue (12) following Glauert's (11) two-layer concept. The point of matching the two solutions occurred between the maximum velocity and the inflexion point in the outer profile, thereby avoiding Glauert's (11) discontinuity in the eddy viscosity.

Escudier and Nicoll (13) developed integral methods for wall jets in pressure gradients where the mean velocity profile was built up by the superposition of a jet component and the logarithmic law of the wall. The velocity profile at the edge of the flow gave a skin friction law. The integral momentum equation provided a second equation, and the third, required to close the solution, was obtained by relating the non-dimensional rate of entrainment to the profile. The choice of the two-parameter profile was, however, restrictive near separation since it specified that the shape of the profile was the same as that of a boundary layer.

A more versatile, but more empirical, method using a four-parameter velocity profile was developed by Gartshore & Newman (14) to predict separation. The profile could, therefore, change in a manner which was relatively independent of the outer flow and a realistic prediction of separation could be obtained. The theory was used for non-self-preserving flows by introducing a time delay based on the estimated life time of a large eddy.

Harris (15) reported an entirely different approach to the problem of a wall jet in a moving stream. He used the momentum and energy integral equations and assumed that the velocity profiles in both the inner and outer regions were everywhere similar. For the evaluation of the integral

$\int \tau \left(\frac{\partial u}{\partial y}\right) dy$ in the energy equation, a skin-friction formula similar to the Blasius expression was employed. Prandtl's mixing-length theory was applied, and the equations were solved by means of a computer. An interesting feature of Harris's theory was that an attempt was made to make some allowance for the fact that the shear stress was not zero at the velocity maximum in wall jets. This was observed experimentally by Bradshaw & Gee (6) and Kruka & Eskinazi (8), and would imply that theories based on the gradient transport of turbulence could not strictly apply. It also suggested that the independence of the inner and outer regions was not a good assumption.

iii) Wall Jet on a Curved Surface

Cooke (16) theoretically investigated two-dimensional wall jets on curved surfaces. He introduced the simplification originally due to Catherall & Mangler (17), whereby a 'displacement body' was supposed to be known, but the true body was to be determined from the solution, using the fact that the velocity components vanish on the true body. External vorticity was not considered but could be included in an extension of the method. Similar solutions were obtained, and it turned out that corresponding first order solutions were the series calculated by Falkner & Skan and Hartree. Earlier calculations by Murphy (18) were shown to be wrong. Cooke found that on convex surfaces the skin friction was reduced and the displacement thickness was increased as compared with the first order solutions. The reverse was the case for concave surfaces. This implies that a convex curvature encourages separation.

Dvorak (19) developed a calculation method for turbulent boundary layers and wall jets in which the effects of large longitudinal surface curvature and the associated normal pressure gradients were included for the first time. This was achieved by using finite difference techniques to represent the equations of mean motion in a system of curvilinear orthogonal coordinates. The Reynolds stress terms in the equations of motion were approximated using an eddy viscosity approach based on the concept of intermittency. Comparisons between theory and experiment for boundary layers and wall jets developing over flat or curved surfaces for a wide variety of pressure distributions showed encouraging agreement.

1.3 Mixing Layers

Contrary to the classical notions of turbulence, recent experimental observations of Brown & Roshko (20), Dimotakis and Brown (21), Hussain & Zaman (22) have revealed that turbulence in two-dimensional mixing layers is far more orderly than previously believed. The turbulence field is found to be dominanted by large vortex-like structures. Motion pictures taken by Brown and Roshko (20) indicate that these large structures are initiated near the trailing edge of the splitter plate which marks the beginning of the mixing layer. These structures grow in size as they are convected downstream. To accommodate this growth the spacings between the neighbouring structures undergo constant changes. Every now and then two (or three) of these vortex-like structures would coalesce to form a single larger structure. This process, which was observed to occur more prominently at low Reynolds number by Winant & Browand (23), is generally referred to as 'vortex pairing' (or tripling). In high Reynolds number flows the pairing process once started is usually completed in very short intervals

of time. It is believed that the large structures actually constitute the dominant part of the turbulence field in what was previously known as fully random turbulent mixing layers. Careful flow-visualization studies have subsequently revealed that the mixing layer is progressively less organized at higher Reynolds numbers and the large-scale structure interactions are considerably more complex, involving tearing and fractional and partial pairings (24,25). Chandrsuda et al. (26) have claimed that the structures in the plane mixing layer are predominantly three-dimensional even though there have been convincing claims that these are indeed two-dimensional (20,27,28). These indicate that many questions remain unanswered in the mixing layers.

1.3a Review of Experimental Investigations

The time-average measures of the axisymmetric mixing layer have been found to be functions of the initial condition, because of the limited extent of the layer (29). Data suggested similar dependence of the plane mixing layer (30 - 32). Hussain (33) speculated that the persisting influence of the initial condition in these data was due to limited streamwise length of the flows investigated. With this in mind, a large plane mixing layer facility was built. It was shown that sufficiently farther downstream from the origin, the mixing layer does achieve a universal state independent of the initial condition (34). They also investigated the coherent structure in the self-preserving region of the mixing layer. In order to eliminate any possible effect of the initial instability, the boundary layer was tripped. Care was taken to ensure that the initial boundary layer satisfied all the criteria of a fully-turbulent boundary layer of the coherent structures. The average passage frequency f_m at any distance x from the tip

depends on x. These structures are detected for the entire length of measurement i.e. for x = 3m or 5000 θ_e. The Strouhal number St_θ ($= f_m \theta/U_e$) remains constant ($\cong 0.024$) at all x. Here θ and θ_e are the local and exit momentum thicknesses and U_e is the free stream velocity (25 m/s). The mixing layer coherent structures have been educed at different stages of their development via an optimized conditional sampling triggered on the peaks of a local reference $\tilde{u}$ - signal obtained from the high-speed edge of the mixing layer.

1.3b Review of Theoretical Investigations

Tam & Chen (35) have proposed a statistical model of turbulence in fully-developed two-dimensional incompressible mixing layers. The statistical model of turbulence consists of representing the turbulent fluctuations by the normal modes of the flow with random amplitudes. The distribution of the amplitudes is determined by the condition that the turbulent wave spectrum at any downstream location could be considered as generated by an initial spectrum whose kinetic energy has no intrinsic length or time scales, namely, a white noise spectrum. The large structures of the mixing layer which are coupled to each other have been represented by linear combination of the hydrodynamic stability modes of the flow, given by the eigensolutions, of the Orr-Sommerfeld equation.

Without taking into account of the internal vortex motion, a quasi-equilibrium statistical model is suggested in a wave representation to predict the second order turbulence statistics, both single-point and two-point space-time correlation functions. It has been found that for a typical mean velocity profile there is only one-family of unstable eigensolutions affecting the flow turbulence. With suitable random amplitude

function the turbulent velocity and pressure fluctuations in the mixing layer have been predicted. This formalism has been subsequantly extended by Plaschko (36).

Some of the important works done on turbulent wall jets and mixing layers by various authors theoretically and experimentally are shown in Table I and Table II respectively.

1.4 Initial Condition

The initial formation of coherent structures in a shear flow is a function of the initial condition i.e. the state of the flow at its initiation point (29,42). Since the instability and roll up of a shear layer into structures and the subsequent evolutions and interactions must in some way depend on the initial condition, careful documentation of the initial condition is very important. It is very unlikely that two different apparatuses can have identical initial conditions. In most previous investigations, the initial condition was never documented presumably because either its significance was not recognized or the flow was sufficiently downstream such that it was considered to be independent of the intial condition.

While the importance of the intial condition in a turbulent shear flow is well recognized, there is as yet no consensus on the measures necessary to identify the initial condition (42 - 46). These measures may include the mean velocity profile and its various characteristic thicknesses (like the boundary layer, displacement and momentum thicknesses) and the shape factor, the pdf's of the velocity fluctuation and the moments, the spectra of velocity fluctuations, spectrum and moments of the Reynolds

TABLE I : RELEVANT ANALYTICAL WORKS ON THE WALL JET.

Authors	Jet Surroundings	Equations	Model	Comment
Glauert (11) 1956	Still Surroundings	Integral i) Mass ii) Momentum	$U_{Jmax} \propto x^a$ $\delta \propto x^b$ $\epsilon \propto x^c$	Similarity solution achieved. Laminar, turbulent, radial and plane jets are analysed.
Schwarz & Cosart (4) 1961	Still Surroundings	Integral i) Mass ii) Momentum	$U_{Jmax} \propto x^a$ $\delta \propto x$ $\epsilon = f(y/\delta)$	Similarity solution achieved. Wall shear stress obtained by momentum integral equation.
Myers et al (5) 1963	Still Surroundings	Integral i) Mass ii) Momentum	$U_{Jmax} \propto x^a$ $\delta \propto x^b$ ϵ by Prandtl's hypothesis.	Regionwise analysis carried out.

TABLE I : (Continued)

Authors	Jet Surrounding	Equations	Model	Comment
Kruka and Eskinazi (8) 1964	Parallel flow	Integral i) Mass ii) Momentum	$U_{Jmax} \propto x^a$ $a \propto (U_{smean}/U_{Jmean})^b$ $\delta \propto x^c$ ϵ by Prandtl's hypothesis.	Similarity solution achieved. Two-layer concept introduced.
Escudier and Nicoll (13) 1966	Parallel flow	Integral i) Mass ii) Momentum	$-m_G = 0.075\ (1-Z_E)$	Prediction equation for shape factor, drag coefficient and momentum thickness are given in terms of entrainment function.
Gartshore and Newman (14) 1969	Parallel flow	Integral i) Mass ii) Momentum	$U_J / U_{Jmax} = (y/y_m)^n$ ϵ by Prandtl's hypothesis.	Used four momentum integral equations taken from the wall to various points in the flow. Wall jet in an arbitrary pressure gradient analysed.

TABLE I : (Continued)

Authors	Jet Surroundings	Equations	Model	Comment
Patel (37) 1971	Parallel flow	Integral i) Continuity ii) Momentum	$\left(\frac{U_{smean}}{U_{Jmax} - U_{smean}}\right)^2 \propto (x-x_o)$ $l_o \propto (x-x_o)^{1/2}$ $\epsilon = f(x)$	Zero pressure gradient. Predicted eddy viscosity Reynolds number.
Newman et al (38) 1972	Still Surroundings	Integral i) Continuity ii) Momentum	$U_{Jmax} \propto x^{-1}$ $\delta \propto x$ $\epsilon = f(y/\delta)$	Three dimensional wall jet originating from a circular orifice
Narayan and Narasimha (39) 1973	Parallel flow	Dimensional analysis	$M_J = U_J^2 D$	Incompressible jet in still air and in parallel flow. Total momentum flux was used as scale.

TABLE II : RELEVANT EXPERIMENTAL WORKS ON THE WALL JET.

Authors	Nozzle Geometry and Jet	Jet Surroundings	Reynolds Number	Variables Measured	Axial distance covered (x/D)
Sigalla (3) 1958	Rectangular nozzle. Plane tangential jet.	Still air	0.23×10^5 to 0.52×10^5	U_J, δ, τ_w	65
Schwarz and Cosart (4) 1961	24"x1" outlet. Plane tangential jet	Still air	0.22×10^5 to 1.06×10^5	U_J, δ, τ_w	84
Myers et al(5) 1963	60" x 0.5" outlet. Plane tangential jet	Still air	0.71×10^4 to 5.65×10^4	U_J, δ, τ_w	180
Kruka and Eskinazi (8) 1964	56" x 0.131" outlet. Plane tangential jet	Parallel air flow	1.3×10^4	U_J, δ, τ_w	305

TABLE II (Continued)

Authors	Nozzle Geometry and jet	Jet Surroundings	Reynolds Number	Variables Measured	Axial Distance covered (x/D)
Newman et al(38) 1972	Circular orifice of diameter 3.175 mm for air, 2 mm for water.	Still air Still water	16400 for air 2800 for water	U_J, δ , P, u'	328 for air 760 for water
Irwin (9) 1973	Rectangular nozzle of depth 6.73 mm. Plane wall jet	Parallel air flow	2.8×10^4	U_J, P, τ_w, u'	260
Bajura and Catalano (40) 1975	Rectangular nozzle of depth 0.0635 cm. Plane wall jet	Still water	100 to 600	Visual observation, u'	960
Rajaratnam and Stalker (41) 1982	Circular nozzle of diameter 0.25 " and 0.75 ".	Parallel water flow	3000 to 25000	U_J, U_s	64 and 21

stress, etc. (29). In view of the sensor resolution problem, one has to be mostly content with the measurement of the longitudinal velocity only. However, care needs to be taken in these measurements to eliminate the probe-induced shear-layer tone (22).

For the sake of simplicity, the initial condition can be divided into four groups: laminar, nominally laminar, highly disturbed and fully turbulent; the first and the last are the two asymptotic limiting states (1). In the first case, the profile is identical with the Blasius profile and the rms longitudinal velocity fluctuation u' decreases monotonically from the 'free-stream' value to zero at the wall. In the nominally laminar case, the mean velocity profile agrees with the Blasius profile but the fluctuation level is comparatively high, typically reaching a peak value (at $y \cong \delta^*$) significantly higher than the free-stream value. The disturbed case has a profile significantly different from the Blasius profile, and typically it denotes a transitional case. The last case represents a fully-developed turbulent boundary layer and is characterised by logarithmic and wake regions in the (u^+, y^+) coordinates with the wake strength and the extent of logarithmic region appropriate for the value of Re_θ (47), a profile of u'/U_e with its peak value in the range 2.54 $\pm$ 10% and located at $y^+ \cong 15$ and monotonically decreasing to the free-stream (48) and a broadband continuous spectrum $\Phi_u(f)$ of u (t). It should be emphasized that the initial condition data are measured at the end of a straight (zero pressure gradient) length of about 100 θ_e following the contraction. While the fully-turbulent case is easily obtained with an appropriate trip placed sufficiently upstream, it is especially important

to document the spectral content of the velocity fluctuations in the other three cases. In addition, the spectrum and free-stream turbulence intensity profile at the initial state must also be documented. The free stream turbulence is not normally the decaying turbulence from the upstream screens but is typically caused by fan blade wake and rotating stall, tunnel settling chamber cavity resonance, laboratory standing acoustic waves, feedback from downstream obstructions, shear-layer tone within and outside of the tunnel, etc. These various disturbances manifest into a peak in u' (y) at $y/\delta^* \cong 1$ (49) where δ^* is the displacement thickness. If any of these frequencies fall within the unstable band of the shear layer, the shear layer will be driven at this frequency. Unless extreme care is undertaken, these free-stream disturbances will be present and the flow will be driven depending on the frequencies and amplitudes of these modes. Because of these, all free shear flows can be considered to be driven, to some extent (1).

If an adequate straight lip is not added following the contraction, the boundary layer profile can deviate from the Blasius profile even when laminar. The use of an appropriate trip is still in the state of an art. Hussain (33) suggests that the optimum trip is a strip with a linear array of teeth aligned spanwise (prepared by cutting a series of notches) projecting into the flow. These teeth should have their width, spacing, height, length (along flow) of about 100 θ_e and placed at least 1000 θ_e upstream from the lip; θ_e is the momentum thickness of the exit boundary layer in the absence of the trip.

Hussain & Clark (49) conducted a number of studies on the effects of the initial condition in a plane jet. They found that evolutions of all time-average measures, including the momentum flux, of a plane jet are strong functions of the initial condition (49). Because of the universal belief in momentum flux invariance of a jet, this result was initially extremely puzzling. Even though complete explanation has not yet been possible because of inherently large uncertainties in hot-wire measurements in jets, the excess momentum flux can be attributed primarily to the negative pressure in the jet supported by the transverse fluctuations and also to the pressure field induced by the entrainment flow. The time-average measures of the axisymmetric mixing layer has also been found to be a function of the initial condition (44 - 46) but not directly of the exit momentum thickness Reynolds number Re_θ (42). On the other hand, the plane mixing layer has been found to achieve a state independent of the initial condition (34). Controlled excitation can alter the initial region of a mixing layer, but not sufficiently farther downstream (50).

1.5 Coherent Structures

A coherent structure results from an instability of one kind or another. While the most common kinds are the Kelvin-Helmholtz instability of free shear layers (mixing layers, jets, wakes) and Tollmien-Schlichting and Gortler instabilities of wall layers, essentially every kind of instability is potentially capable of generating coherent structures (for example, Benard cells due to Benard and Marangoni instabilities). There are, of course, special cases of coherent structure

formation like puffs and slugs (51, 52) in pipe and channel flows and spiral turbulence in circular Couette flow (53-55). Perhaps the simplest example of coherent structures are the Taylor cells in the circular Couette flow. Because the structure size can be made to remain invariant with time and unlike in shear flows like jets and wakes, these structures are stationary in the laboratory frame, the Taylor cells are extremely attractive for coherent structure studies (56, 57) even though no one has attempted a detailed study from this point of view. The instability from which coherent structures result does not have to be of a laminar flow (58,59,60). Vortex formation from a turbulent wake was demonstrated by Taneda (60). The instability and roll-up of an axisymmetric mixing layer originating from a fully-turbulent boundary layer was first reported by Clark & Hussain (61) who also claimed that coherent structures in an initially fully-turbulent axisymmetric mixing layer were more organized and more compact than when the mixing layer was initially laminar. For an initially fully-turbulent plane mixing layer, the formation, evolution and the equilibrium state of large-scale coherent structures have been documented by Hussain & Zaman (33).

In order to either understand the physics of coherent structures or be able to include these explicitly in a new (and hopefully viable) turbulence theory, it is necessary to first experimentally determine the properties of these structures. The coherent structure is quite periodic and repeatable in the early stages of formation when these result from instability of laminar flows. The periodicity can be enhanced via

controlled excitation. In either case, the structure properties can be determined via phase-locked measurements (62). However, in the fully-developed turbulent shear flows, there is a large dispersion in the shape, size, orientation, strength, and convection velocity of the coherent structures, and the structures pass by at random intervals; the dispersion increases with increasing distances from the point of structure formation. These present formidable constraints in the eduction of coherent structures (63 - 65). Even in periodically induced structures, the constraints become serious with increasing distances from the point of periodic formation of structures.

The understanding of coherent structures in turbulent wall layers and wall jets is considerably much poorer than in free shear flows. Even though the inhibition of transverse wandering of the structures by the presence of the wall is a decided advantage for eduction purposes, the wall itself is the root of the problems. The poorer understanding is due to the fact that the most significant zone of activity, say $y^+ \lesssim 100$, is too narrow a slice of the boundary layer and too close to the wall to allow detailed and accurate measurements as well as flow - visualization. Motion in the boundary layer is expected to be complex. Intuitively, unlike the free shear flows, the boundary layer is not characterized by a single length scale and a single time scale. For these very reasons, the motion in the wall jets are far more complex and have escaped any serious investigation so far.

1.6 Motivation and Objectives

a) Motivation

The flow phenomenon which one can observe in a turbulent wall jet is theoretically appealing as well as practically useful. Such a flow is produced by the downwards-directed jet from a vertical-take-off and landing (VTOL) aircraft spreading out over the ground. The impingement of the jet causes erosion of the ground -- a well known problem in aviation. Another example of the practical application of the wall jet is found in jet-flaps. Initially, the jet flap arrangement consisted of a thin jet sheet ejected at the trailing edge of an aerofoil. This configuration was later modified to include a small trailing-edge flap over which the jet is blown; the basic principle is to energise the boundary layer by blowing a high velocity jet into it and thereby avoid separation. In this way, blowing has been used to reduce the take-off and landing speeds of aircrafts.

Another important application of the wall jet is found in air-cushion vehicles. In such vehicles, an annular jet of air is blown inwards around the periphery of the wheel to establish the base pressure which lifts the vehicle off the ground.

Practical cases of turbulent wall jets are often encountered in marine hydrodynamics, specially when the jet-propelled vessel operates in shallow and restricted water where a high-velocity water jet impinging on the canal bed causes erosion.

The flow through a partially opened sluice gate takes the form of a turbulent wall jet and is important for its scouring effect.

Different schemes are adopted for discharging effluents (after some degree of treatment) from pulp mills, mines, and municipal sewage treatment plants into rivers. In one scheme, the effluent is discharged from a large pipe (buried in the riverbed) through a series of short pipes or nozzles, often as coflowing circular wall jets (66). If the spacing between these jets is small, they merge after some distance, and the effluent discharge behaves like a plane wall jet in a coflowing stream. If, on the other hand, the spacing of the jets is relatively large, in the region before they merge, they can be treated as circular wall jets in a coflowing stream.

The flow of a jet along a curved wall (popularly known as Coanda effect) has a great many applications, mostly in the field of aviation and mechanical engineering. Such a flow is used in fluid logic devices. The general principle is based on the facts that a jet discharged into a diverging channel is free to attach itself to either wall and that it may be forced to separate from one wall and attach to the other. This attachment can be controlled by some auxiliary jets emerging from holes on each side acting as activating signals. The system acts as a relay, or an amplifier.

Still another application is found in swirl atomisers (16). Air is blown down in the middle of the nozzle and swirling liquid round the

rounded lip. With a sharp-edged lip, atomization was found to be poor. With a curved lip, the Coanda effect operated, and atomization was very good.

An older technology is the jet pump in which a primary jet, often steam, is used to entrain and, therefore, pump a surrounding secondary flow of air. The existence of the surrounding walls in the region of entrainment characterises it as a wall jet.

The theory of wall jet has been applied for solving the problem of ventilation in auditoria and other buildings to get an optimum air distribution without appreciable draft. The vortex tube refrigeration is being understood in a better way with the help of the wall jet theory.

Since the wall jet flow is used, and can further be used, for a variety of practical applications, a knowledge of the development of flow properties is called for. For example, in some applications the requirement of the wall jet flow may have to be achieved with minimum energy dissipation whereas in some cases the objective may be dissipation of energy itself. Since such extreme demands may be made on the flow, unless a precise knowledge of the flow development in all its aspects is acquired, the design of the wall jet is of a hit and trial type. Although the simple cases of wall jet flows, both laminar and turbulent, have been investigated theoretically as well as experimentally, some of the more complicated cases still remain unexplored.

The combination flow of two interacting wall jets is one such unexplored area. Formulation of a turbulence model for the initial region of a plane turbulent mixing layer is an extremely difficult task. Existing theoretical methods are not yet powerful enough to give an exact or even an approximate solution to this problem. This is why experimental data must be relied upon to a considerable extent. The present experimental investigation in the initial region of a plane turbulent mixing layer was undertaken keeping the above issues in view.

b) Objectives

The primary objective of the present investigation is to study the initial region of a plane wall jet which is essentially a mixing layer. This includes measurements of mean axial velocity and static pressure at the nozzle exit and also at different axial distances. The exit condition will be identified in terms of the mean and fluctuating velocity profiles and the Reynolds number, and their effects on the jet development will be studied. The experimental data will be used to compute the various flow properties viz., the boundary layer, displacement and momentum thicknesses, the shape factor, the Reynolds number etc. at the exit plane and the geometry of the jet in its motion. The mean velocity development within the jets along the axial direction will be determined and interpreted. Finally, the experimental results will be compared with the available informations in the existing literature.

In order to perform the experiments, a subsonic wind tunnel will be fabricated, installed, commissioned and calibrated. Then nozzles of different aspect ratios (i.e. width/depth) will be installed in turn in the test section to generate two-dimensional wall jets.

CHAPTER - II

THE EXPERIMENTAL SET-UP AND EXPERIMENTS

2.1 Design of the Wind Tunnel

The basic experimental facility used in this work was a 36 ft (10.973 m) long subsonic wind tunnel with a test section having a cross section 1.5 ft x 1.5 ft (45.72 cm x 45.72 cm). The wind tunnel was originally designed by Islam (67) as a closed-circuit wind tunnel. The basic considerations for the design of the wind tunnel can be summarised as follows.

The design of each component has been carried out keeping in mind that the energy losses in these parts should be minimum. The converging section has been designed as a profile of streamline for a potential flow in the duct. Since air possesses a low viscosity and its boundary layer thickness is small compared to the duct dimension, the assumption of potential flow is quite justified. The test section has been designed such that a stable, uniform, undisturbed flow is achieved through it. While designing the diverging duct, special care was taken to minimise frictional and expansion losses. The angle of divergence as well as the length of the duct were chosen such that separation never occurs in the duct.

The wind tunnel was redesigned as an open tunnel and necessary modifications were done keeping the test section dimensions the same as in the original design.

2.2 Construction of the Wind Tunnel

The schematic diagram of the wind tunnel is shown in Figure 2.1A. Figures 2.1B and 2.1C show the different views of the wind tunnel. The principal components of the wind tunnel are the converging section, the flow straighteners, the test section, the diverging section and the fan. The particulars of the components are given in Appendix I.

The wind tunnel has been constructed with locally available materials in the university workshop. The general arrangements of the aforesaid components are shown in Figure 2.1A. The fan is placed at the exit of the diverging duct downstream of the test section to produce a suction flow through the wind tunnel. This arrangement gives a more uniform, stable and undisturbed flow through the test facility. A wire net strainer was fitted at the inlet of the converging section in order to prevent the entrance of foreign solid particles into the wind tunnel. At the exit of the converging section a flow straightener made of wire net was placed in order to produce low turbulence uniform flow.

Four consecutive square sections forming the test section followed the exit of the converging duct. During calibration of the wind tunnel, the first section to follow the converging duct was made of G. I. sheet. The second and the third sections were made of perspex sheet while the fourth one was of wood. The individual sections were connected to each other by nuts and bolts. But at the

time of performing experiments with jets, the G. I. section following the converging duct was replaced by a wooden section incorporating the test nozzle and the upper channel for producing two jets. At the exit of the upper channel two flow straighteners were installed to produce a lower flow velocity than that of the nozzle. Eleven circular holes, each of 0.25 inch (0.635 cm) diameter, were made at an interval of 6 inches (15.24 cm) on the central line of the bottom of the perspex sections. These permitted the traversing of the Pitot-static tube across the duct vertically at different sections of the tunnel.

All the component parts of the wind tunnel have been mounted on fourteen pair of stands made of G. I. pipe. The base plate of each stand was bolted to the floor of the laboratory. Special care was taken to ensure proper alignment of the ducts so that a horizontal flow can be achieved in the test section. The central longitudinal axis of the wind tunnel was maintained at a constant height (viz. 4 ft 2.5 inches) from the floor throughout the length of the tunnel. Duct surfaces were matched properly at the joints so that the streamlines are not disturbed while passing from one duct to another. Rubber pad gaskets were placed between adjacent sections to avoid any leakage of air.

The motor and the fans were installed on a special foundation isolated from the remaining floor by an air gap. This ensures the isolation of mechanical vibration from the remaining components of the wind tunnel.

2.3 Calibration of the Wind Tunnel

The installation of the wind tunnel was followed by its calibration. For this purpose, the Pitot-static tube was traversed vertically up and down by rack and pinion arrangement over a stand with vernier to read upto 0.01 inch (0.0254 cm). The United Sensor Pitot-static tube, one-sixteenth inch (0.159 cm) in outer diameter, was connected to an inclined draft gauge (manufactured by Ellison Draft Gauge Company, Chicago, USA) graduated to read 0.02 inch (0.0508 cm) of water gauge. The draft gauge was set horizontally by the help of the spirit level fixed to the casing of the gauge. The liquid used in the manometer was petroleum oil of specific gravity 0.834.

In order to prevent undue vibration of the sensor, the Pitot-static tube was supported by a brass rod 0.25 inch (0.635cm) in diameter. The sensing point was 4 inches (10.16 cm) above the end of the brass rod to avoid any major disturbance in the flow due to the presence of the brass rod. Before taking the Pitot-static tube reading at a station care was taken to align it in the flow direction to give the correct reading. The correct alignment was found out by trial and error with changing of the horizontal orientation of the sensor through a small angle.

In order to determine the velocity profile, the pressure distribution and other related flow properties in the test section, the velocity heads and the pressure heads were recorded at four

stations viz., x/D_T = 0, 1, 2 and 3 respectively, where x is the axial distance measured from the inlet of the test section, and D_T is the depth of the test section.

Subsequently, the reproducibility of readings was checked. For this purpose, the Pitot-static tube was placed at the centre of the test section at x/D_T = 2 and the manometer reading was recorded at a random interval of time. The duration of each experiment was two hours. Seven such experiments were performed over a period of one month keeping the Pitot-static tube in the same position. The reproducibility of the readings was found to be within $\pm$ 1%.

2.4 Experimental Procedure

2.4a Mixing of Two Turbulent Streams in the Presence of a Wake

After the calibration the G.I. duct placed at the exit of the converging section was taken out and replaced by the wooden duct mounted with the nozzle and the upper channel. The main experiments leading to the investigation of confined turbulent wall jets were conducted. The nozzle had an exit area of 18" x 6" (45.72 cm x 15.24 cm). Air was allowed to flow through the nozzle and through the upper portion of the duct. A schematic diagram of the experimental set-up is shown in Figure 2.2A and a pictorial view is shown in Figure 2.2B. At the exit section of the nozzle a 1 inch (2.54 cm) high step was built, and the jet spreaded over the lower plate (i.e. the test section floor).

The jet spread on the upper side in the presence of another jet of air flowing over the nozzle through the upper channel. These twin jets, confined by the wall of the wind tunnel test section, were allowed to grow in the downward direction over a perspex floor.

In order to determine the jet growth along the axial direction, the mean velocity and static pressure were recorded at stations x/D = 0, 1, 2, 3 . . . . 10, where x is the axial distance measured from the nozzle exit, and D is the depth of the nozzle. In the central part of the jet the manometer reading was quite stable, whereas it fluctuated near the wall over a narrow range. However, the values of the velocities or pressures presented in this thesis are the average of atleast three values obtained at a particular point.

Then a second converging nozzle with an exit area 18" x 4" (45.72 cm x 10.16 cm) was fitted in the test section replacing the first nozzle. Similar turbulent jet flow was produced in the test section and all relevant measurements as with the first nozzle were again taken.

At the beginning and at the end of each experiment, the room temperature and pressure were taken, and the average of the two was taken as the recorded data for the experiment.

It is a well known fact that a jet must travel some distance from the exit of the nozzle before it attains stability with the surrounding fluid. The flow is quite unstable in the initial region (close to the exit plane) and hence it is difficult to take any measurement with the Pitot-static tube. In the present investigation an attempt was made to determine at what distance from the exit the flow starts stabilising. Three additional circular holes were made in the test section floor at distances of 2,3 and 4.5 inches (5.08 cm, 7.62 cm and 11.43 cm) from the exit, and measurements were taken at each of these stations. Significant fluctuation was observed in the manometer reading, especially in the region of mixing of the two jets. The fluctuation in reading was 21% at $x/D = 0.5$ and 9% at $x/D = 0.75$.

2.4b Mixing of Two Streams in the Absence of a Wake

A knife edged splitter was placed at the midsection of the duct. The knife edged splitter was 3 ft. long and 1.5 ft. wide. The leading edge was given a parabolic shape to maintain a smooth flow. The splitter covered the entire width of the duct and the flow was assumed to be two-dimensional. For this case the two shear layers from either side mix without any wake between them. The mixing of the two shear layers in the initial region was studied experimentally. Finally, measurements were also taken by traversing the Pitot-static tube horizontally, and the mean velocities were found uniform across the cross section except the boundary layers close to the walls. This proves that the flow within the mixing region is two-dimensional.

CHAPTER - III

RESULTS AND DISCUSSION

3.1 General

As mentioned in the preceding chapter the velocity and the pressure heads have been measured at different points in the flow field with the help of a sensitive Pitot-static tube and an inclined draft gauge. All these experimental data have been analysed to produce information regarding the flow and to determine geometrical characteristics of the jets. All computations and data analyses were performed by using an IBM 370-115/2 computer, and the computer programs are given in Appendix III.

3.2 Calibration of the Wind Tunnel

For the calibration of the tunnel, the velocity and the pressure in the test section were measured. The purpose was to achieve a uniform velocity and zero pressure gradient in the test section for experiments. The experimental results have been plotted to compare with the expected results for calibration. Figure 3.1 shows the measured mean axial velocity distribution in the test section at four axial distances, i.e., x/D_T = 0, 1, 2 and 3, where x is the axial distance measured from the inlet of the test section and D_T is the depth of the test section. It is seen that the velocity profiles are similar at all the four stations, and the experimental points for all the stations collapse on a single curve. Therefore, it can be noted that there exists no velocity gradient in the axial direction. The velocity distribution is also found to maintain symmetry about the centreline as shown in Figure 3.1. The velocity profile is flat across

the test section except for a small boundary layer at the top and bottom walls of the test section. The shape of the velocity profile is similar to a typical profile for a uniform turbulent flow between two parallel plates. The area under the velocity profile was computed by using Simpson's first rule for numerical integration, and therefrom the mean velocity across the test section was determined. Reynolds number of the flow was calculated on the basis of the mean velocity and the test section depth. The boundary layer thickness was obtained by measuring the distance, y, from the wall for which $U_T/U_{Tmax} = 0.99$. The computed values of different flow parameters for the test section are given in Table III.

TABLE - III : Velocity Profile Characteristics in the Test Section.

Parameters	Values
Centre-line Velocity, U_{Tmax}	68.155 ft/sec (20.774 m/sec)
Mean Velocity, U_{Tmean}	67.497 ft/sec (20.573 m/sec)
Reynolds Number, Re_{D_T}	5.832×10^5
Boundary Layer Thickness, δ	0.7997 in. (2.031 cm)
δ/D_T	0.04412

The boundary layer thickness is less than 4.5% of the depth of the test section which may be assumed to be small to validate the assumption that the velocity profiles in the test section

are uniform. The Reynolds number for this flow is sufficiently high ($Re_{D_T} = 5.832 \times 10^5$) compared to a typical value for which the flow in a duct may be assumed to be turbulent.

Figure 3.2 shows the distribution of the pressure coefficient, C_p, in the test section at four axial distances, i.e., $x/D_T = 0$, 1, 2 and 3. It is observed that the pressure distribution is similar at all the four axial locations. The four sets of experimental points at the four locations fall on a single curve as shown in Figure 3.2. This implies that there exists no pressure gradient in the axial direction within the test section. The pressure distribution at a particular section is found to be uniform across the depth of the test section. This is justified from the fact that the boundary layer is very thin.

The reproducibility of the data obtained for the calibration of the wind tunnel has also been checked. Figure 3.3 depicts the reproducibility of experimental results for mean axial velocity. The points in Figure 3.3 represent the mean axial velocity measured at a particular point, $x/D_T = 2$ and $y/D_T = 0.5$, on the centre-line of the test section. The tip of the Pitot-static tube was placed at the location and readings were taken as per procedure already mentioned in Chapter II. Seven sets of experiments were performed and these experimental values are plotted in Figure 3.3. The experimental points are found to be scattered about a mean value line forming a small band of 1% variation. Such deviations in readings may be due to

a variation in voltage, humidity, pressure, temperature and such other environmental factors. The deviation of readings within $\pm$ 1% shows a satisfactory reproducibility of the experimental results. Reproducibility was also examined at several other points across the test section depth, and it was never found to exceed $\pm$ 1.5% even close to the walls. Reproducibility of the results for pressure was also examined, and its variation was found to be less than $\pm$ 1%. Such a range of values for reproducibility was also found to be present in the jet flows when the nozzles were installed in the test section of the wind tunnel.

3.3 Mixing of Two Shear Layers in the Presence of a Wake

The nozzle exit condition of the jet was identified by the exit mean axial velocity and the displacement thickness of the profile. Measured values of mean axial velocity at the exit of the nozzle are shown in Figures 3.4 and 3.5 for nozzle depths, D = 4 in. (10.16 cm) and 6 in. (15.24 cm) respectively. The velocity profile is found to be symmetrical about the nozzle centreline. The experimental points were fitted to the equation, $U_N/U_{Nmax} = (Y/\delta)^{1/n}$, and the value of n was computed by the method of least squares. The curves corresponding to the equation, $U_N/U_{Nmax} = (Y/\delta)^{1/n}$ are also given in Figures 3.4 and 3.5. The boundary layer thickness was obtained by plotting the experimental values of mean axial velocity at different distances from the wall and then measuring the distance for which $U_N/U_{Nmax} = 0.99$. The displacement thickness, δ^*, the momentum thickness, θ, and the shape factor, H, of the velocity profile were calculated by using the equations,

$$\delta^*/\delta = \int_0^1 \left(1 - \frac{U_N}{U_{Nmax}}\right) d(y/\delta),$$

$$\theta/\delta = \int_0^1 \frac{U_N}{U_{Nmax}} \left(1 - \frac{U_N}{U_{Nmax}}\right) d(y/\delta),$$

$$H = \delta^*/\theta$$

respectively. The area under the velocity profile at the exit was integrated by using Simpson's first rule and subsequently the area-average velocity at the exit was computed.

The experimental values of mean axial velocity within the boundary layer at the exit plane were fitted to the universal velocity profile at the wall given by the following equation :

$$U^+ = \frac{1}{k} \ln y^+ + A$$

where $U^+ = U/U_*$, $y^+ = yU^*/\nu$, and k and A are constants. U^* is the shear velocity. In the procedure of fitting by the least square method the values of k and A were obtained for various values of U^* starting from 1 ft/sec to 10 ft/sec, and the corresponding rms errors of the mean axial velocities were computed. The optimum values of A, k and U^* were selected on the basis of the least rms error which was within $\pm$ 3% of the maximum velocity. The best fit line with k = 1/2.989 and A = 4.395 is shown in Figure 3.6, and the constants found are very close to the values, k = 1/2.5 and A = 4.9 obtained by Coles (68) in the turbulent wall layer.

The Reynolds number, Re_D, was calculated on the basis of the area-average axial velocity and the nozzle depth, D. The computed values of all the parameters which identify the exit conditions are given in Table IV. Considering these characteristics of the velocity profile, the boundary layer at the nozzle exit was assumed to be turbulent. It is worth mentioning in this context that the growth of the jet investigated here would deviate if the exit conditions are changed. Hussain and Zedan (42,43) investigated the flow through circular jets identifying the exit conditions. The exit conditions were identified to be turbulent by considering turbulence, momentum thickness and the hot-wire signal characteristics at the exit plane. The characteristics of the jet flow were found to vary with the variation of the exit conditions. Here also it is expected that the flow characteristics of the interacting jets would vary with the exit conditions. The study of interacting jets or the plane jets identifying the exit condition practically does not exist in the literature. Table IV shows some characteristics of the velocity profile at the exit plane.

The jet issuing from the nozzle is obstructed by the wind tunnel test section floor on the bottom side and spreads on the top side where another stream with a relatively lower average velocity exists. The velocity profiles of the stream above the jet are presented in Figures 3.7 and 3.8 for jets of depth 4 in.(10.16 cm) and 6 in. (15.24 cm) respectively. The velocity profile of the upper stream is approximately flat with a small boundary layer at the top

TABLE IV : The Nozzle Exit Conditions

Parameter	Depth of the nozzle, D	
	4 in. (10.16 cm)	6 in. (15.24 cm)
Mean axial velocity, U_{Nmean}	82.70 ft/sec (25.21 m/sec)	77.19 ft/sec (23.53 m/sec)
Maximum axial velocity, U_{Nmax}	84.16 ft/sec (25.65 m/sec)	80.58 ft/sec (24.56 m/sec)
Power of the velocity profile, n	6.80	6.29
Boundary layer thickness, δ	0.464 in. (1.18 cm)	0.618 in.(1.57 cm)
Ratio of displacement thickness to boundary layer thickness, δ^*/δ	0.128	0.137
Ratio of momentum thickness to boundary layer thickness, θ/δ	0.099	0.104
Shape factor, H	1.294	1.318
Reynolds number based on the nozzle depth, Re_D	1.65×10^5	2.27×10^5
Reynolds number based on the momentum thickness, Re_θ	1912	2410
Maximum velocity in the upper stream, U_{smax}	55.50 ft/sec (16.92 m/sec)	55.10 ft/sec (16.79 m/sec)
Mean axial velocity in the upper stream, U_{smean}	54.05 ft/sec (16.47 m/sec)	52.24 ft/sec (15.92 m/sec)
Momentum thickness of the boundary layer in the upper channel, θ_s	0.0067 in.(0.017 cm)	0.0278 in.(0.071cm)
Depth of the upper channel, D_s	12.25 in.(31.11 cm)	10.25 in.(26.03 cm)

and the bottom. The oncoming flow from the nozzle interacts with the upper stream having profiles given in Figures 3.7 and 3.8.

The mean velocity across the test section has been measured at different axial distances, viz. at an interval of 6 inches (15.24 cm) from the exit plane of the nozzles. This interval corresponds to $\Delta x/D = 1$ and 1.5 for D = 6 inches (15.24 cm) and 4 inches (10.16 cm) respectively, where Δx is the axial distance between the centres of any two consecutive holes. The experimental results have been presented in Figures 3.9 and 3.10 for the nozzle depths, D = 4 inches (10.16 cm) and 6 inches (15.24 cm) respectively. From the mean velocity profile development in Figures 3.9 and 3.10, it appears that the small wake between the streams at the start of the jet influences the flow. But this effect decays with the increase of axial distance as the wake disappears gradually. The mixing of the jet with the upper stream is notably slow, as is obvious from the nature of the velocity profile. This may be due to the presence of low momentum gradient between the two streams. The velocity profile in the region of mixing is not self-preserving within the experimental range. But it is expected to become self-preserving far downstream from the exit. The velocity profile in the region of mixing grows monotonously after the decay of the wake. In this investigation the two jets emanate from the nozzle exit with different average axial velocities, i.e., the lower jet having a higher average velocity than the upper one. The excess mean axial velocity is obtained by

subtracting the maximum mean axial velocity of the upper stream, U_{smax}, from the mean axial velocity of the lower jet, U_J. Figures 3.11 and 3.12 represent the distribution of the measured excess mean axial velocity at different axial distances for the nozzle depths, D = 4 inches (10.16 cm) and 6 inches (15.24 cm) respectively. The formation of a wake in the region of mixing of the two streams is very clearly observed in these figures. The wake is formed behind the plate of thickness 0.75 inch (1.905 cm) and the size of the wake is approximately the same as the plate thickness. The excess velocity in the wake is less than zero which implies that it would absorb energy from both sides. The wake size close to the nozzle exit is sufficiently big to affect the flow but it gradually decreases and then disappears at an axial distance of x/D = 7.5 for D = 4 inches (10.16 cm), and x/D = 7 for D = 6 inches (15.24 cm). It is observed that for both the cases the wake disappears at an approximately the same axial distance of x/D = 7. For both the cases the boundary layer thickness at the nozzle exit is approximately the same as shown in Table IV. It is also observed that the mean excess velocities at the exit for both the cases are approximately the same. So the disappearance of the wakes at the same axial distance, x/D = 7, seems to be quite reasonable, although the exit Reynolds numbers are different.

The mean static pressure has been measured at different axial distances, and subsequently the coefficient of pressure, C_p, has been computed. The experimental values of the pressure coefficient across the jet are plotted in Figures 3.13 and 3.14 for

nozzle depths, D = 4 inches (10.16 cm) and 6 inches (15.24 cm) respectively. The distribution of the pressure coefficient is found to be approximately uniform across the jets at all axial distances except through the wake but this is not clear from Figures 3.13 and 3.14 which are drawn to a compressed scale. This is, however, clear from Figure 3.15 drawn to an enlarged scale.

The maximum mean axial velocity decays in the downward direction as shown in Figure 3.16. The velocity is found to decay in a linear fashion as shown in Figure 3.16 for both the nozzles. The experimental values are fitted to straight lines by the least square method and the following equations are obtained.

$$\frac{U_{Jmax}}{U_{Nmax}} = -0.016\ (x/D) + 0.965 \qquad [3.1]$$

for $D_s/D_T = 0.68$, and

$$\frac{U_{Jmax}}{U_{Nmax}} = -0.026\ (x/D) + 0.971 \qquad [3.2]$$

for $D_s/D_T = 0.57$.

It may be noted that equations [3.1] and [3.2] correspond to the experimental values of velocities for nozzle depths, D = 4 inches (10.16 cm) and 6 inches (15.24 cm) respectively.

The decay of the maximum mean axial velocity within the jet observed by various authors is shown in Table V. These results are applicable to the developed region, whereas the present study is in the near region of the jet, and the results differ from those in the aforesaid Table.

Figures 3.17 and 3.18 represent the maximum mean axial velocity distribution in both the lower jet and the upper stream along the axial direction for nozzle depths, D = 4 inches (10.16cm) and 6 inches (15.24 cm) respectively. This will help one to get an idea about the actual range of speeds in which the jet behaviour has been investigated. It is seen that the maximum mean axial velocity of the lower and the upper streams decreases linearly except close to the nozzle. The rate of decay of the lower jet velocity is faster than that of the upper stream. This may be attributed to the fact that the lower jet having higher average velocity imparts momentum to the upper stream having relatively lower average velocity.

A typical sketch of a jet velocity profile in streaming flow is presented in Figure 3.19. Two tangents AB and CD can be drawn to the two flat velocity profiles of the faster and the slower streams respectively. A third line EF is drawn through the experimental points lying in the region of mixing of the two streams. The angle, ϕ, between AB and EF is the slope of the mixing profile. The value of ϕ has been computed at different axial distances and

plotted in Figure 3.19. It is seen that the slope of the mixing profile, ϕ, decreases in a nonlinear fashion along the downward direction. It should be mentioned in this context that as a result of exchange of momentum between the two streams, the slope of the jet boundary decreases along the axial direction. And at some point far away from the nozzle exit it will reduce to zero.

The mid point of the uniform velocity portion of the jet is plotted in Figures 3.20 and 3.21 for nozzle depths, D = 4 inches (10.16 cm) and 6 inches (15.24 cm) respectively. The experimental values for the mid points, except those very close to the exit plane, lie on a straight line obtained by the curve-fitting principle. These points on the velocity profile fall below the geometric central line close to the nozzle exit and then gradually move up to merge with the geometric central line. This phenomenon indicates that the bottom plate of the nozzle affects the velocity profile close to the nozzle exit. This is probably due to the existence of the stagnant eddies at the step corner beneath the jet. As the eddy growth due to recirculation gradually disappears in the downstream, the velocity profile regains its shape with axial distance. The geometric centre-line and the uniform velocity portion centre-line merge at x/D = 10.5 and 9 for nozzle depths, D = 4 inches (10.16 cm) and 6 inches (15.24 cm) respectively.

A comparison of the present experimental results with the experimental results of Irwin (9) shows that the excess mean axial velocity decay agrees satisfactorily for the nozzle of depth, D = 4 inches (10.16 cm) but the agreement is not satisfactory for the nozzle of depth, D = 6 inches (15.24 cm). Figure 3.22 shows the variation of mean excess velocity along the axial direction. Irwin (9) carried out his experiment at a Reynolds number of 2.80×10^5. The depth of the nozzle was 0.265 inch. Actually Irwin's (9) results were for the developed portion of the jet. So the present experimental results are likely to differ from Irwin's (9) results.

The minimum distance from the wall at which the maximum velocity is attained is called the width for maximum velocity, y_m, of the jet. The experimental values of the width for maximum velocity were plotted in Figure 3.23. It is seen that the width for maximum velocity increases linearly along the axial direction for both the nozzle depth, D = 4 and 6 inches. A straight line was fitted to the experimental points by the method of least squares and equations [3.3] and [3.4] were obtained for D = 4 in. (10.16 cm) and 6 in. (15.24 cm) respectively.

$$y_m/D = 0.0136\ (x/D) + 0.3636 \qquad [3.3]$$

$$y_m/D = 0.0235\ (x/D) + 0.2107 \qquad [3.4]$$

The present experimental results are compared with those of Irwin (9) who has confirmed linear variation of the width for maximum velocity.

TABLE V : Compilation of Half-width Growths and Maximum Mean Axial Velocity Decay for Wall Jets of Various Geometries.

Type of flowfield	Investigators	Streamwise variation of half-width growth, $y_{m/2}$	Axial decay of maximum mean velocity, U_{Jmax}
Two - Dimensional wall jet.	Glauert (11)	$x^{1.0}$	$x^{-0.583}$
	Sigalla (3)	$x^{1.0}$	$x^{-0.50}$
	Bradshaw and Gee (6)	$x^{0.91}$	$x^{-0.53}$
	Schwarz and Cosart (4)	$x^{1.0}$	$x^{-0.555}$
Radial wall jet	Bakke (69)	$x^{0.94}$	$x^{-1.12}$
	Poreh et al (70)	$x^{0.9}$	$x^{-1.1}$
Three - dimensional wall jet	Sforza and Herbst (7)	$x^{0.78 \pm 0.07}$ (for all conventional orifices tested, in both Characteristic Decay and Radial Type Decay regions)	Characteristic Decay region e = 0.025 : $x^{-0.41}$ e = 0.05 : $x^{-0.43}$ e = 0.10 : $x^{-0.16}$ Radial Decay region $x^{-1.1}$ (all conventional orifices tested).

The half-width, $y_{m/2}$, of a jet is the distance from the wall where half of the maximum velocity is attained in the outer region of the profile. The variation of the half - width of the jet in the axial direction is shown in Figure 3.24. The variation is observed to be nonlinear. These results have been compared with those of Irwin (9) who has shown the variation to be linear for the developed region. The present experimental results are applicable to the initial region of the jet where the flow is not self-preserving. The growth of the half-width for wall jets of various geometries observed by different authors is shown in Table V.

3.4 Mixing of Two Shear Layers in the Absence of a Wake

The exit conditions of the streams on either side of the splitter were identified by measuring the exit mean axial velocity and calculating the displacement thickness of the velocity profiles. Measured values of mean axial velocity at the exit of the nozzle are shown in Figure 3.25 and 3.26 for the lower and the upper stream respectively. For each stream the velocity profile is found to be symmetrical about the nozzle centreline. The experimental points were fitted to the equation, $U_N/U_{Nmax} = (y/\delta)^{1/n}$, and the values of n were computed by the method of least squares to be 6.47 and 6.57 for the lower and the upper stream respectively. The boundary layer thickness, the momentum thickness, the shape factor, the average axial velocity

and the Reynolds number of the flow were calculated in the manner described earlier, and these values are shown in Table VI. Considering these characteristics of the velocity profile, the boundary layers were assumed to be turbulent for streams on either side of the splitter.

The two shear layers separate from the knife edge of the splitter and mixing starts from the exit. The mean velocity across the test section has been measured at different axial distances, viz at an interval of 6 inches (15.24 cm) from the exit plane of the nozzles. The experimental results are presented in Figure 3.27. From the mean velocity profile development in Figure 3.27, it appears that the mixing of the two streams is slow compared to that in presence of a wake. The velocity is uniform in the central portion of the two streams. The velocity gradients occur at the interacting regions. The gradient becomes more gentle as one moves away from the nozzle to the downstream side. This phenomenon indicates that energy is being transferred from the lower stream to the upper stream.

Figure 3.28 represents the maximum mean axial velocity distribution in both the lower and the upper streams along the axial direction. It is seen that the maximum mean axial velocities of both the streams decrease linearly. The rate of decay of the lower stream is faster than that of the upper stream. The reason is that the lower stream having higher average velocity imparts momentum to the upper stream having relatively lower average velocity.

TABLE VI : Exit Conditions of the Velocity Profile for the Knife Edged Splitter

Parameter	Lower Stream	Upper Stream
Depth of the nozzle	9 in (22.86 cm)	9 in.(22.86cm)
Average axial velocity	62.62 ft/sec (19.09 m/sec)	53.99 ft/sec (16.46 m/sec)
Maximum axial velocity	64.815 ft/sec (19.76 m/sec)	55.971 ft/sec (17.06 m/sec)
Power of the velocity profile, n	6.47	6.57
Boundary layer thickness, δ	0.581 in. (1.476 cm)	0.531 in. (1.349 cm)
Ratio of displacement thickness to boundary layer thickness, δ^*/δ	0.134	0.132
Ratio of momentum thickness to boundary layer thickness, θ/δ	0.102	0.101
Shape factor, H	1.309	1.304
Reynolds number based on the nozzle depth, Re_D	2.74×10^5	2.37×10^5
Reynolds number based on momentum thickness, Re_θ	1808	1417

The mean axial velocity difference of the two streams at different axial locations are plotted in Figure 3.29. This velocity difference decreases linearly at a slow rate compared to that in presence of a wake.

The width for maximum velocity, y_m, was calculated at different axial distances and plotted in Figure 3.30. The values of y_m increase in the axial direction, and fit to a straight line given by the equation :

$$\frac{y_m}{D} = 0.0074 \left(x/D \right) + 0.0766 \qquad [3.5]$$

The pressure was measured at different axial distances, and was found to be uniform across the streams as shown in Figure 3.31. As this mixing of shear layers takes place in the absence of a wake, there appears no pressure drop in the neighbourhood of the exit although it did exist in case of mixing in the presence of a wake.

CHAPTER - IV

CONCLUSION

The present investigation is on the interaction of two asymmetric confined turbulent streams. Experimental results are obtained primarily from the data of the mixing zone of the two streams and the conclusions drawn are more qualitative than quantitative.

A wind tunnel of test section 1.5 ft x 1.5 ft x 10 ft 8 inches (45.72 cm x 45.72 cm x 325.12 cm) has been installed and all its components except the fan have been fabricated with locally available materials. The wind tunnel was calibrated and found to show a uniform velocity distribution in the test section with no pressure gradients, and the flow was found to be two-dimensional. Nozzles were set up within the test section to produce jets.

The characteristics of mixing of two shear layers depend upon the exit conditions which were identified here. The displacement thicknesses at the exit planes were $\delta^*/\delta = 0.128$ and 0.137 corresponding to Reynolds numbers $Re_D = 1.65 \times 10^5$ and 2.27×10^5 respectively. The boundary layer was turbulent at the beginning of the jet flow, and they formed the mixing layers with a wake between them. A similar flow was generated by using a knife edged splitter to have the mixing layers without wake.

The mean axial velocity and the mean static pressure have been measured across the jets, and the experimental results are compared with those of other investigators, and the results are found to agree satisfactorily except close to the exit. The mean velocity profile within the mixing region of two streams was found to show a high shear due to the presence of a high velocity gradient. This velocity gradient gradually decreases in the downward direction, but the rate of decrease is not as high as in the case of free jets. The velocity profile in the mixing region does not show self-preserving character. This is probably due to the presence of large eddies and their coalescence and subsequent break down. The thin plate between the two streams created a wake which may also be a cause for non-self-preservation of the flow.

The maximum mean axial velocity was observed to decay linearly except close to the outlet for both the lower jet and the upper stream. The rate of decay of the mean axial velocity was higher for the faster moving jet compared to that for the slower moving upper stream in both the cases, viz. D = 4 inches (10.16 cm) and 6 inches (15.24 cm).

No potential core was observed for the jet. The process of mixing of the jet with the upper stream was slow for the low momentum gradient across the streams, and it was monotonic.

No pressure gradient was found to exist across the jets except for a small pressure drop in the wake ahead of the thin plate which separates the two streams.

The width for the maximum velocity, y_m, increases linearly along the axial direction.

The wake formed between the two interacting streams disappears approximately at the same axial distance, x/D, for both the jets because the excess mean velocity is approximately the same in both the cases.

The slope of the mixing profile decreases along the axial direction in a nonlinear fashion.

The small step at the bottom side of the nozzle exit affects the mean flow upto a small distance from the exit plane due to the formation of recirculating flow ahead of the step.

The velocity and pressure distribution in the mixing layer in the absence of wake was found to maintain a trend similar to those with wake. But the velocity in the mixing layer developed at a comparatively slow rate which was probably

due to the absence of wake. The width for maximum velocity, y_m, for this case also varied linearly with the axial distance. The pressure was found to be uniform across the streams at all axial distances.

- o -

REFERENCES

1. Hussain, A.K.M.F., "The Role of Coherent Structures in Turbulent Shear Flows", Proceedings of the Indian Academy of Science (Engr. Sci.) 4, 1981, pp 129 - 175.

2. Forthman, E., " Turbulent Jet Expansion", Ingenieur Archiv. 1, 1934. Trans: N.A.C.A.T.M. 789, 1936.

3. Sigalla, A., " Experimental Data on Turbulent Wall Jets", Aircraft Engineering, Vol. 30, p 131, 1958.

4. Schwarz, W.H. and Cosart, W.P., " The Two-Dimensional Turbulent Wall Jet", Journal of Fluid Mechanics, Vol. 10, Part 4, 1961, pp 481-495.

5. Myers, G.E., Schauer, J.J. and Eustis, R.H., " Plane Turbulent Wall Jet Flow Development and Friction Factor", Journal of Basic Engineering, Transactions of the ASME, Vol. 85(2), p 47, 1963.

6. Bradshaw, P. and Gee, M.T., " Turbulent Wall Jets with and without an External Stream", ARC 22,008, FM 2971, 1960.

7. Sforza, P.M. and Herbst, G., " A Study of Three Dimensional Incompressible Turbulent Wall Jets", AIAA Journal, Vol. 8, No. 2, February, 1970, pp 276 - 283.

8. Kruka, V. and Eskinazi, S., " The Wall Jet in a Moving Stream", Journal of Fluid Mechanics, Vol. 20, Part 4, pp 555 - 579, 1964.

9. Irwin, H.P.A.H., " Measurements in a Self-Preserving Plane Wall Jet in a Positive Pressure Gradient", Journal of Fluid Mechanics, Vol. 61, Part I, 1973, pp 33 - 63.

10. Sawyer, R.A., " Two-Dimensional Reattaching Jet Flows including the Effects of Curvature on Entrainment ", Journal of Fluid Mechanics, Vol. 17, p 481, 1963.

11. Glauert, M.B., " The Wall Jet ", Journal of Fluid Mechanics, Vol. 1, 1956, pp 625 - 643.

12. Eichelbrenner, E.A., and Dumargue, P., " The Problem of the Plane Turbulent Wall Jet with an External Flow of Constant Velocity ", Journal De Mechanique, Vol. 1, p 109, 1962.

13. Escudier, M.P. and Nicoll, W.B., " The Entrainment Function in Turbulent Boundary Layer and Wall Jet Calculations ", Journal of Fluid Mechanics, Vol. 25, Part 2, pp 337 - 366, 1966.

14. Gartshore, I.S. and Newman, B.G., " The Turbulent Wall Jet in an Arbitrary Pressure Gradient ", The Aeronautical Quarterly, Vol. 20, p 25, 1969.

15. Harris, G.L., " The Turbulent Wall Jet on Plane and Curved Surfaces Beneath an External Stream ", Von Karman Institute TN 27, 1965.

16. Wille, R. and Fernholz, H., " Report on the First European Mechanics Colloquium on the Coanda Effect", Journal of Fluid Mechanics, Vol. 23, Part 4, pp 801 - 819, 1965.

17. Catherall, D. and Mangler, K.W., " An Indirect Method for the Solution of the Navier - Stokes Equations for Laminar Incompressible Flow at Large Reynolds Numbers", RAE Rep. Aero. 2683, 1963.

18. Murphy, J.S., " Extension of the Falkner - Skan Similar Solution of the Laminar Boundary Layer Equations to Flows with Surface Curvature", Douglas Aircraft Corp. Rep. ES 40487, 1962.

19. Dvorak, F.A., " Calculation of Turbulent Boundary Layers and Wall Jets over Curved Surfaces", AIAA Journal, Vol. 11, No. 4, April, 1973.

20. Brown, G.L. & Roshko, A., " On Density Effects and Large Structure in Turbulent Mixing Layers", J. Fluid Mechanics, Vol. 64, pp 775 - 816, 1974.

21. Dimotakis, P.E. & Brown, G.J., " The Mixing Layer at High Reynolds Number : Large - Structure Dynamics and Entrainment", J. Fluid Mechanics, Vol. 78, pp 535 - 560, 1976.

22. Hussain, A.K.M.F. & Zaman, K.B.M.Q., " The Free Shear Layer Tone Phenomenon and Probe Interference", J. Fluid Mechanics, Vol. 87, Part 2, 1978, pp 349 - 383.

23. Winant, C.D. & Browand, F.K., " Vortex Pairing : The Mechanism of Turbulent Mixing Layer Growth at Moderate Reynolds Numbers ", J. Fluid Mechanics, Vol. 63, pp 237 - 255, 1974.

24. Clark, A.R., Ph.D. Thesis, University of Houston, 1979.

25. Hussain, A.K.M.F. and Clark, A.R., " On the Coherent Structure of the Axisymmetric Mixing Layer : A Flow - Visualization Study", J. Fluid Mechanics, Vol. 104, 1981, pp 263 - 294.

26. Chandrsuda, C., Mehta, R.D., Weir, A.D. and Bradshaw, P., " Effect of Free - Stream Turbulence on Large Structures in Turbulent Mixing Layers.", J. Fluid Mechanics, Vol. 85, pp 693 - 704, 1978.

27. Browand, F.K. and Troutt, T.R., " A Note on Spanwise Structure in the Two - Dimensional Mixing Layer ", J. Fluid Mechanics, Vol. 97, 1980, pp 771 - 781.

28. Kleis, S.J. and Hussain, A.K.M.F., " The Asymptotic State of the Plane Mixing Layer ", 32nd Regular Meeting of the American Physical Society Division of Fluid Dynamics, American Physical Society, November 18 - 20, 1979, University of Notre Dame.

29. Bradshaw, P., " The Effect of Initial Conditions on the Development of a Free Shear Layer ", J. Fluid Mechanics, Vol. 26, 1966, pp 225 - 236.

30. Batt, R.G., " Some Measurements on the Effect of Tripping the Two Dimensional Shear Layer ", A. I. A. A. J., Vol. 13, 1975, pp 245 - 247.

31. Liepmann, H. & Laufer, J., " Investigations of Free Turbulent Mixing.", N. A. C. A. Tech. Note 1257, 1947.

32. Wygnanski, I. & Fiedler, H.E., " The Two - Dimensional Mixing Region. ", J. Fluid Mech., Vol. 41, 1970, pp 327 - 361.

33. Hussain, A.K.M.F., " Coherent Structures - Reality and Myth ", To be published in Physics of Fluids, 1983.

34. Kleis, S.J., and Hussain, A.K.M.F., " The Asymptotic State of the Plane Mixing Layer ", Bull. Am. Phys. Soc. Ser. II, Vol. 24, 1132, 1979.

35. Tam, C.K.W. and Chen, K.C., " A Statistical Model of Turbulence in Two - Dimensional Mixing Layers. ", J. Fluid Mechanics, Vol. 92, Part 2, 1979, pp 303 - 326.

36. Plaschko, P., " Stochastic Model Theory for Coherent Turbulent Structures in Circular Jets ", Physics of Fluids, Vol. 24 (2), February, 1981.

37. Patel, R.P., " Turbulent Jets and Wall Jets in Uniform Streaming Flow ", The Aeronautical Quarterly, Vol. XXII, November, 1971, pp 311 - 326.

38. Newman, B.G., Patel, R.P., Savage, S.B., and Tjio, H.K., " Three Dimensional Wall Jet Originating from a Circular Orifice.", The Aeronautical Quarterly, Vol. XXIII, 1972, pp 188 - 200.

39. Narayan, K.Y., and Narasimha, R., " Parametric Analysis of Turbulent Wall Jets.", Aeronautical Quarterly, August 1973, pp 207 - 218.

40. Bajura, R.A. and Catalano, M.R., " Transition in a Two-Dimensional Plane Wall Jet.", Journal of Fluid Mechanics, Vol. 70, Part 4, 1975, pp 773-799.

41. Rajaratnam, N. and Stalker, M.J., " Circular Wall Jets in Coflowing Streams.", Journal of the Hydraulics Division, Proceedings of the American Society of Civil Engineers, Vol. 108, No. HY2, February 1982, pp 187-198.

42. Hussain, A.K.M.F. and Zedan, M.F., " Effects of the Initial Condition on the Axisymmetric Free Shear Layer: Effects of the Initial Momentum Thickness.", Physics of Fluids, Vol. 21, No. 7, July 1978, pp 1100 - 1112.

43. Hussain, A.K.M.F. and Zedan, M.F., " Effects of the Initial Condition on the Axisymmetric Free Shear Layer: Effect of the Initial Fluctuation Level.", Physics of Fluids, Vol. 21, No. 9, September 1978, pp 1475 - 1481.

44. Husain, Z.D. and Hussain, A.K.M.F., " An Experimental Study of Instability and Natural Roll - up of the Free Shear Layer ", American Physical Society Division of Fluid Dynamics Meeting, November 18 - 20, 1979, South Bend, Indiana; Bull. Am. Phys. Soc. Ser. II, 24, 1144, 1979.

45. Hussain, A.K.M.F. and Hussain, Z.D., " The Turbulence Structure in the Axisymmetric Mixing Layer. ", AIAA Journal 18, 1980, pp 1462 - 1469.

46. Husain, Z.D., Ph.D. Thesis, University of Houston, 1982.

47. Coles, D.E., Rand Corpn. Rept. R - 403PR, 1962.

48. Purtell, L.P., Klebanoff, P.S. and Buckley, F.T., Phys. Fluids, Vol. 24, 1981, p 802.

49. Hussain, A.K.M.F. and Clark, A.R., Physics of Fluids, Vol. 20, 1977, p 1416.

50. Kita, Y., Hussain, A.K.M.F. and Kleis, S.J., " Controlled Perturbation of the Plane Mixing Layer.", American Physical Society Division of Fluid Dynamics Meeting, November 22 - 24, 1980, Cornell University. Bull. Am. Phys. Soc., Series II 25, p 1070.

51. Wygnanski, I.J. and Champagne, F.H., " On Transition in a Pipe. Part 1. The Origin of Puffs and Slugs and the Flow in a Turbulent Slug ", J. Fluid Mech., Vol. 59, 1973, pp 281 - 335.

52. Wygnanski, I.J., Sokolov, M. and Friedman, D., " On Transition in a Pipe. Part 2. The Equilibrium Puff ", J. Fluid Mech., Vol. 69, 1975, p 283 - 304.

53. Coles, D.E., " Transition in Circular Couette Flow ", J. Fluid Mech., Vol. 21, 1965, pp 385 - 425.

54. Van Atta, C.W., " Exploratory Measurements in Spiral Turbulence ", J. Fluid Mech., Vol. 25, 1966, pp 495 - 512.

55. Koschmieder, E.L., " Turbulent Taylor Vortex Flow ", J. Fluid Mech., Vol. 93, 1979, pp 515 - 527.

56. Batchelor, G.K., Private Communication, 1982.

57. Hunt, J.C.R., Private Communication, 1982.

58. Reynolds, W.C., " Large - scale Instabilities of Turbulent Wakes ", J. Fluid Mech., Vol. 54, 1972, pp 481 - 488.

59. Bevilaqua, P.M. and Lykoudis, P.S., " Turbulence Memory in Self - preserving Wakes ", J. Fluid Mech., Vol. 89, 1978, pp 589 - 606.

60. Taneda, S., J. Phys. Soc., Japan, Vol. 14, 1959, p 843.

61. Clark, A.R. and Hussain, A.K.M.F., in Turb. Shear Flows (London), 1979, p 2.30.

62. Hussain, A.K.M.F. and Zaman, K.B.M.Q., "Vortex Pairing in a Circular Jet under Controlled Excitation. Part 2. Coherent Structure Dynamics.", Journal of Fluid Mechanics, Vol. 101, 1980, pp 493 - 544.

63. Blackwelder, R.F., Physics of Fluids Suppl., Vol. 20, S232, 1977.

64. Yule, A.J., in Turb. Shear Flows (London), 1979, p 7.1.

65. Sokolov, M., Hussain, A.K.M.F., Kleis, S.J. and Hussain, Z.D., "Turbulent Spot in an Axisymmetric Free Shear Layer, Part 1.", J. Fluid Mechanics, Vol. 98, 1980, pp 65 - 95.

66. Clay, C.H., and Gordon, R.M., "Experiments with Industrial Effluent Outfalls on the Pacific Coast of Canada", Eleventh Congress of the International Association of Hydraulic Research, Leningrad, Soviet Union, Vol. 2, 1965.

67. Islam, S.M.N., "Design and Construction of a Closed Circuit Wind Tunnel", M.Sc. Engg. Thesis, Department of Mechanical Engineering, BUET, Dhaka, 1975.

68. Schlichting, H., "Boundary Layer Theory", McGraw Hill Book Company, New York, N.Y., 1968.

69. Bakke, p., "An Experimental Investigation of a Wall Jet", Journal of Fluid Mechanics, Vol. 2, p 467, 1957.

70. Poreh, M., Tsuei, Y. G., and Cermak, J.E., "Investigation of a Turbulent Radial Wall Jet", Transactions of the ASME, Journal of Applied Mechanics, June 1967, pp 457 - 463.

F I G U R E S

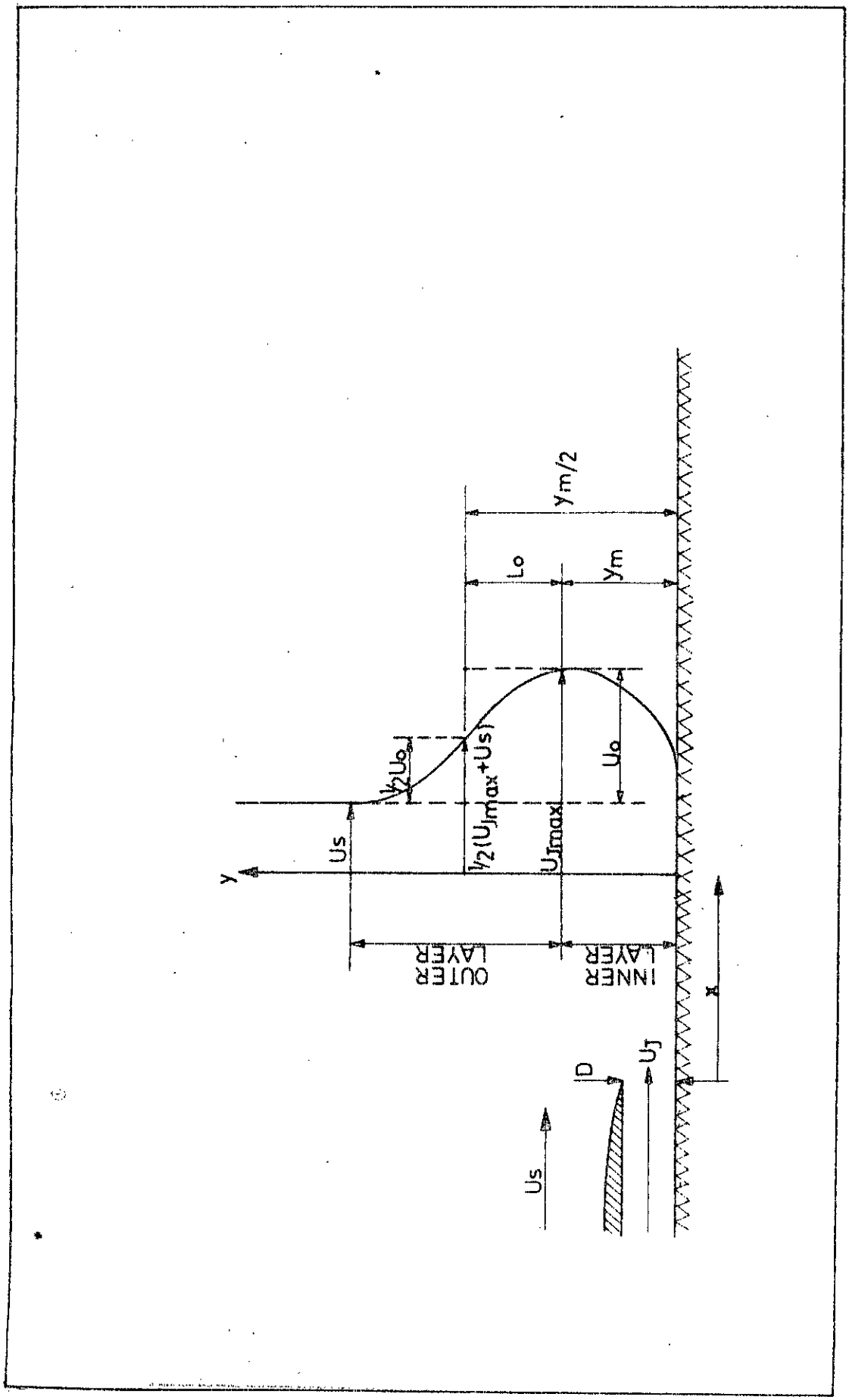

FIG. 1.1. TWO-DIMENSIONAL TURBULENT WALL JET IN STREAMING FLOW.

1. CONVERGING DUCT
2. WOODEN DUCT (1'-6" x 1'-6")
3. PERSPEX DUCT (1'-6" x 1'-6")
4. PERSPEX DUCT (1'-6" x 1'-6")
5. WOODEN DUCT (1'-6" x 1'-6")
6. DIVERGING DUCT
7. AXIAL FAN
8. AXIAL FAN
9. WIRE NET (MESH SIZE : 16 HOLES/INCH)

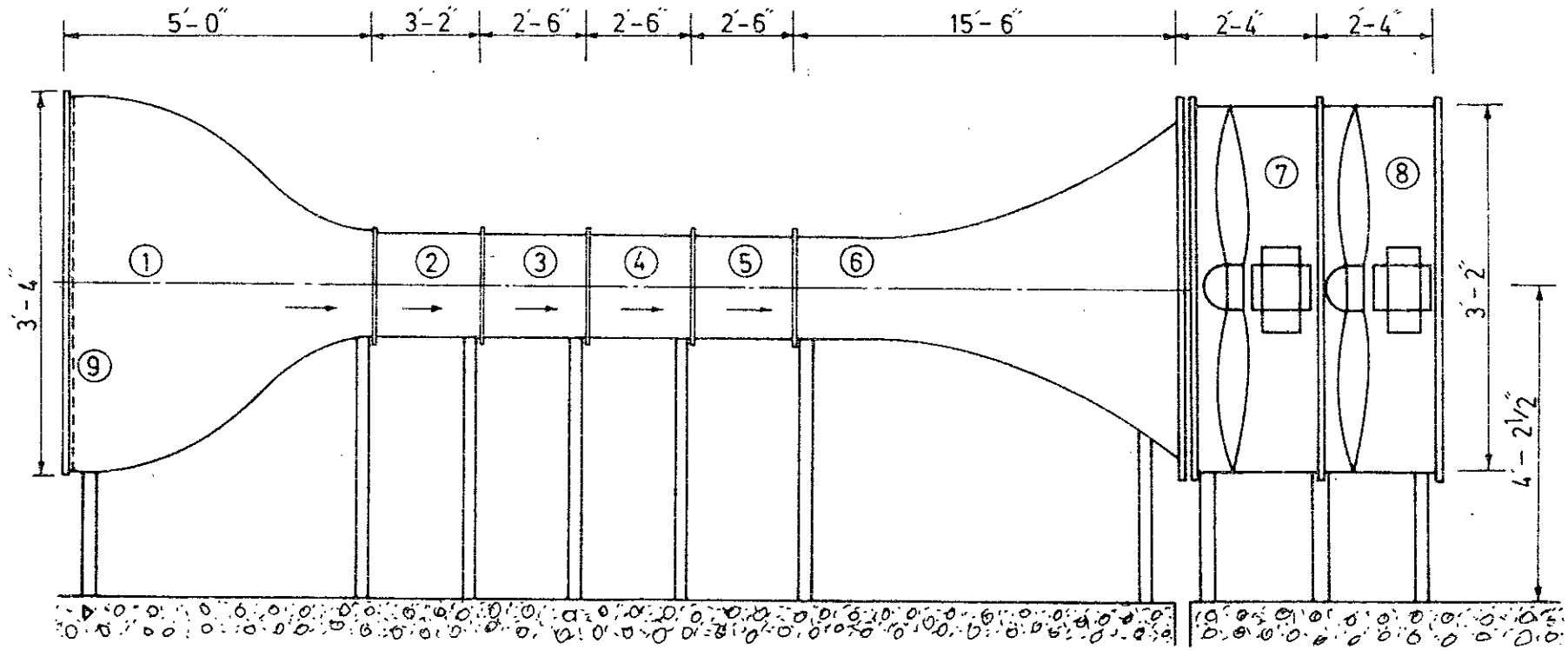

FIG. 2.1 A. SCHEMATIC DIAGRAM OF THE WIND TUNNEL USED FOR THE EXPERIMENT.

FIG. 2.1B. A FRONT VIEW OF THE WIND TUNNEL USED FOR THE EXPERIMENT.

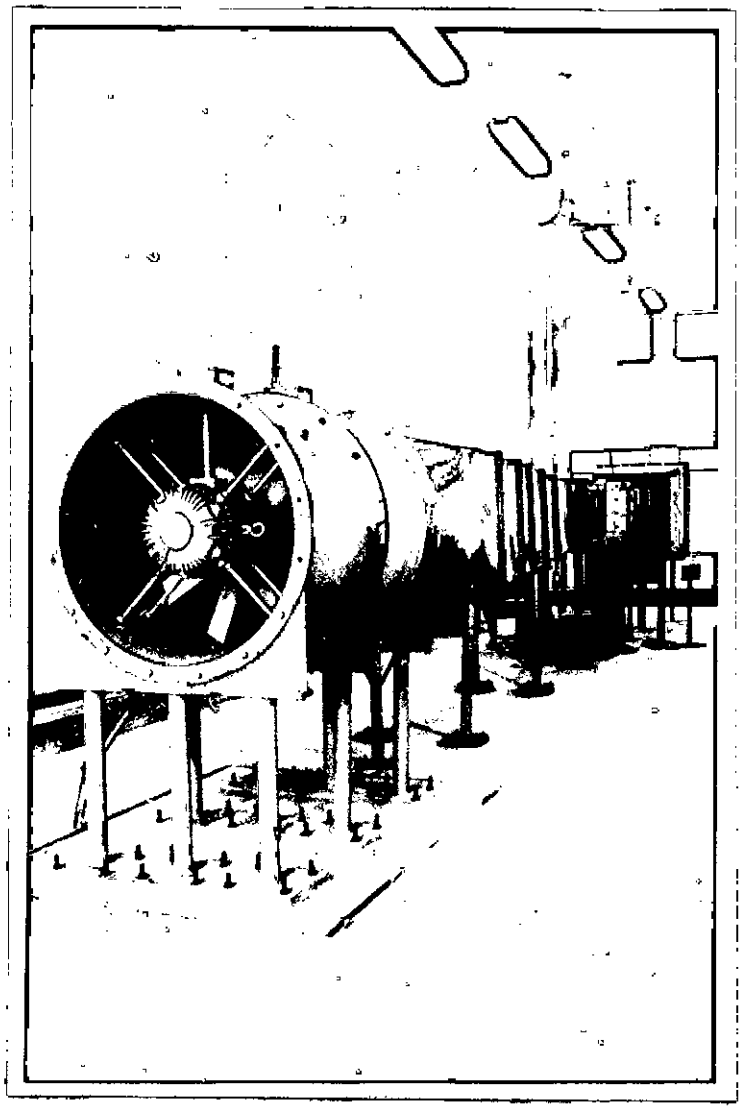

FIG. 2.1C. A REAR VIEW OF THE WIND TUNNEL USED FOR THE EXPERIMENT.

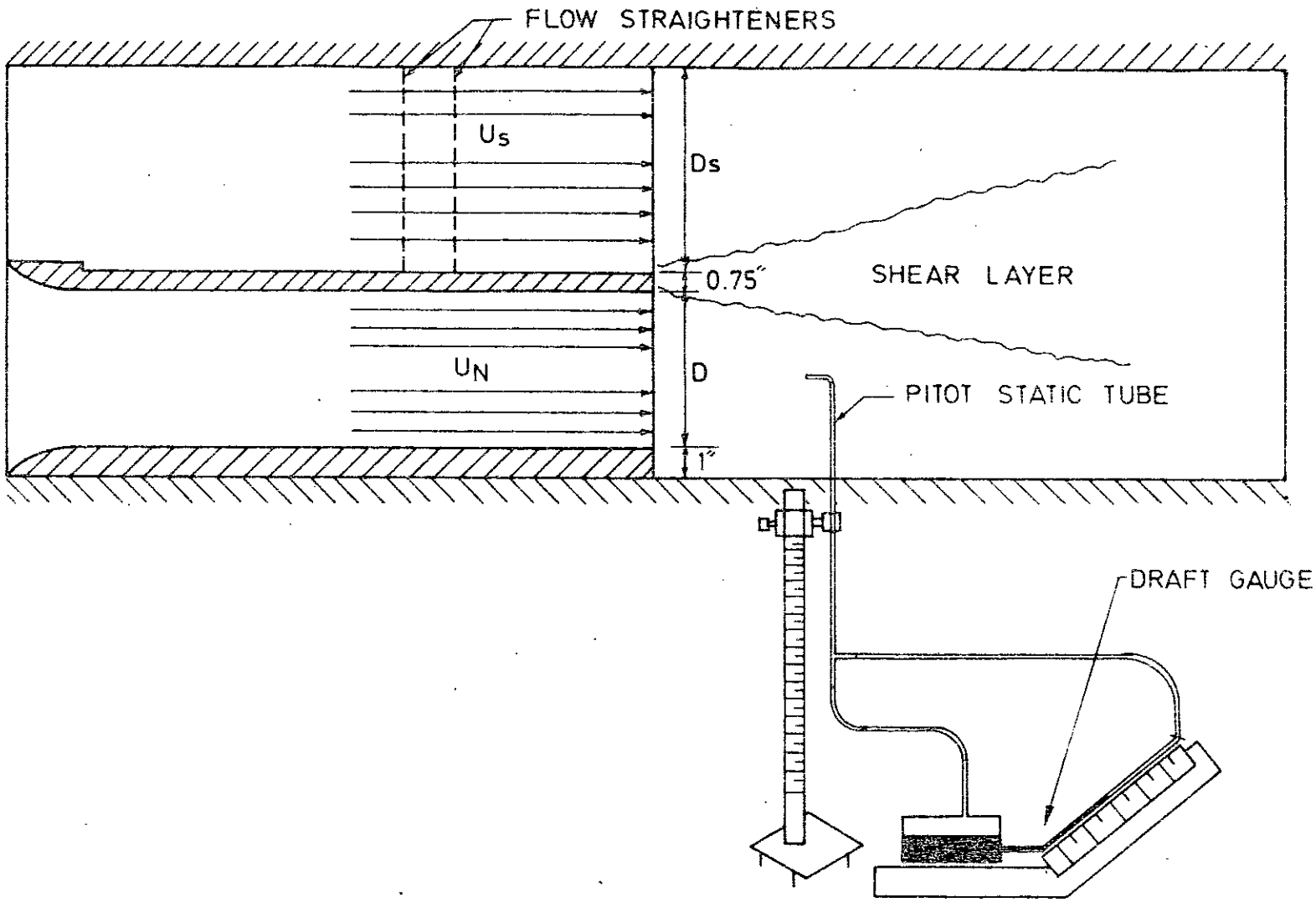

FIG. 2.2 A. SCHEMATIC DIAGRAM OF THE EXPERIMENTAL SET-UP.

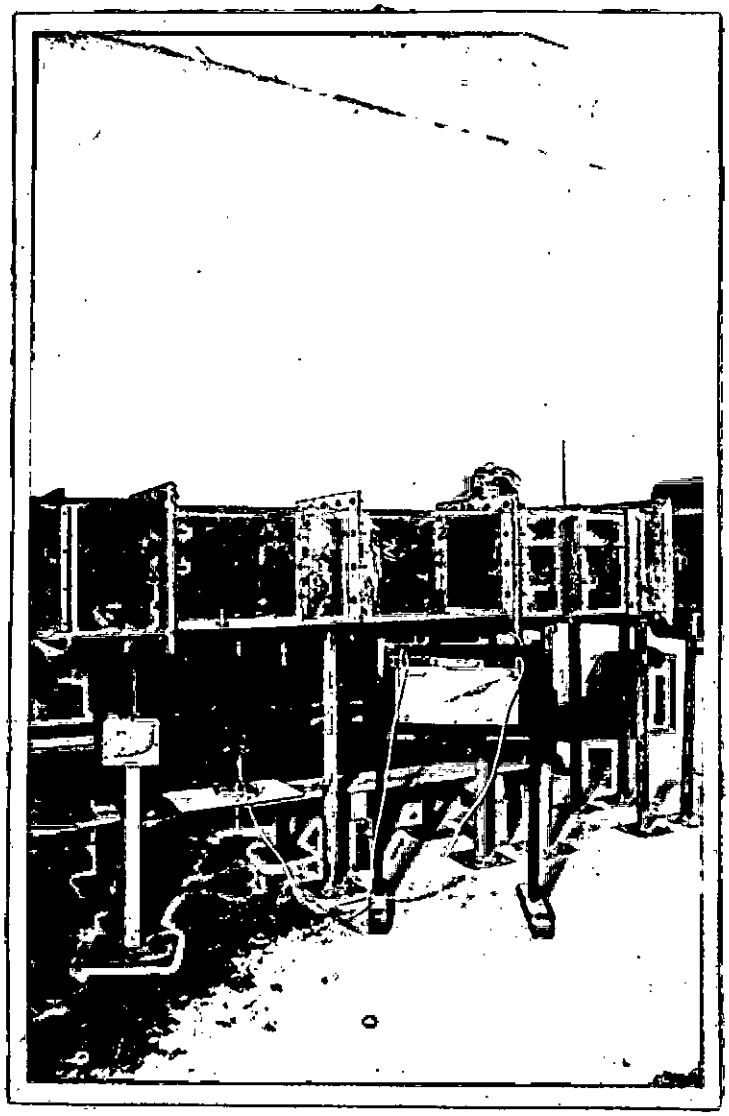

FIG. 2.2B. A VIEW OF THE EXPERIMENTAL SET-UP.

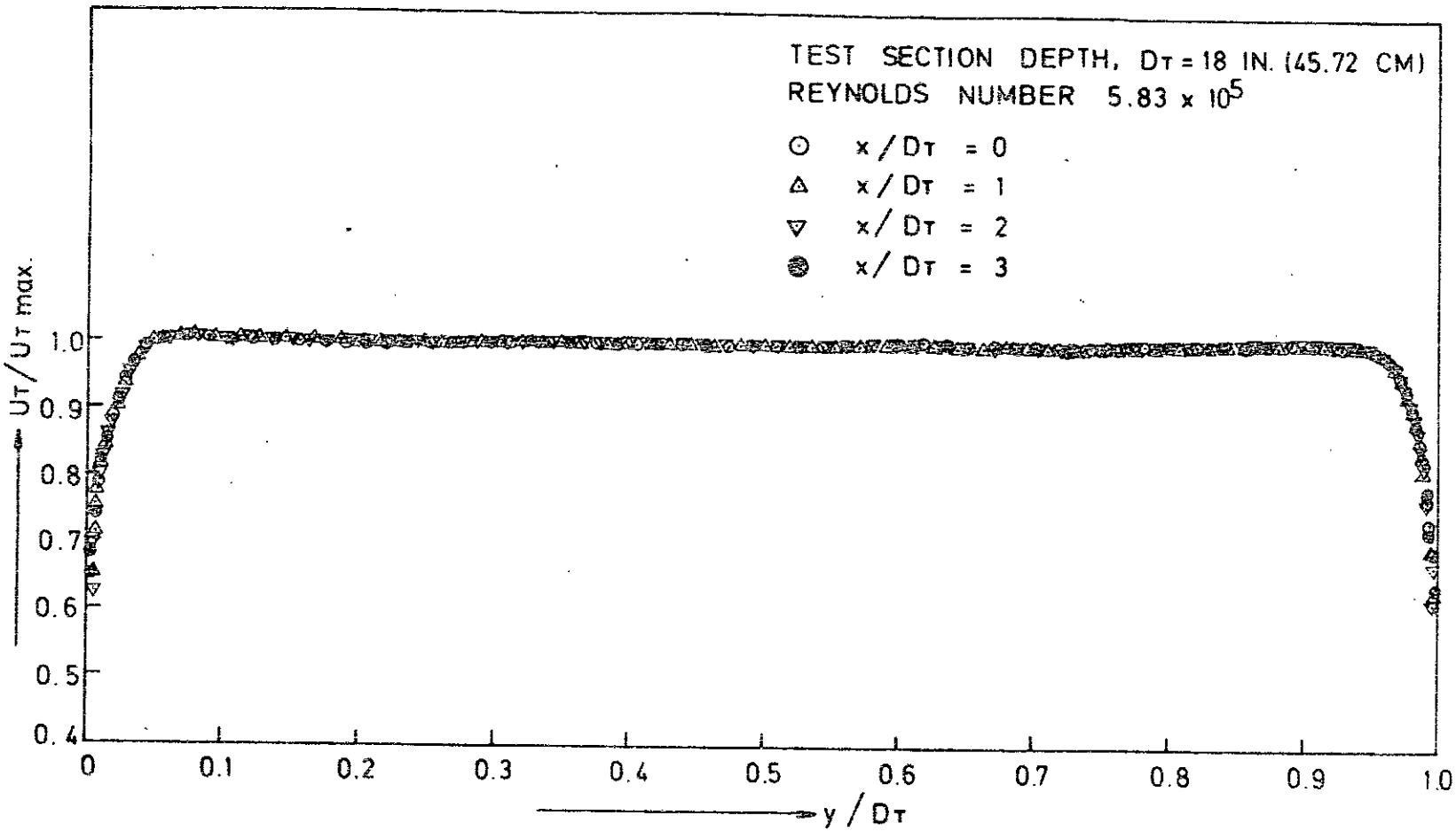

FIG. 3.1 MEASURED MEAN AXIAL VELOCITY DISTRIBUTION IN THE TEST SECTION AT DIFFERENT AXIAL DISTANCES.

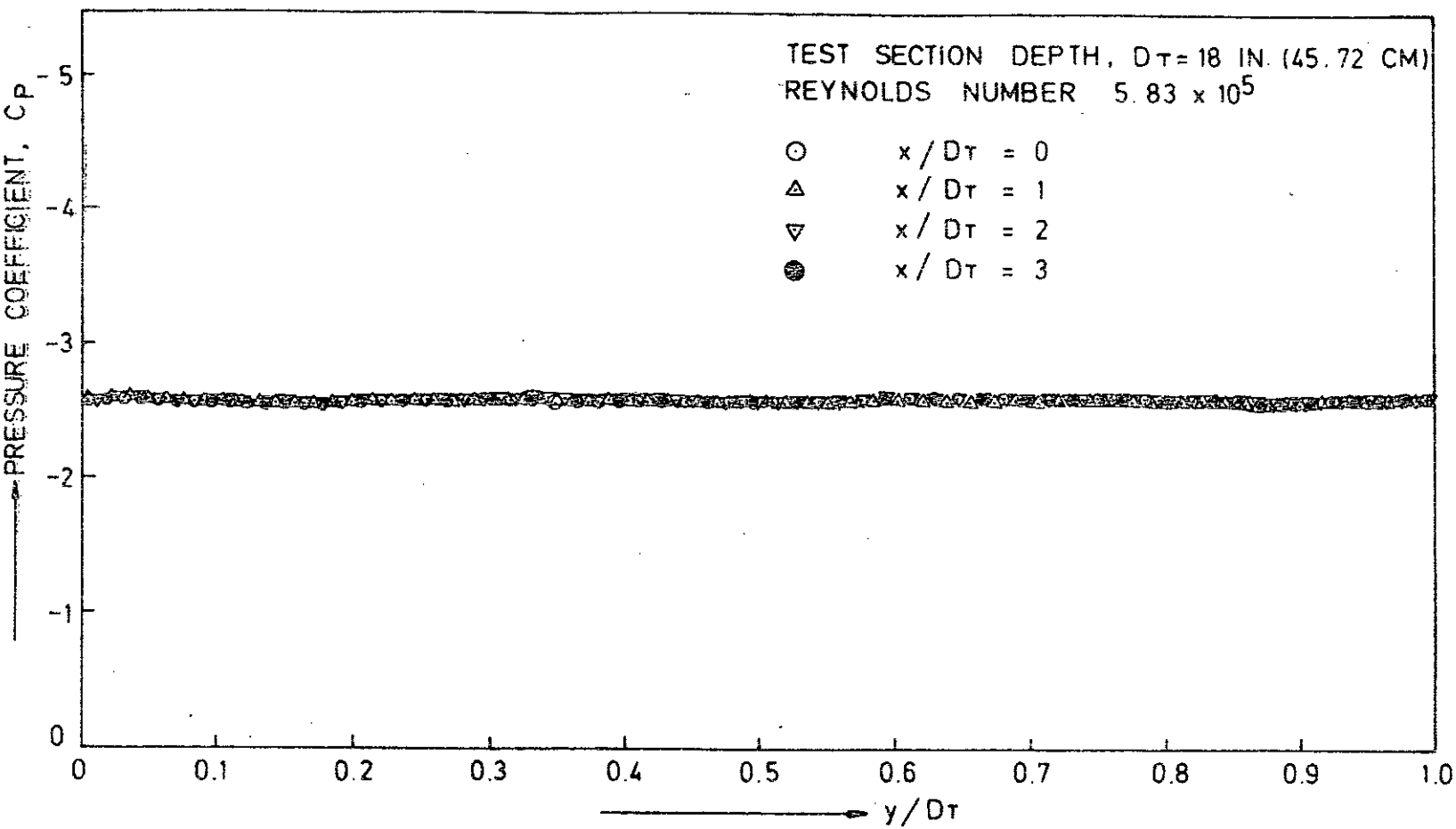

FIG. 3.2 DISTRIBUTION OF THE PRESSURE COEFFICIENT IN THE TEST SECTION AT DIFFERENT AXIAL DISTANCES.

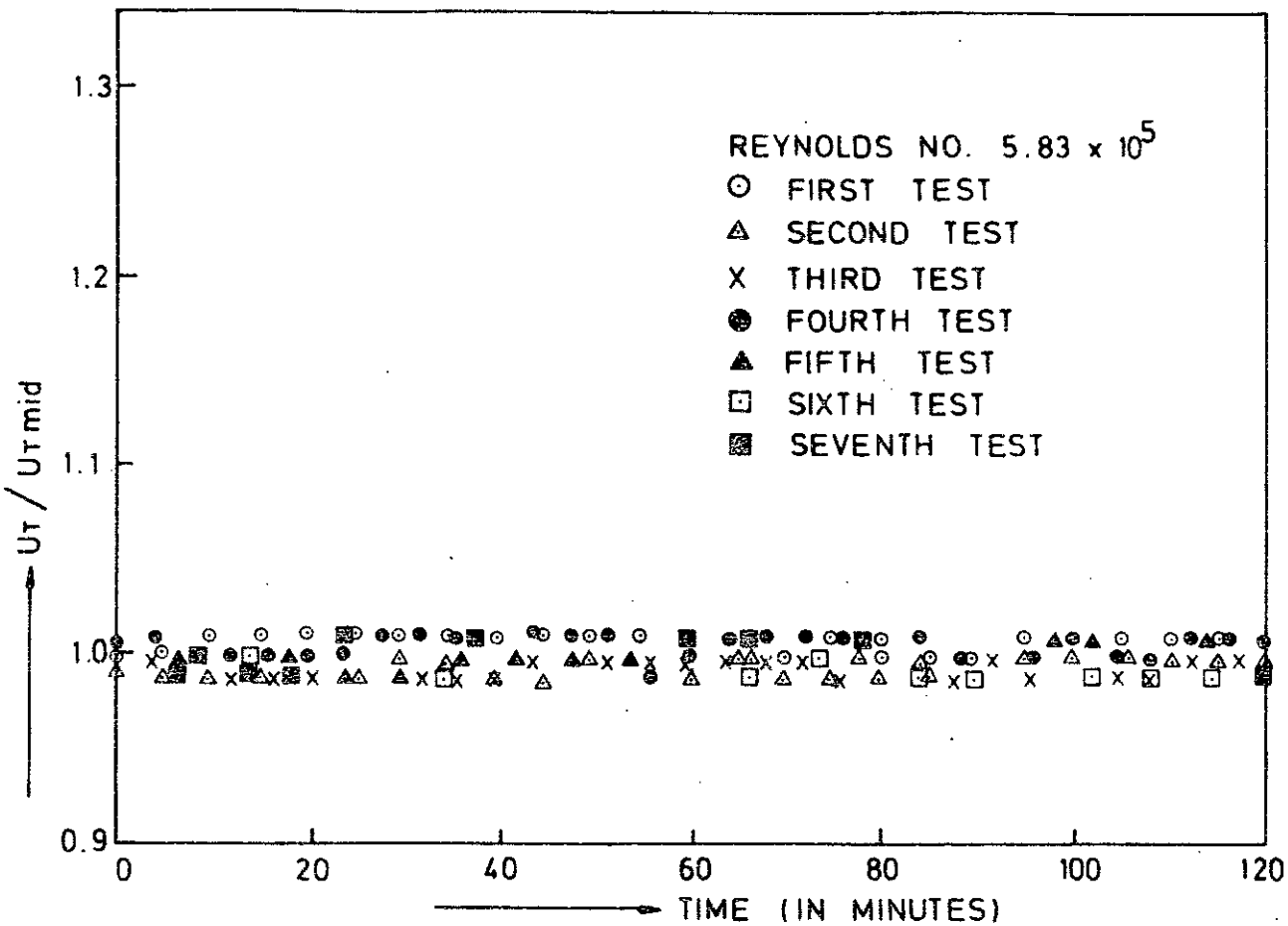

FIG. 3.3 REPRODUCIBILITY OF MEAN AXIAL VELOCITY WITH TIME AT THE CENTRE OF THE TEST SECTION.

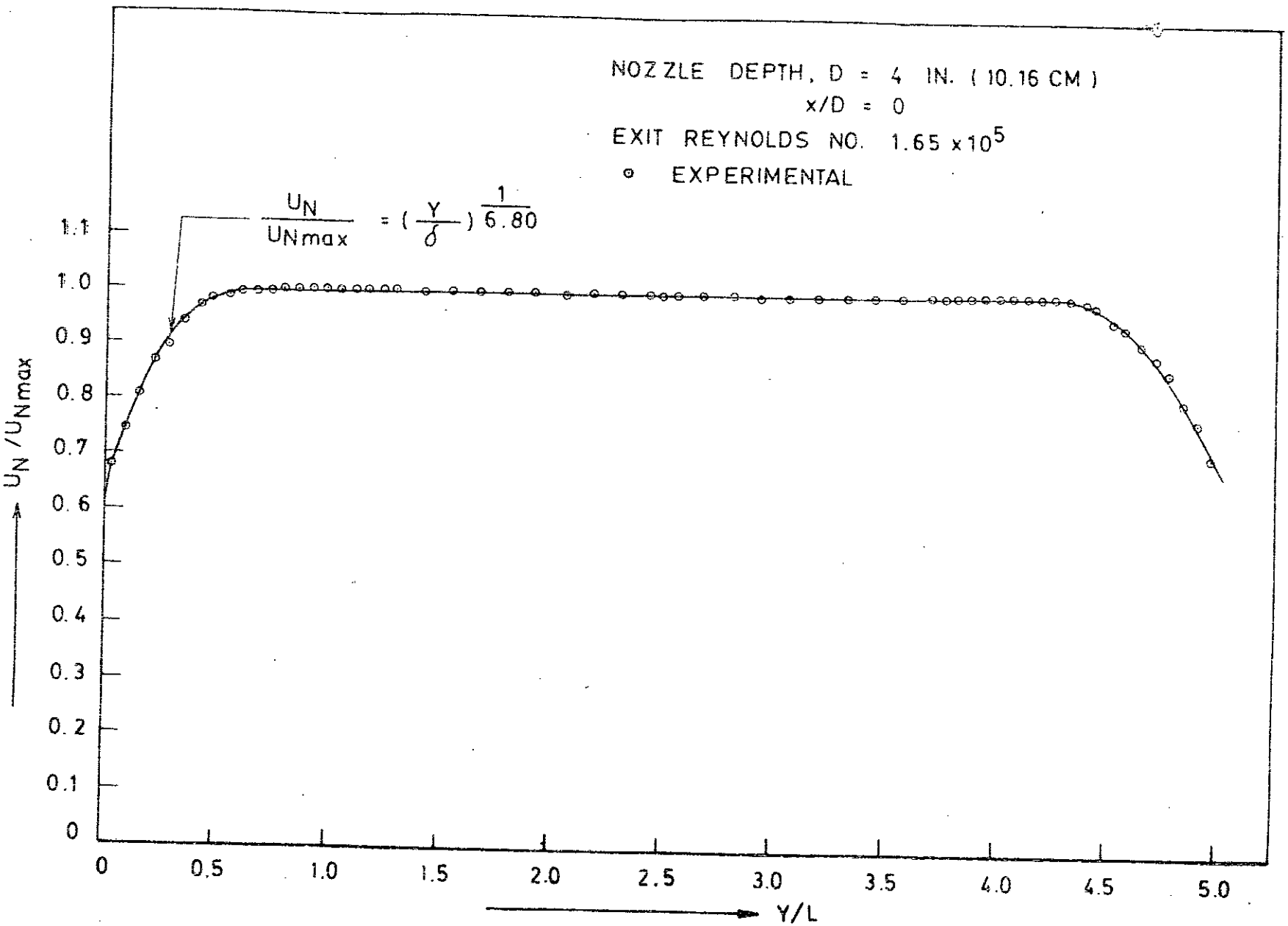

FIG. 3.4 MEASURED MEAN AXIAL VELOCITY DISTRIBUTION IN THE NOZZLE AT THE EXIT PLANE

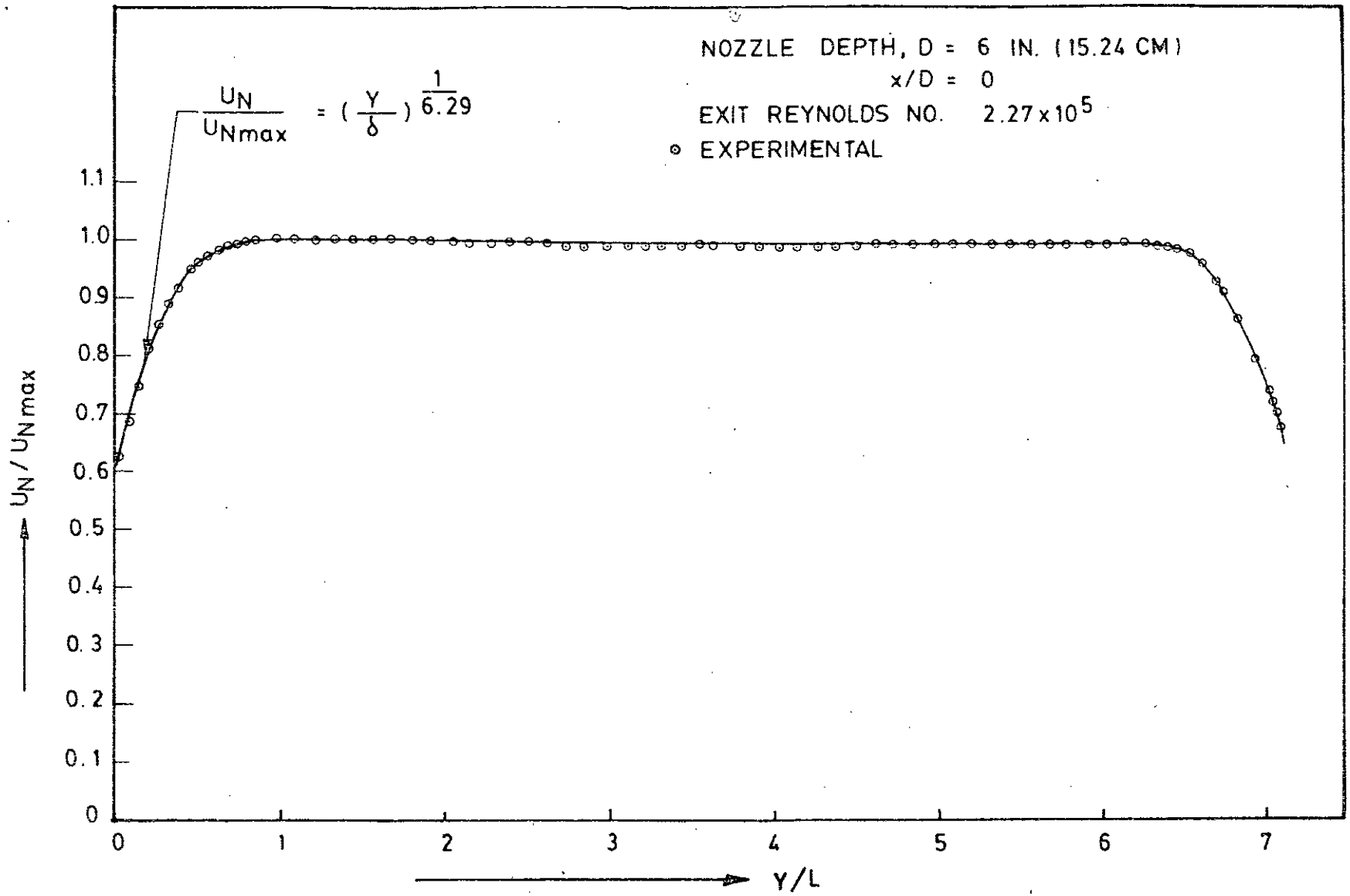

FIG. 3.5 MEASURED MEAN AXIAL VELOCITY DISTRIBUTION IN THE NOZZLE AT THE EXIT PLANE.

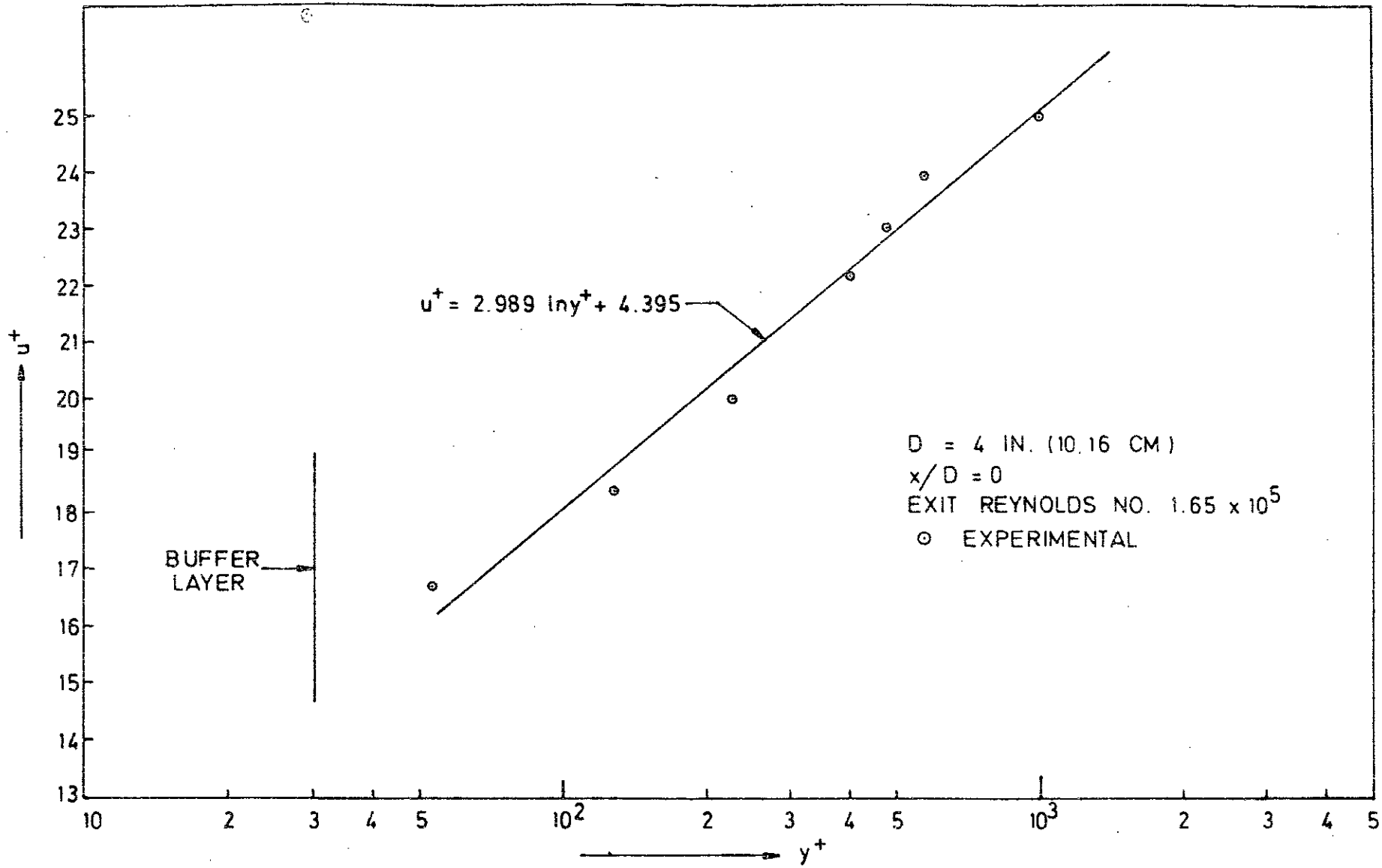

FIG. 3.6 UNIVERSAL VELOCITY PROFILE AT THE NOZZLE EXIT.

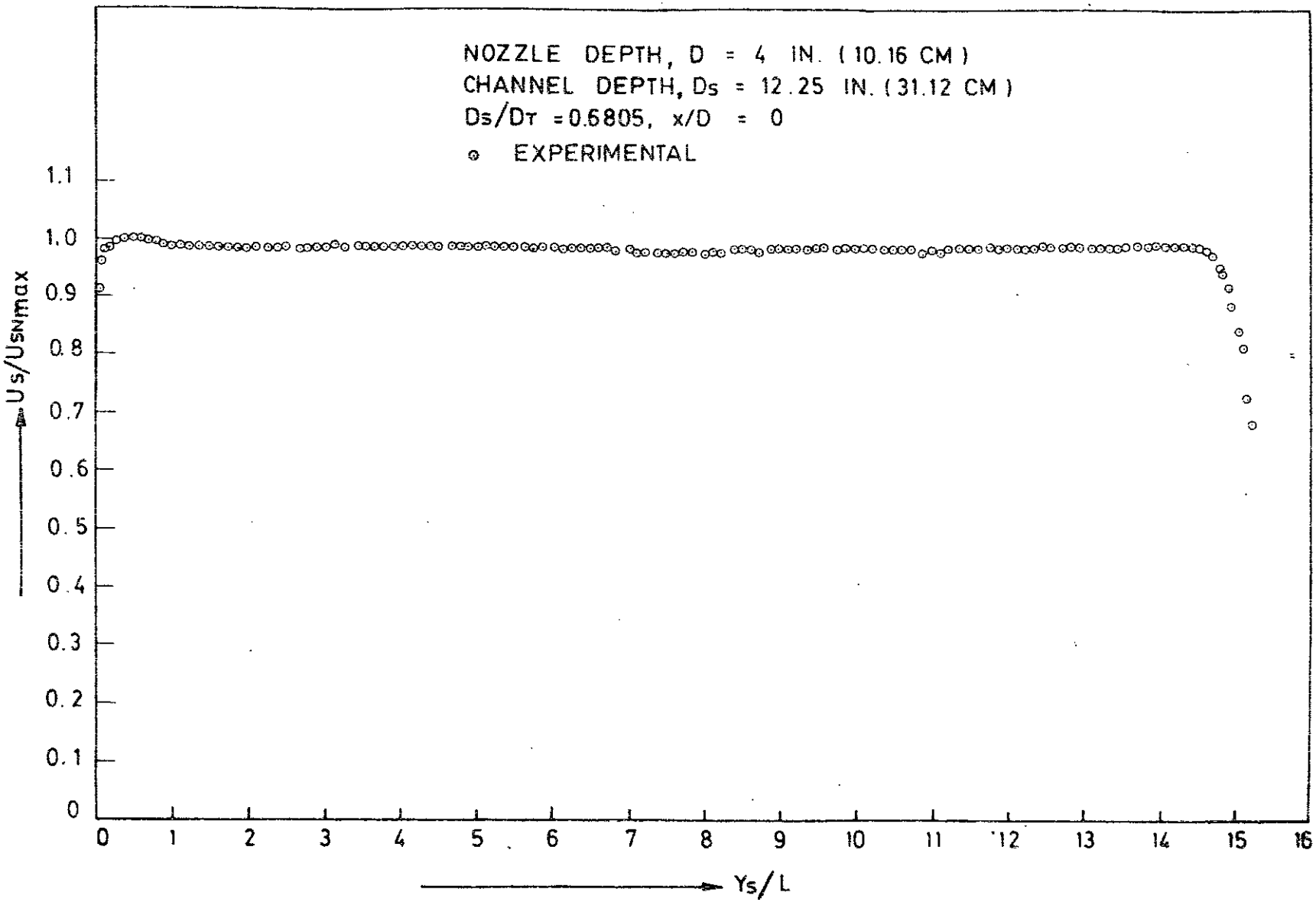

FIG. 3.7 MEASURED MEAN AXIAL VELOCITY DISTRIBUTION IN THE SUPERIMPOSING CHANNEL AT THE EXIT PLANE.

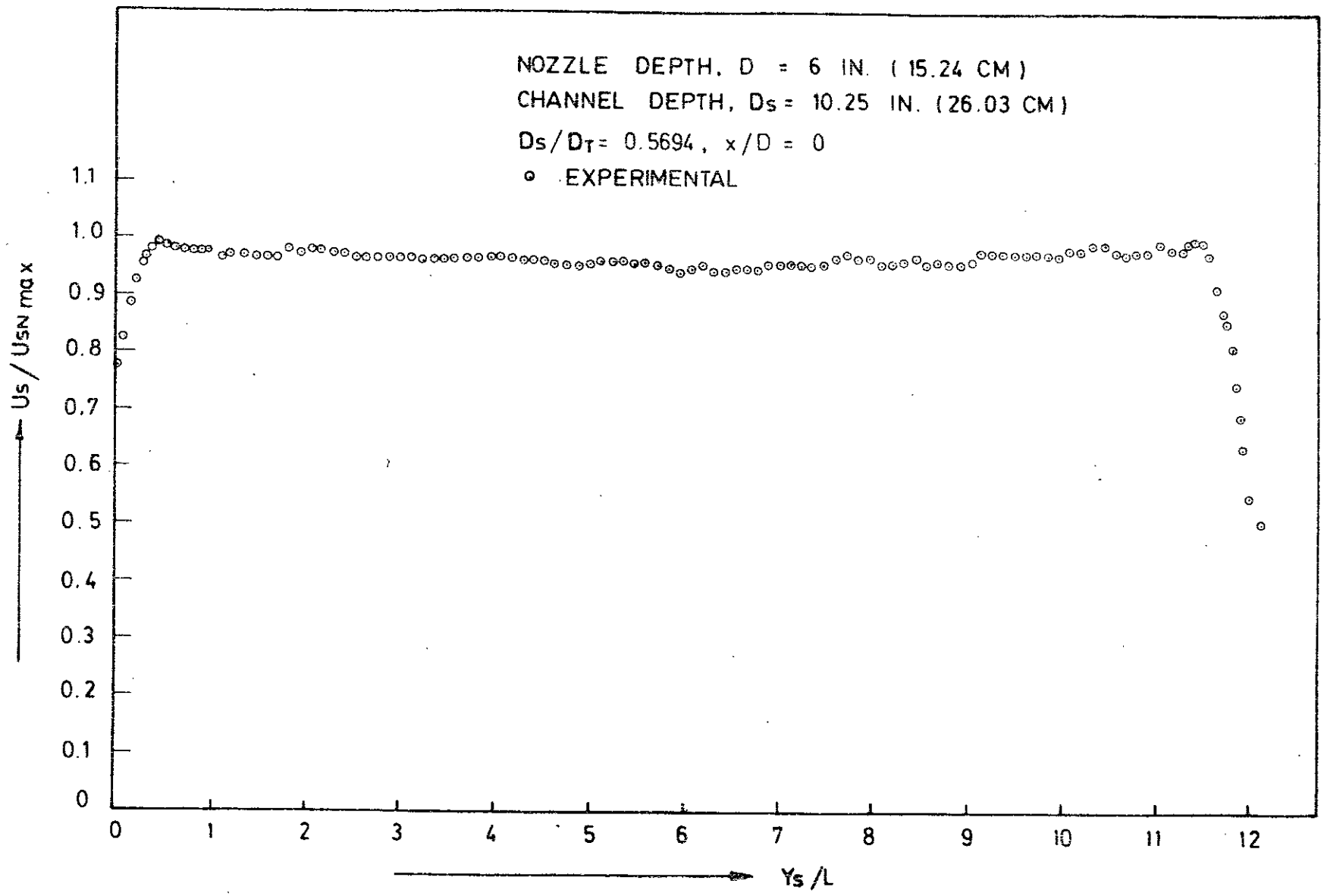

FIG. 3.8 MEASURED MEAN AXIAL VELOCITY DISTRIBUTION IN THE SUPERIMPOSING CHANNEL AT THE EXIT PLANE.

NOZZLE DEPTH, D = 4 INCHES (10.16 CM)
Ds/Dт = 0.6805

EXIT REYNOLDS NO. 1.65×10^5

⊙ EXPERIMENTAL

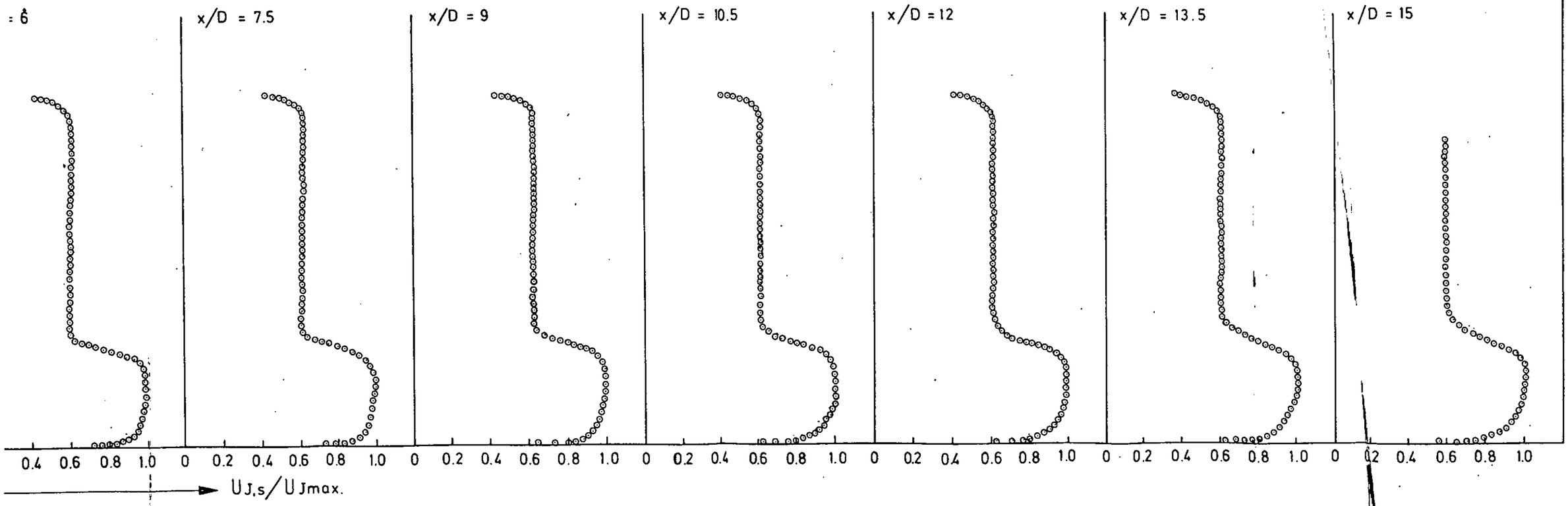

DISTANCES.

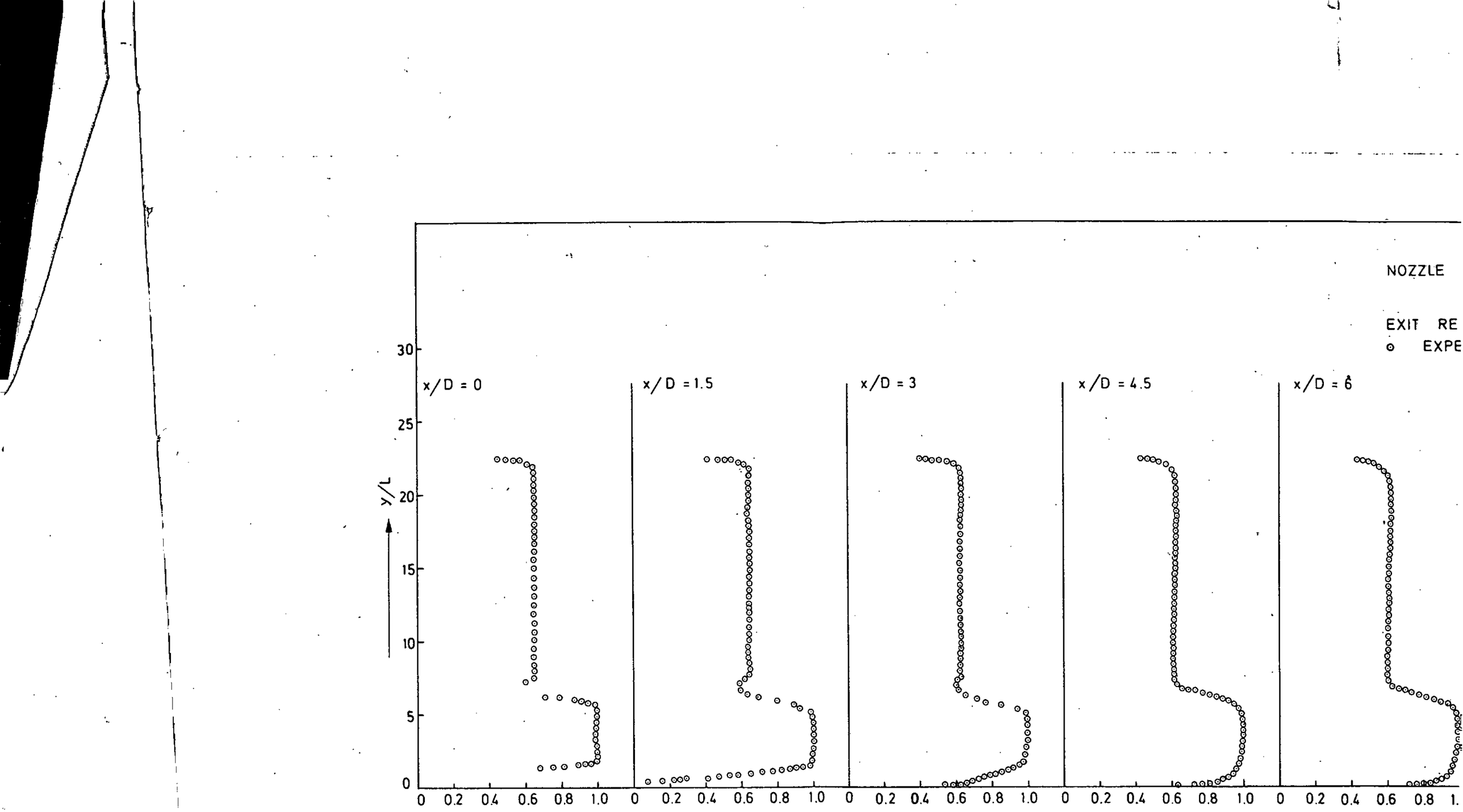

FIG. 3. 9 MEASURED MEAN AXIAL VELOCITY DISTRIBUTION IN THE JET AT DIFFERENT AXIAL DISTANCES.

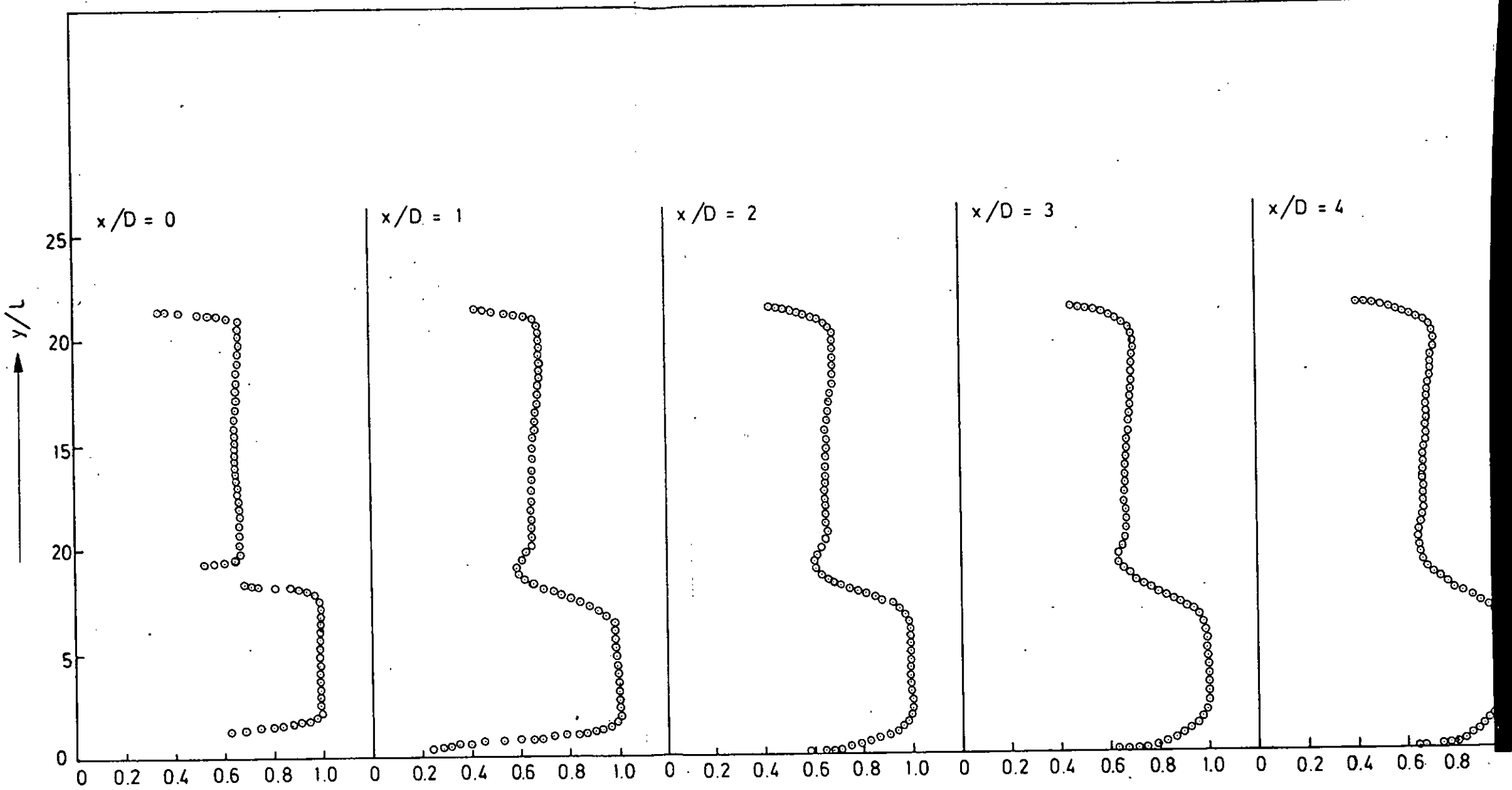

FIG. 3.10 MEASURED MEAN AXIAL VELOCITY DISTRIBUTION IN THE JET AT DIFFERENT AXIAL DISTANCES.

ZLE DEPTH, D = 6 INCHES (15.24 CM)
D_s/D_T = 0.5694

REYNOLDS NO. 2.27×10^5
EXPERIMENTAL

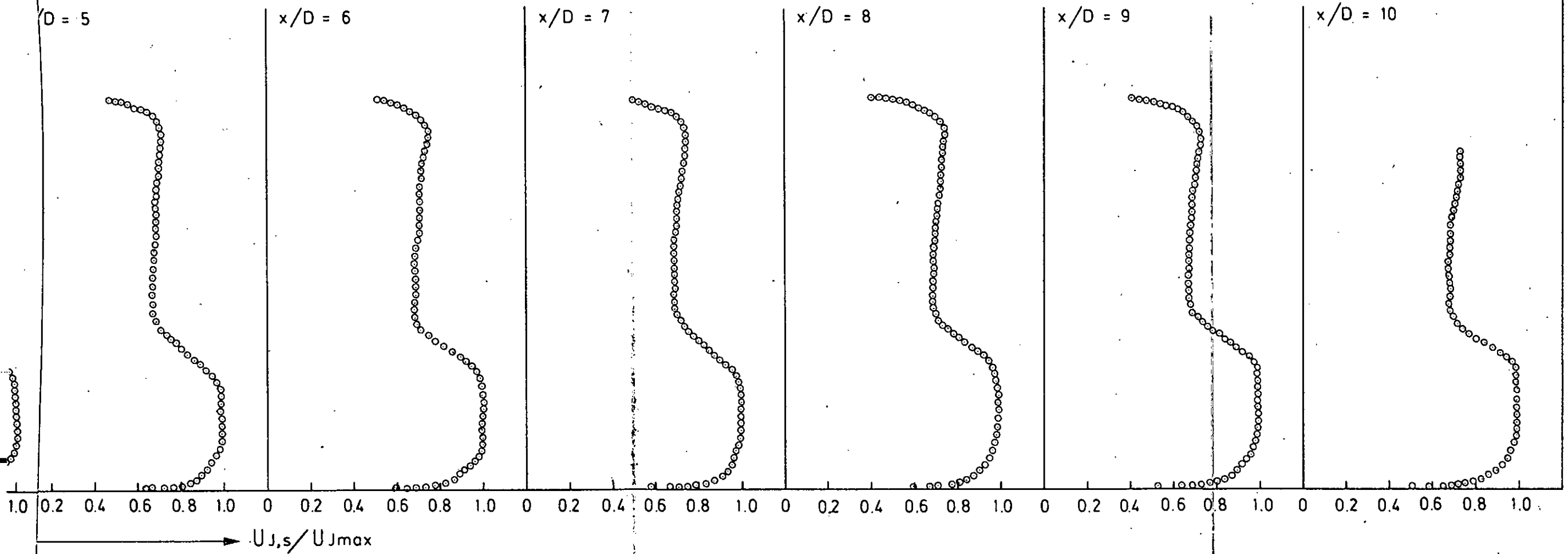

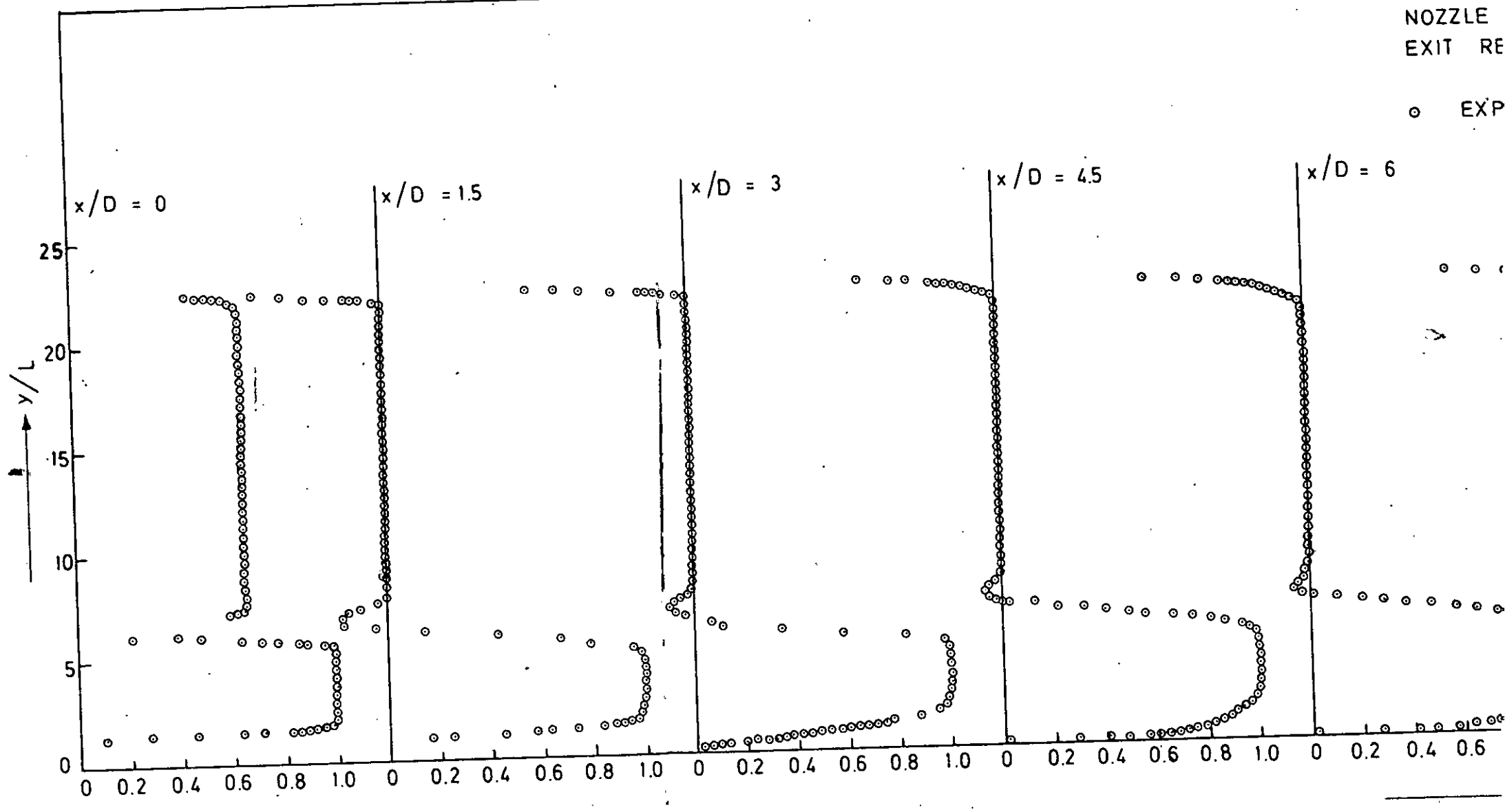

FIG. 3.11 MEASURED MEAN EXCESS VELOCITY DISTRIBUTION IN THE JET AT DIFFERENT AXIAL DISTANCES.

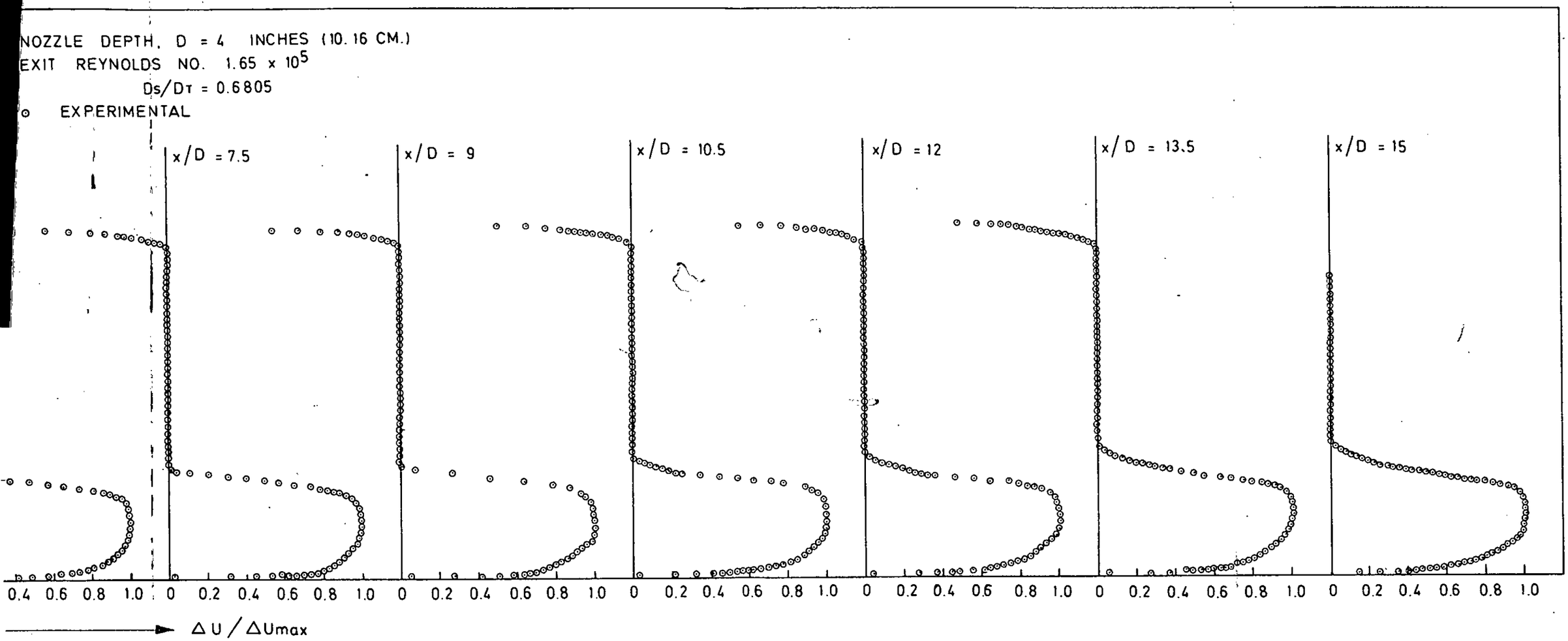
NOZZLE DEPTH, D = 4 INCHES (10.16 CM.)
EXIT REYNOLDS NO. 1.65 x 10^5
Ds/Dt = 0.6805
EXPERIMENTAL
x/D = 7.5
x/D = 9
x/D = 10.5
x/D = 12
x/D = 13.5
x/D = 15
0.4 0.6 0.8 1.0
0 0.2 0.4 0.6 0.8 1.0
ΔU / ΔUmax

ANCES.

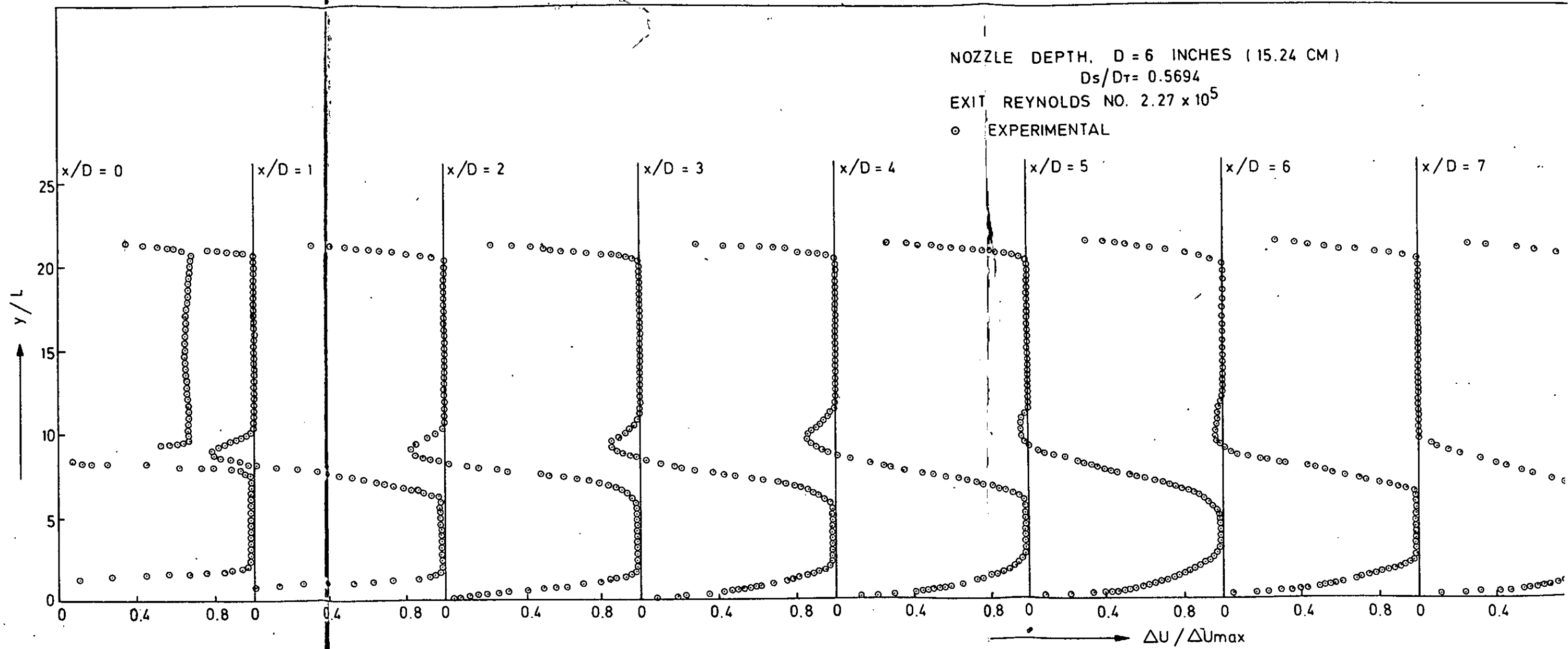

FIG. 3.12 MEASURED MEAN EXCESS VELOCITY DISTRIBUTION IN THE JET AT DIFFERENT AXIAL DISTANCES.

ZLE DEPTH, D = 6 INCHES (15.24 CM)
Ds/DT= 0.5694
REYNOLDS NO. 2.27 x 10^5
EXPERIMENTAL

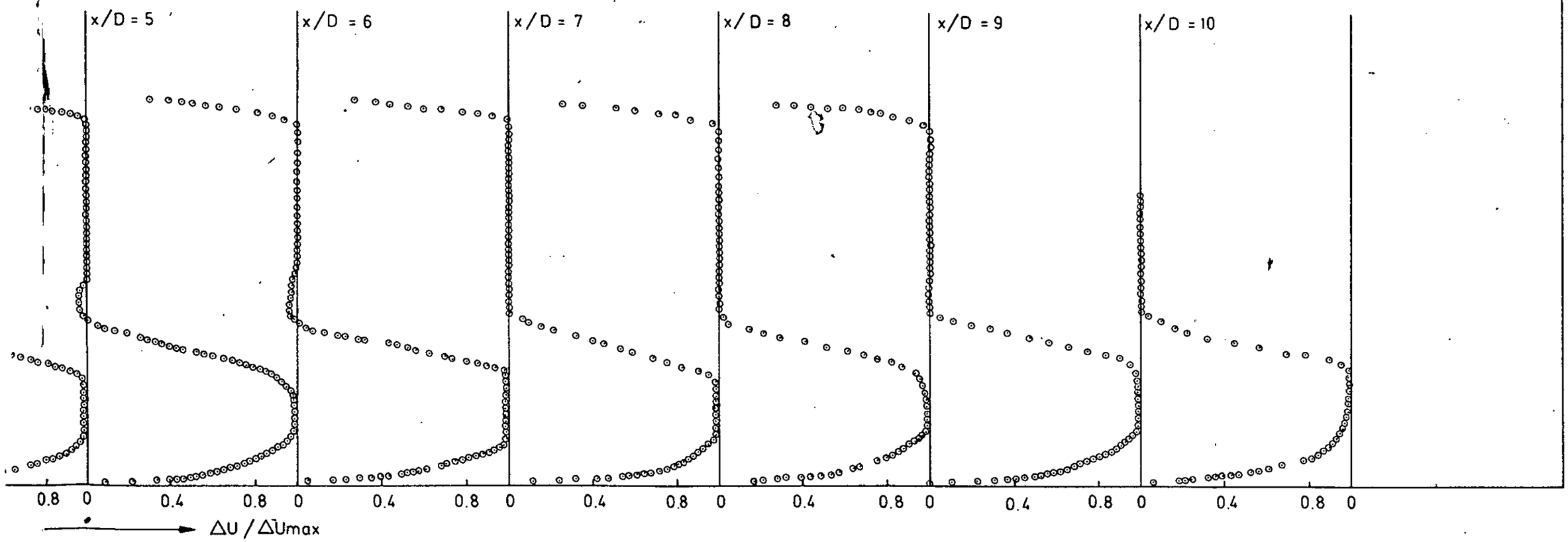

DISTANCES.

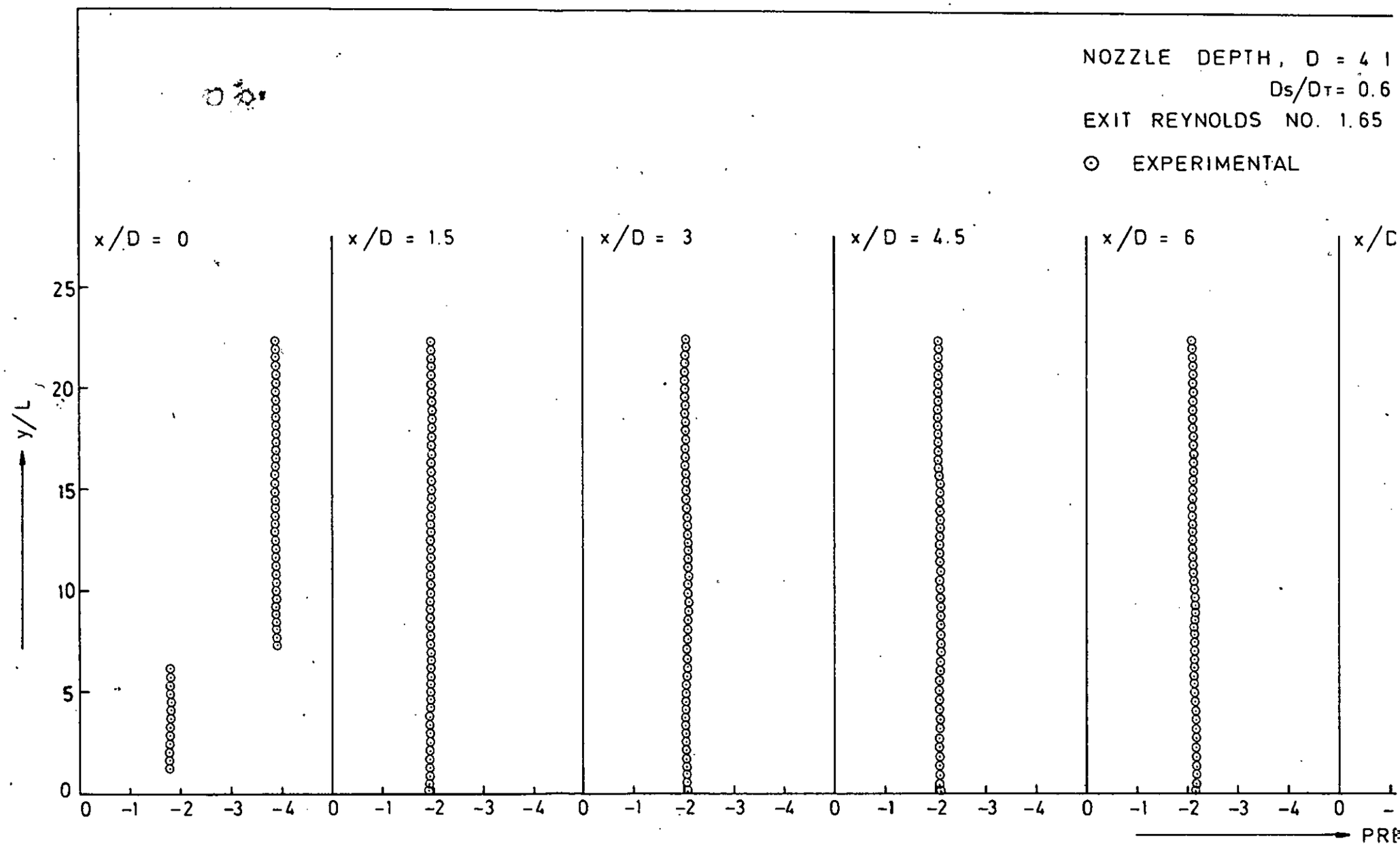

FIG. 3.13 DISTRIBUTION OF THE PRESSURE COEFFICIENT IN THE JET AT DIFFERENT AXIAL DISTANCES.

NOZZLE DEPTH, D = 4 INCES (10.16 CM)

D_s/D_T = 0.686

EXIT REYNOLDS NO. 1.65×10^5

⊙ EXPERIMENTAL

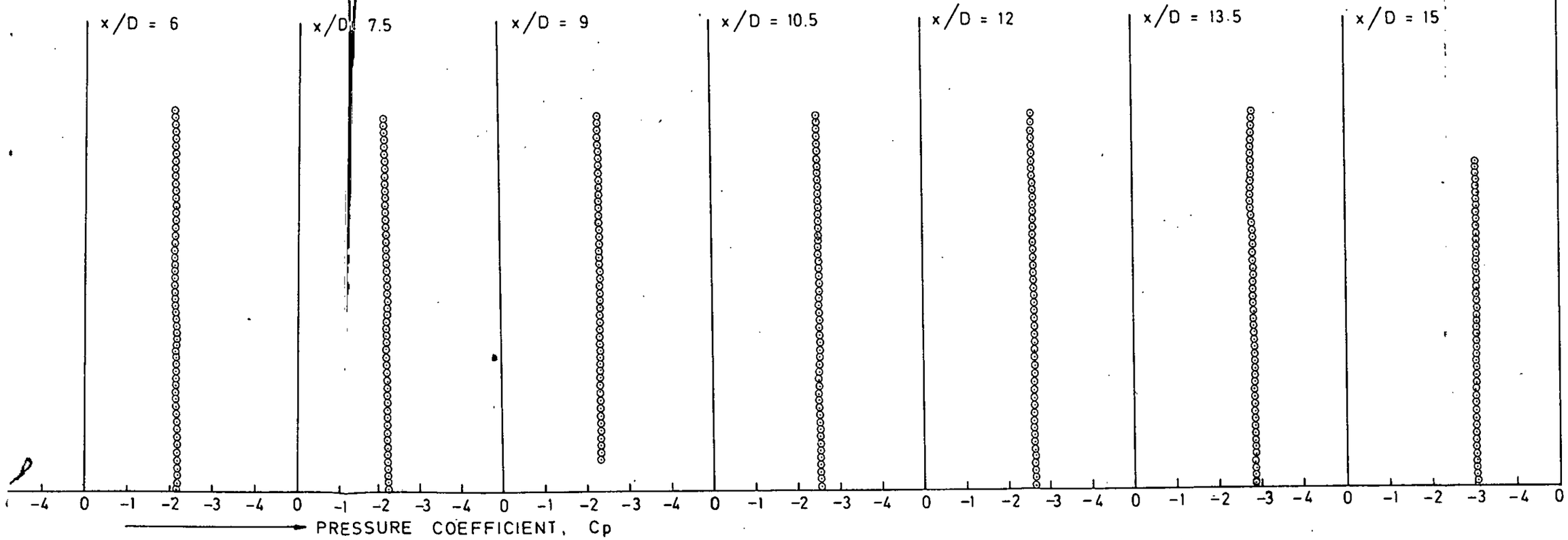

DIFFERENT AXIAL DISTANCES.

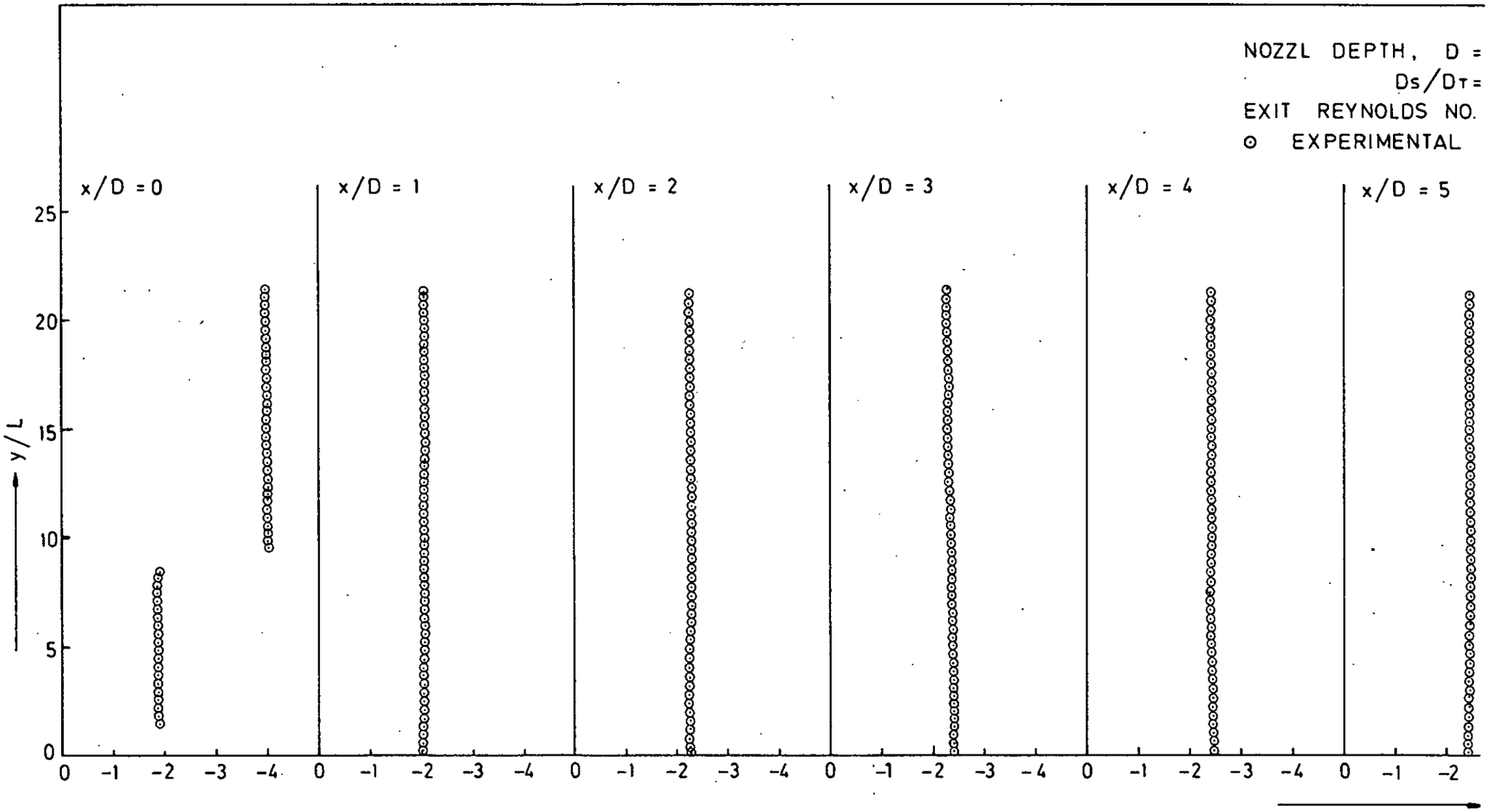

FIG. 3.14 DISTRIBUTION OF THE PRESSURE COEFFICIENT IN THE JET AT DIFFERENT AXIAL DISTANCES.

DEPTH, D = 6 IN. (15.24 CM)
Ds/DT = 0.5694
EYNOLDS NO. 2.27×10^5
ERIMENTAL

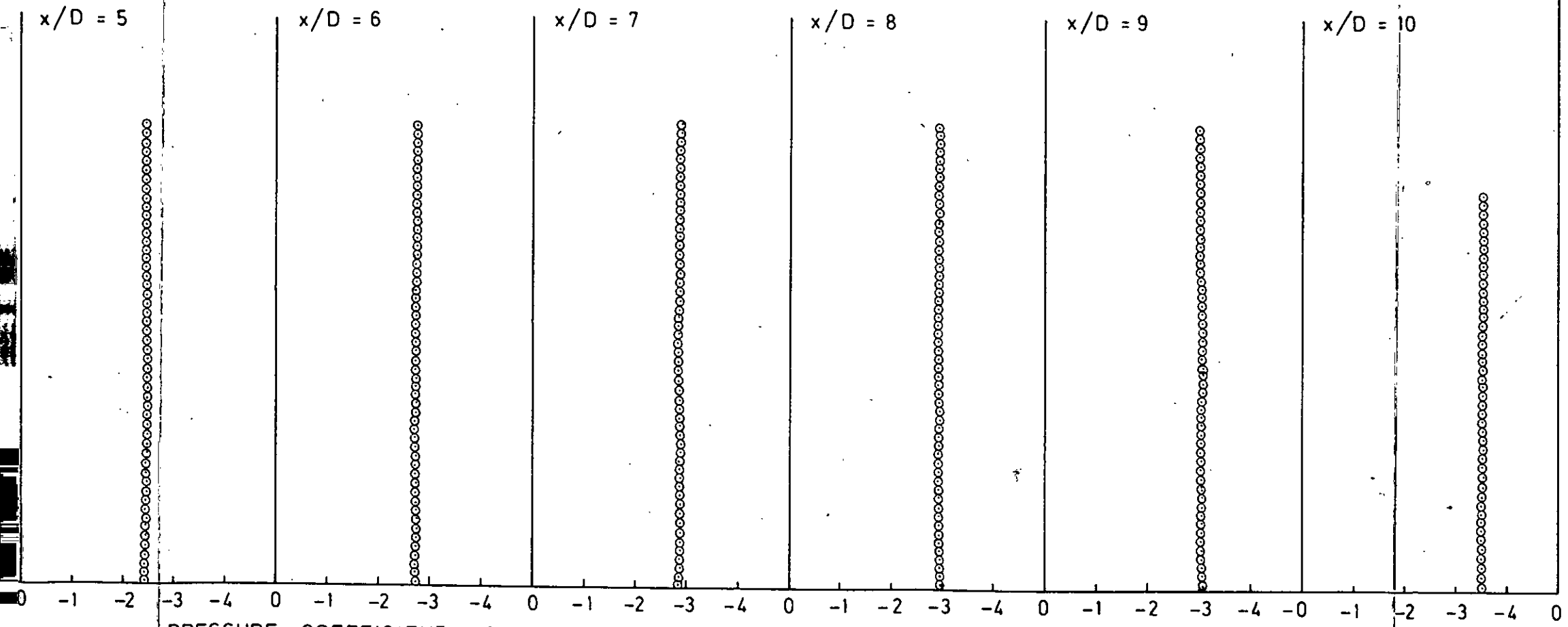

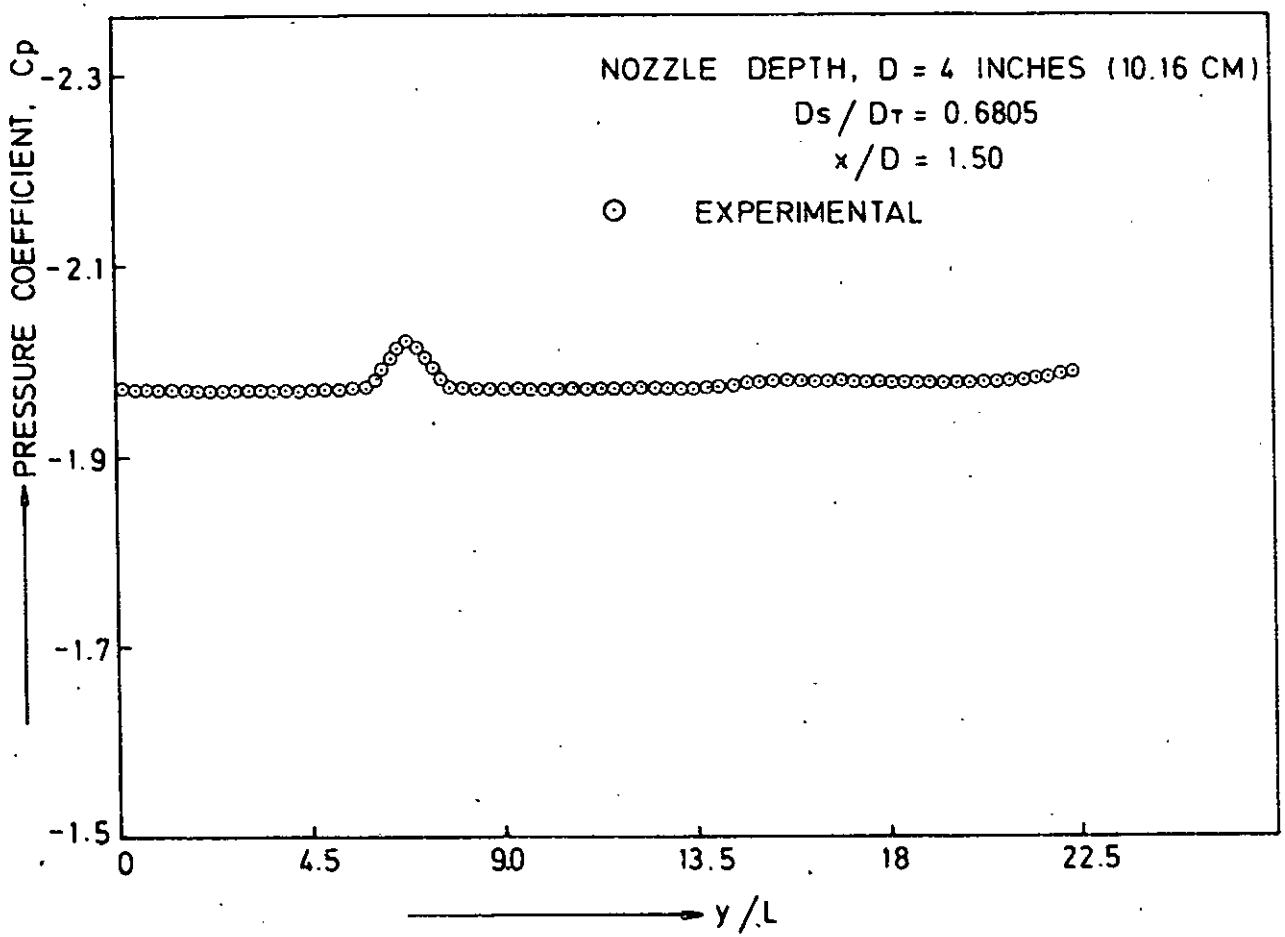

FIG. 3.15 DISTRIBUTION OF THE PRESSURE COEFFICIENT IN THE JET.

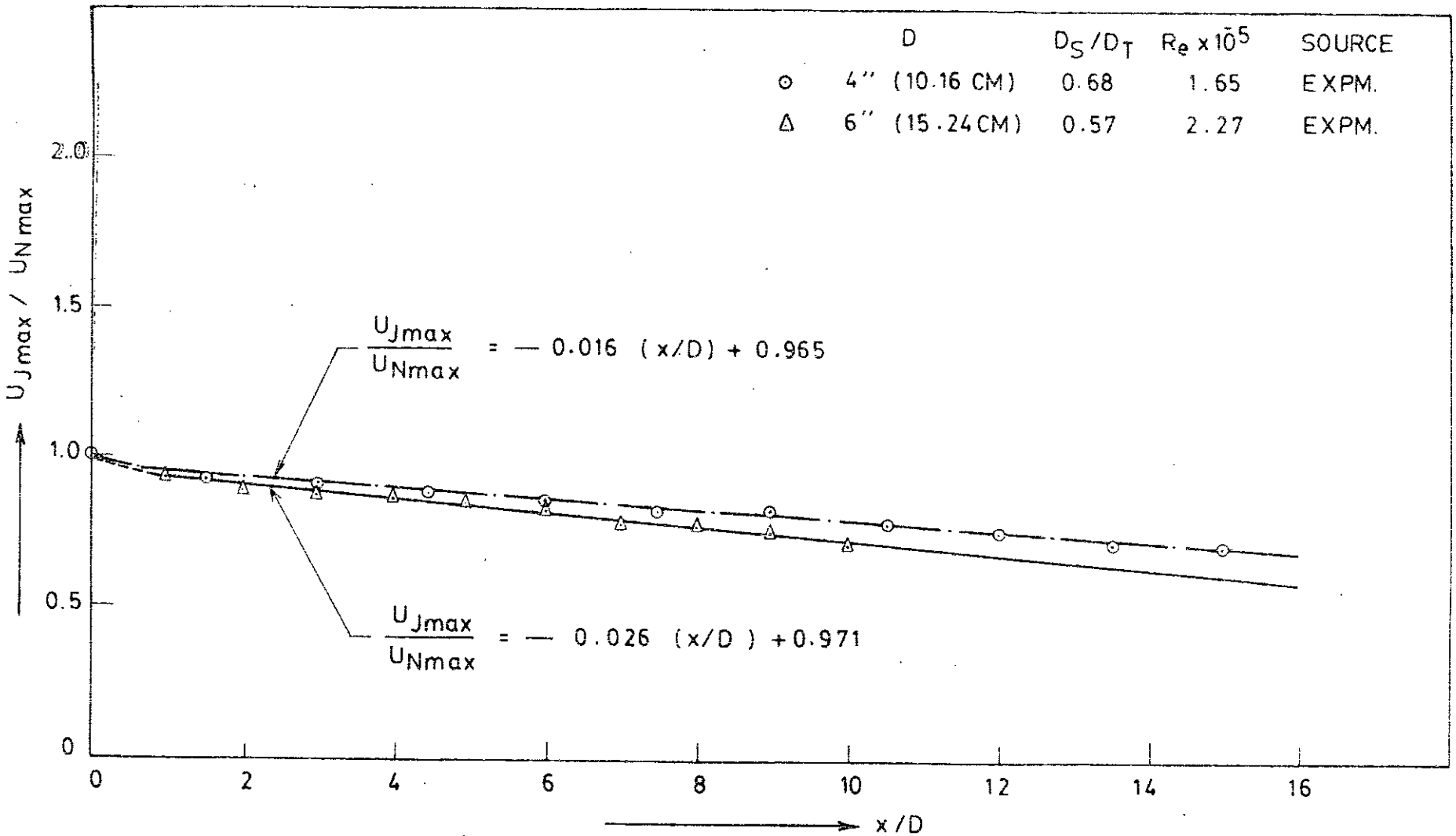

FIG. 3.16 MAXIMUM MEAN AXIAL VELOCITY DISTRIBUTION IN THE JET ALONG THE AXIAL DIRECTION.

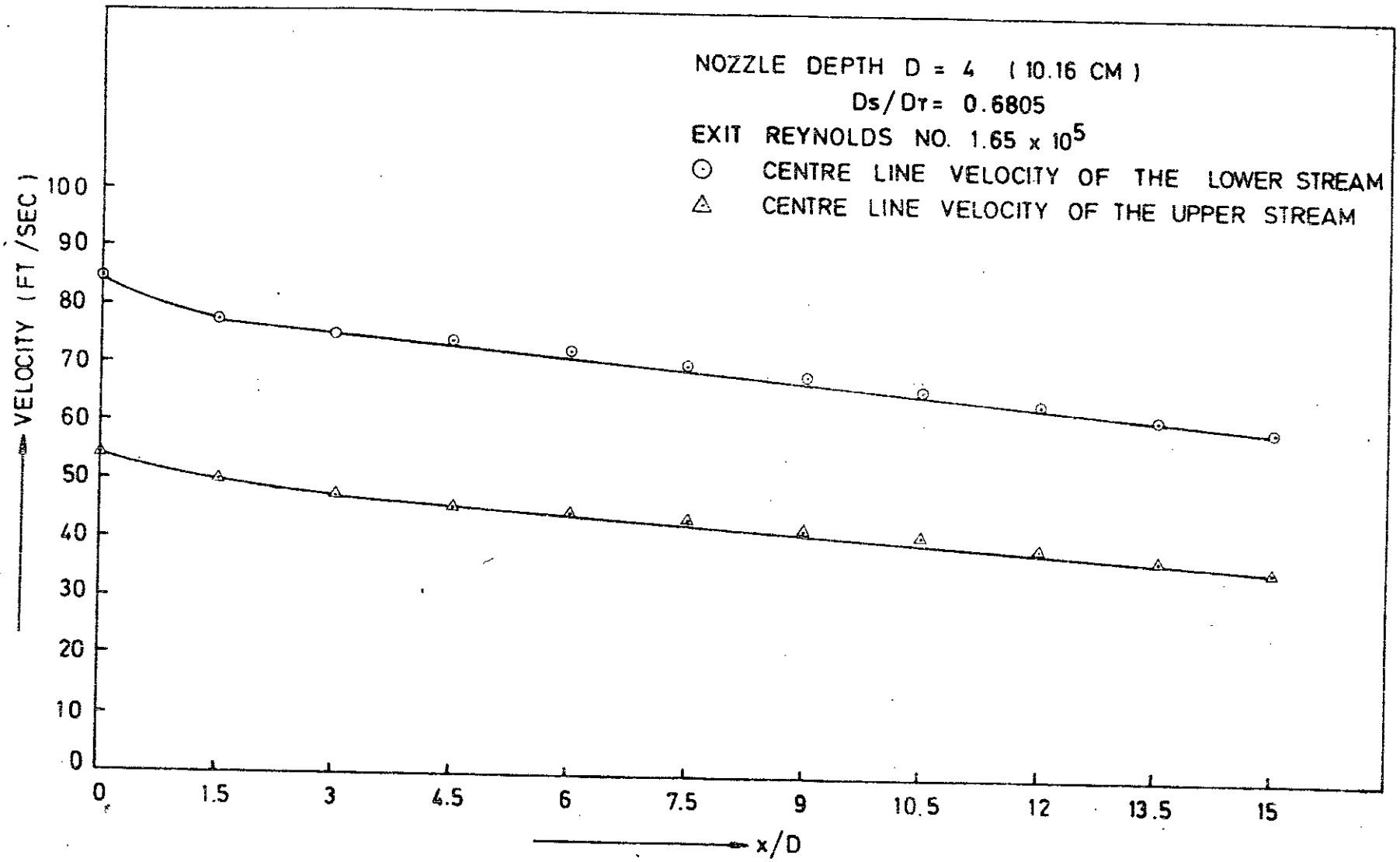

FIG. 3.17 MAXIMUM MEAN AXIAL VELOCITY DISTRIBUTION IN THE TWO STREAMS ALONG THE AXIAL DIRECTION.

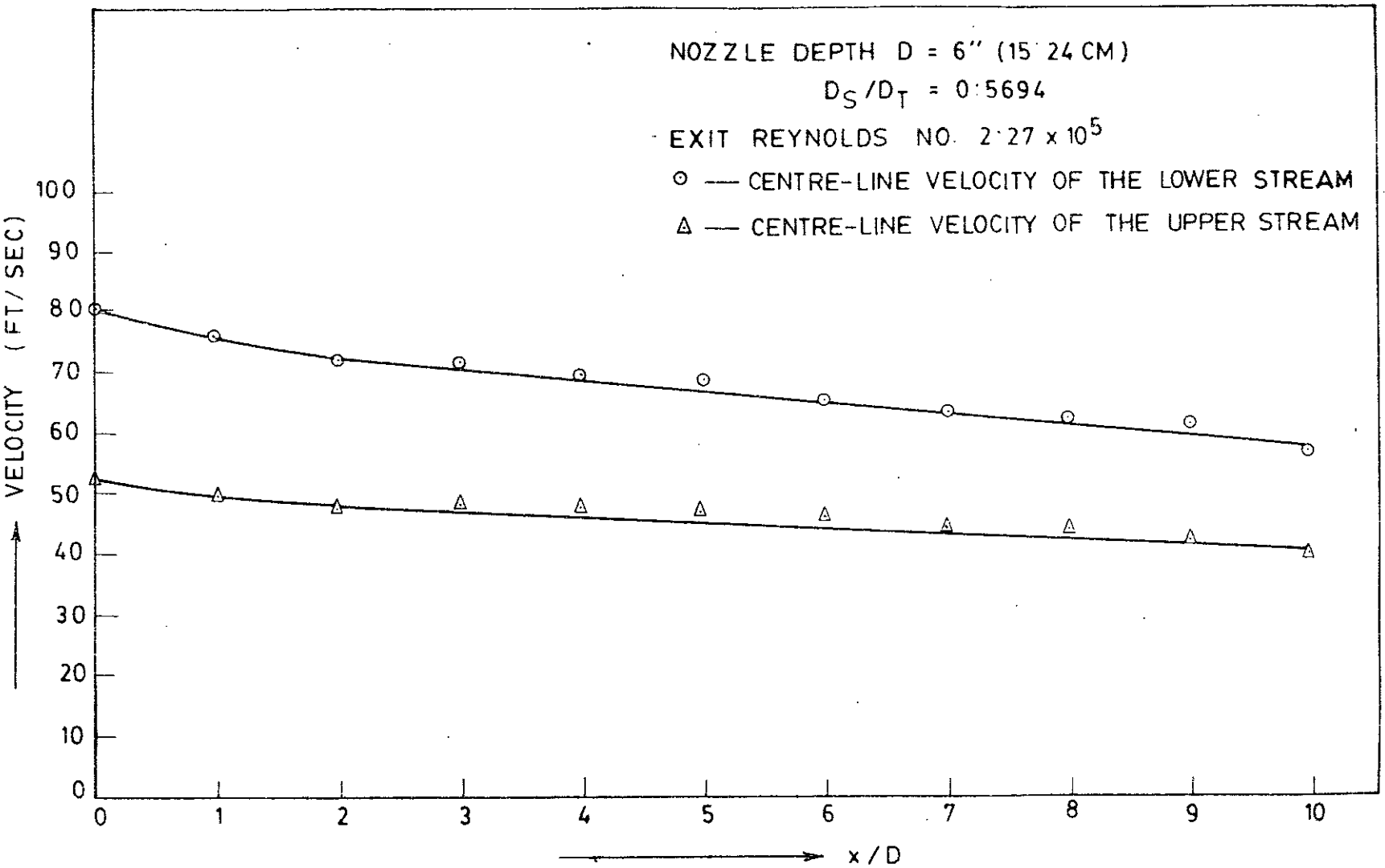

FIG. 3.18 MAXIMUM MEAN AXIAL VELOCITY DISTRIBUTION IN THE TWO STREAMS ALONG THE AXIAL DIRECTION.

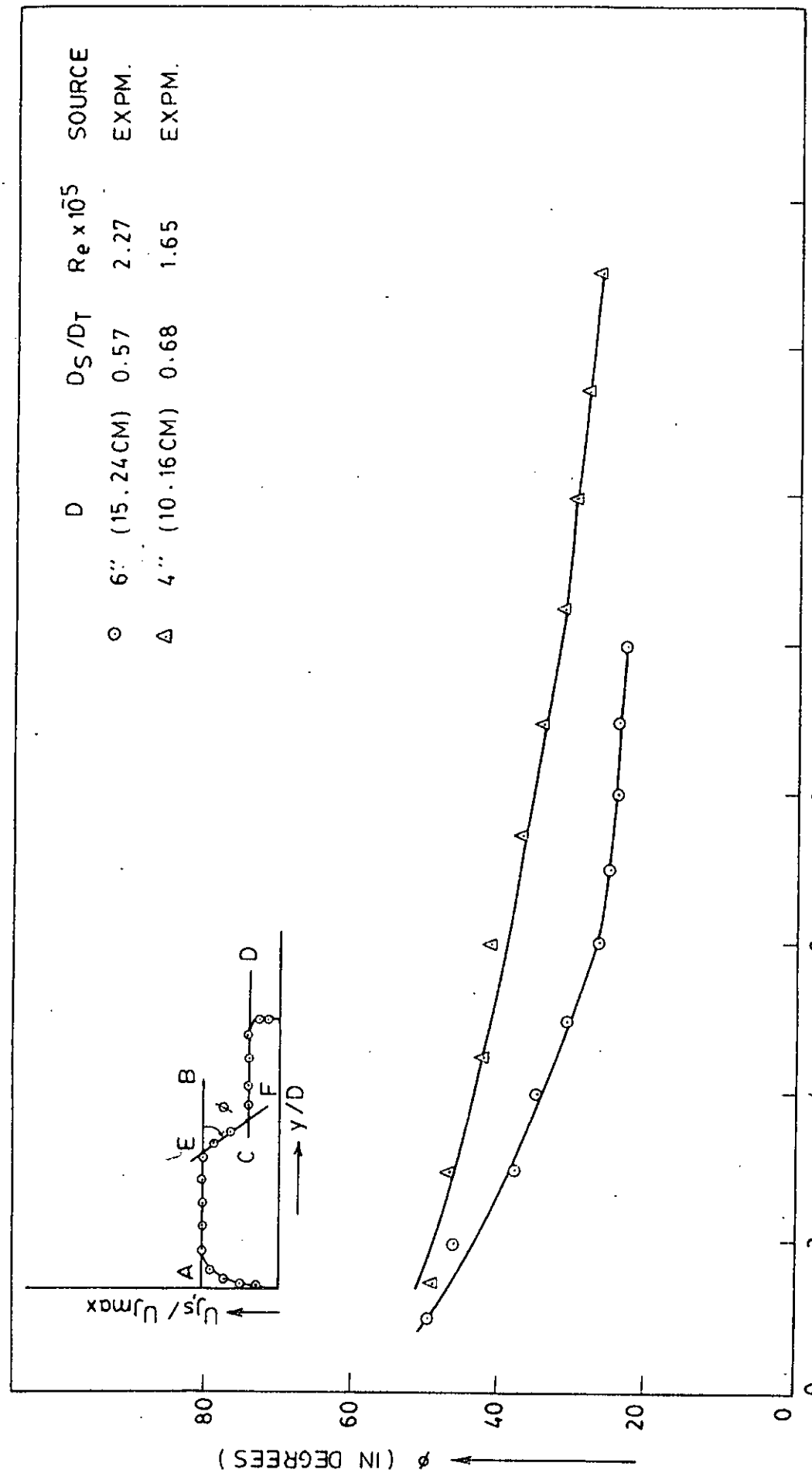

FIG. 3.19 VARIATION OF THE SLOPE OF THE MIXING PROFILE ALONG THE AXIAL DIRECTION.

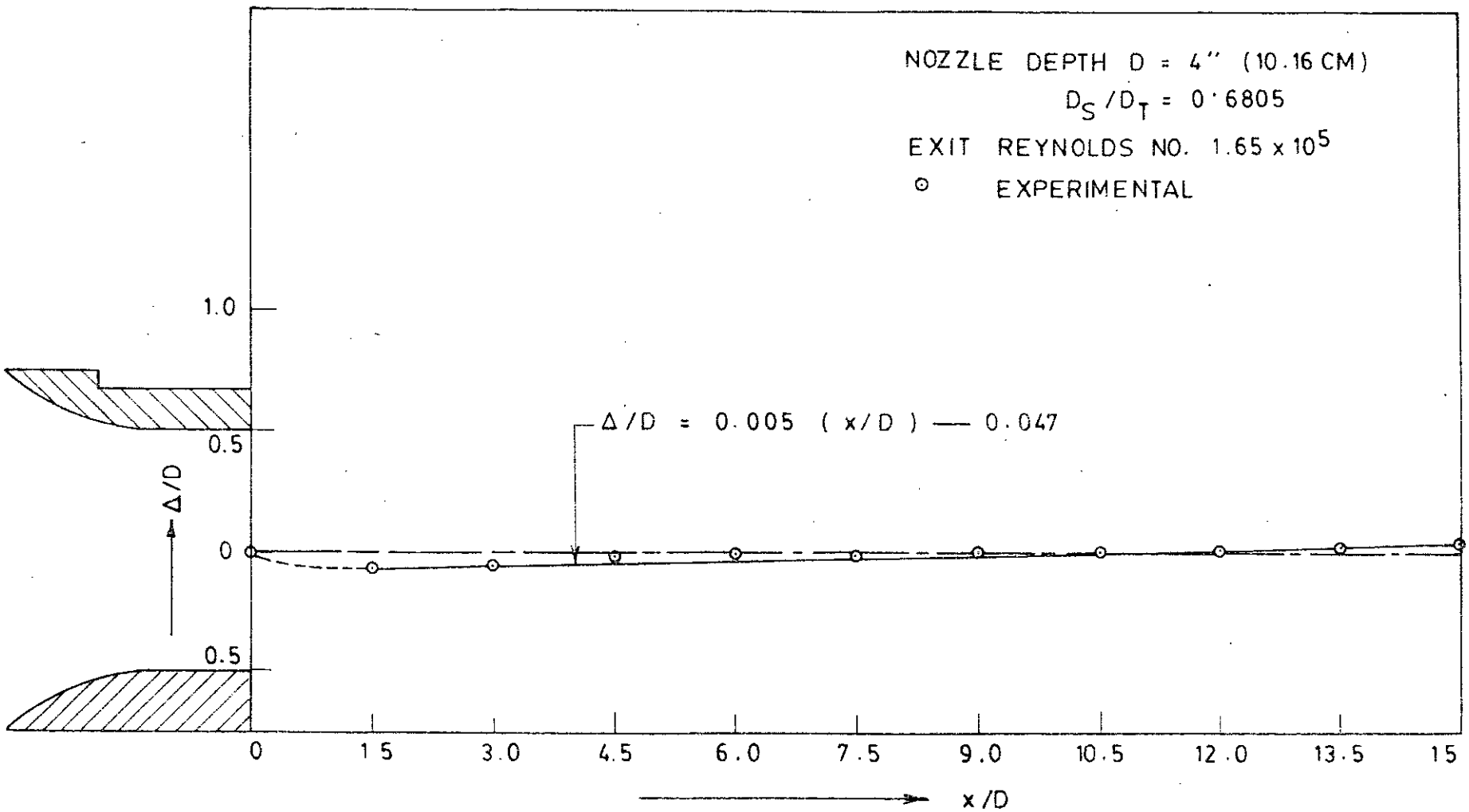

FIG. 3.20 DEVIATION OF THE CENTRE OF THE JET VELOCITY PROFILE FROM THE GEOMETRIC CENTRE LINE OF THE NOZZLE ALONG THE JET AXIS.

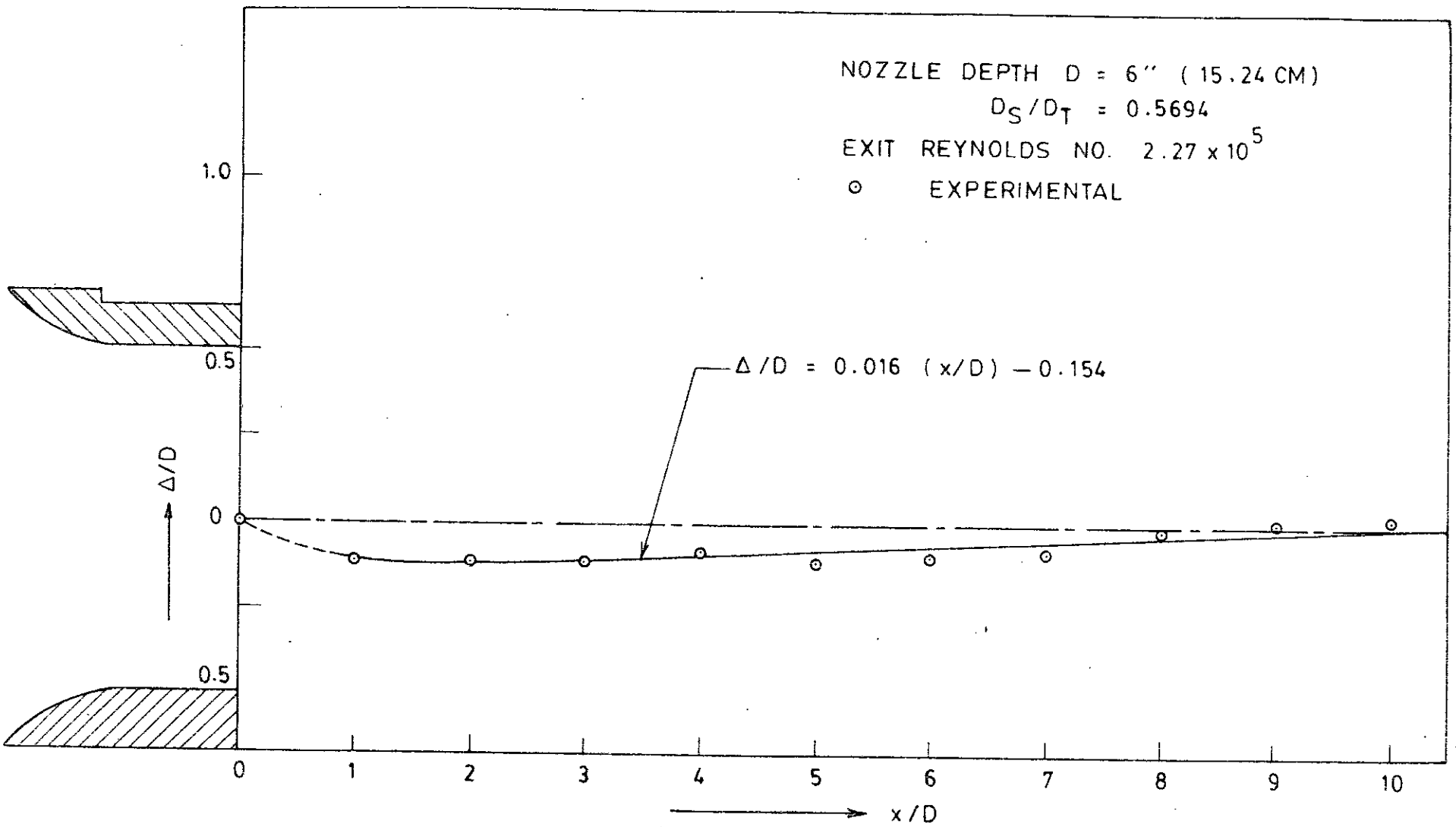

FIG. 3.21 DEVIATION OF THE CENTRE OF THE JET VELOCITY PROFILE FROM THE GEOMETRIC CENTRE LINE OF THE NOZZLE ALONG THE JET AXIS.

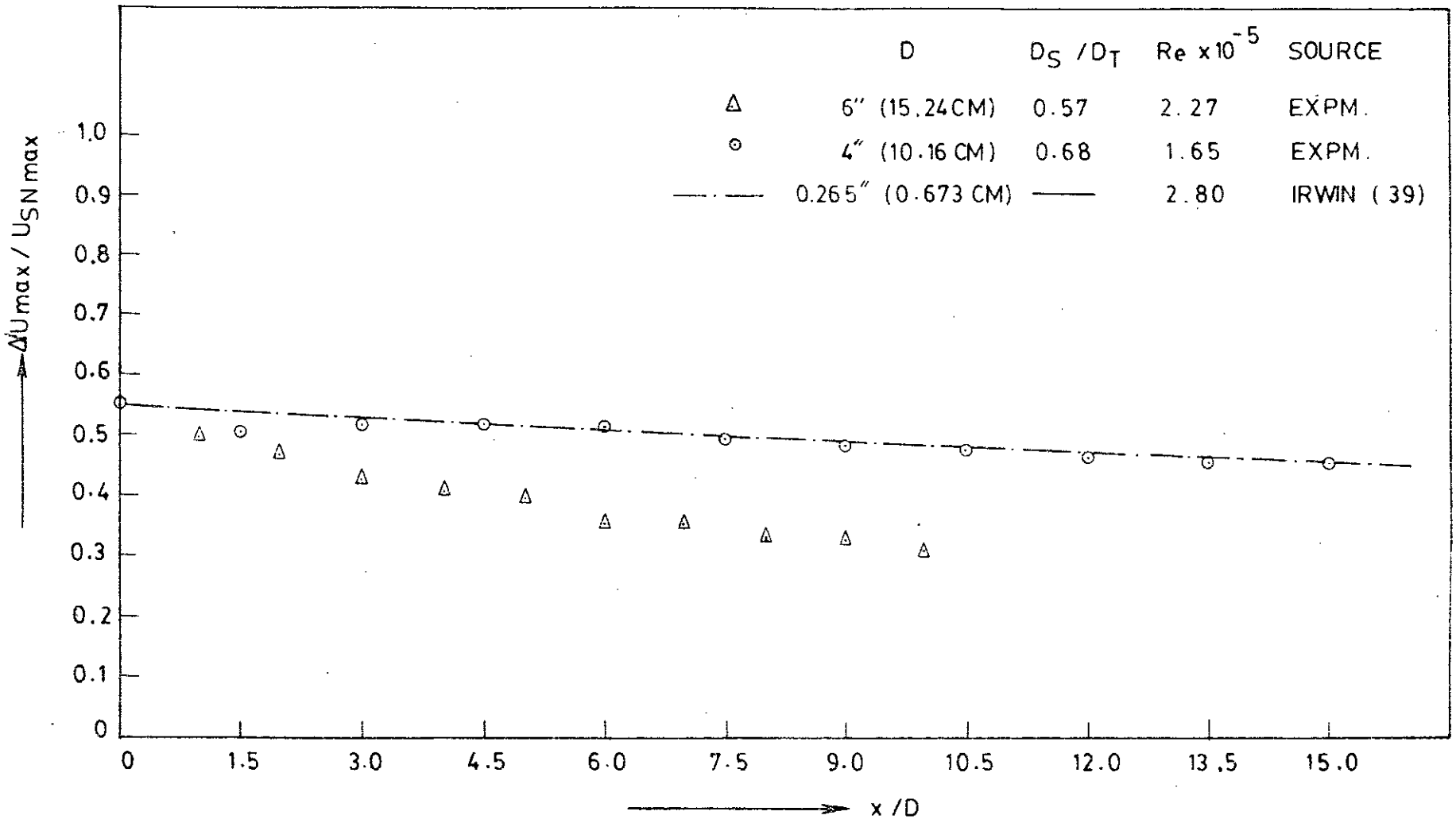

FIG. 3.22 EXCESS MEAN AXIAL VELOCITY DISTRIBUTION IN THE JET ALONG THE AXIAL DIRECTION.

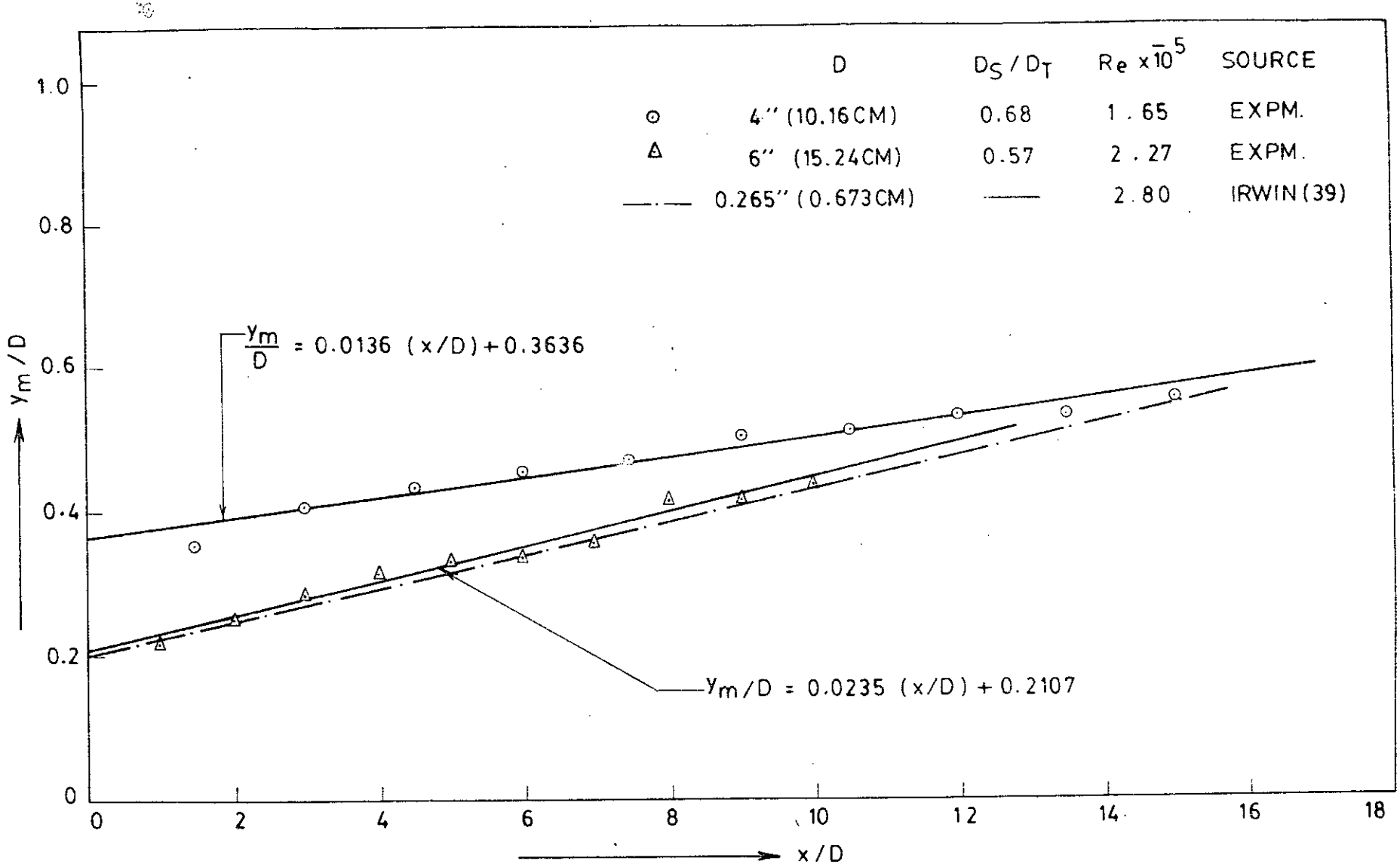

FIG. 3.23 VARIATION OF THE WIDTH FOR MAXIMUM VELOCITY ALONG THE AXIAL DIRECTION.

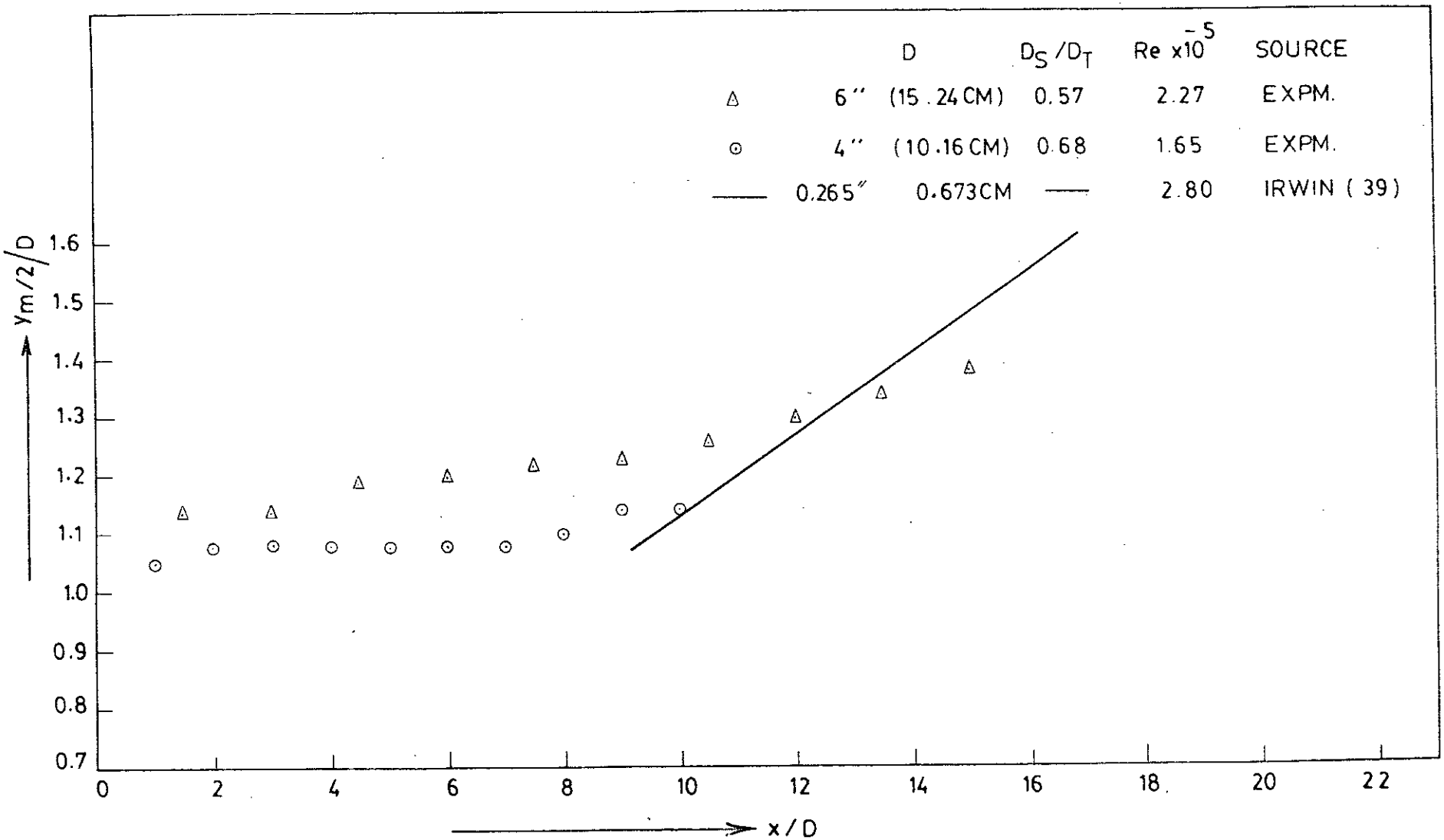

FIG. 3.24 VARIATION OF HALF WIDTH OF THE JET ALONG THE AXIAL DIRECTION

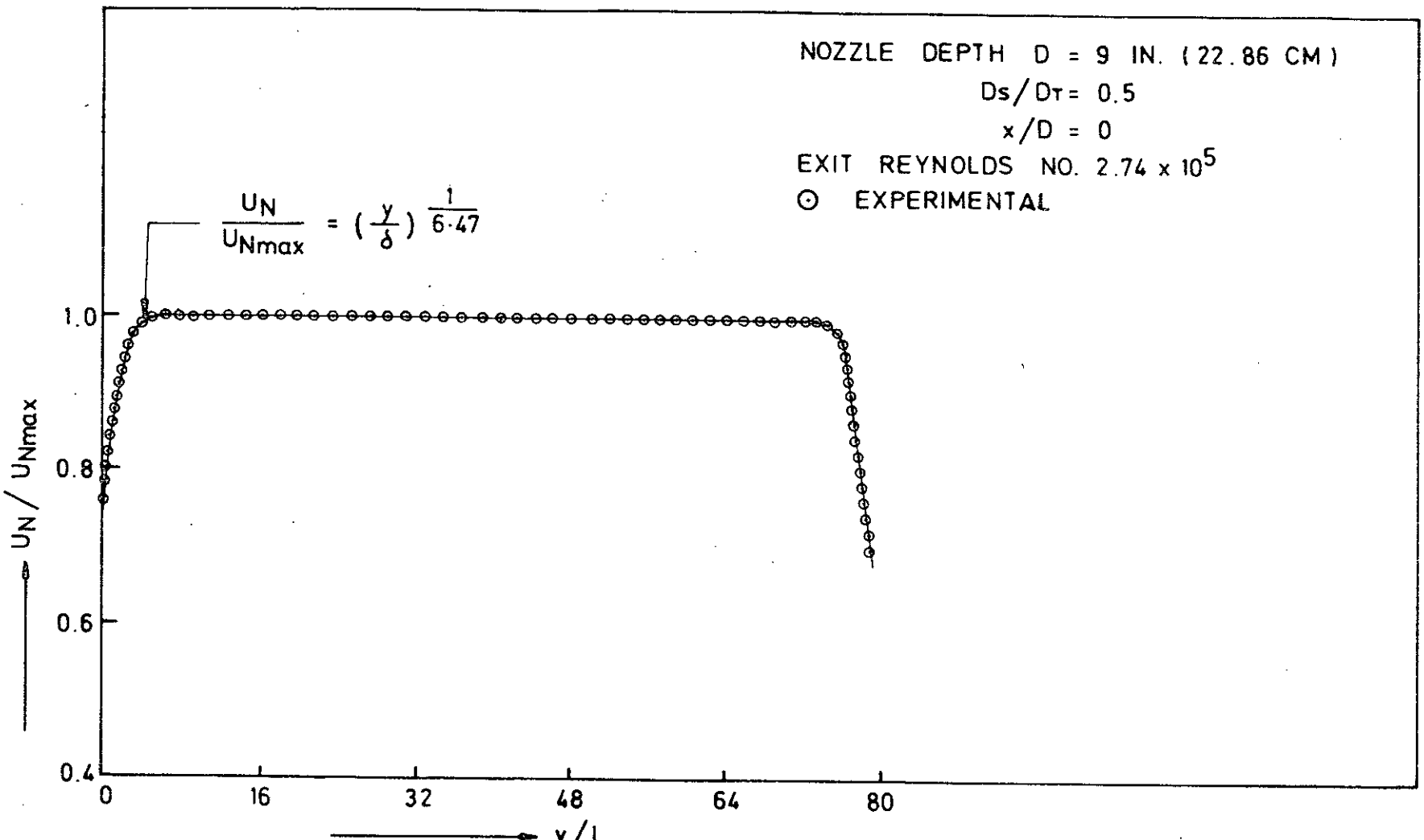

FIG. 3.25 MEASURED MEAN AXIAL VELOCITY DISTRIBUTION IN THE NOZZLE AT THE EXIT PLANE.

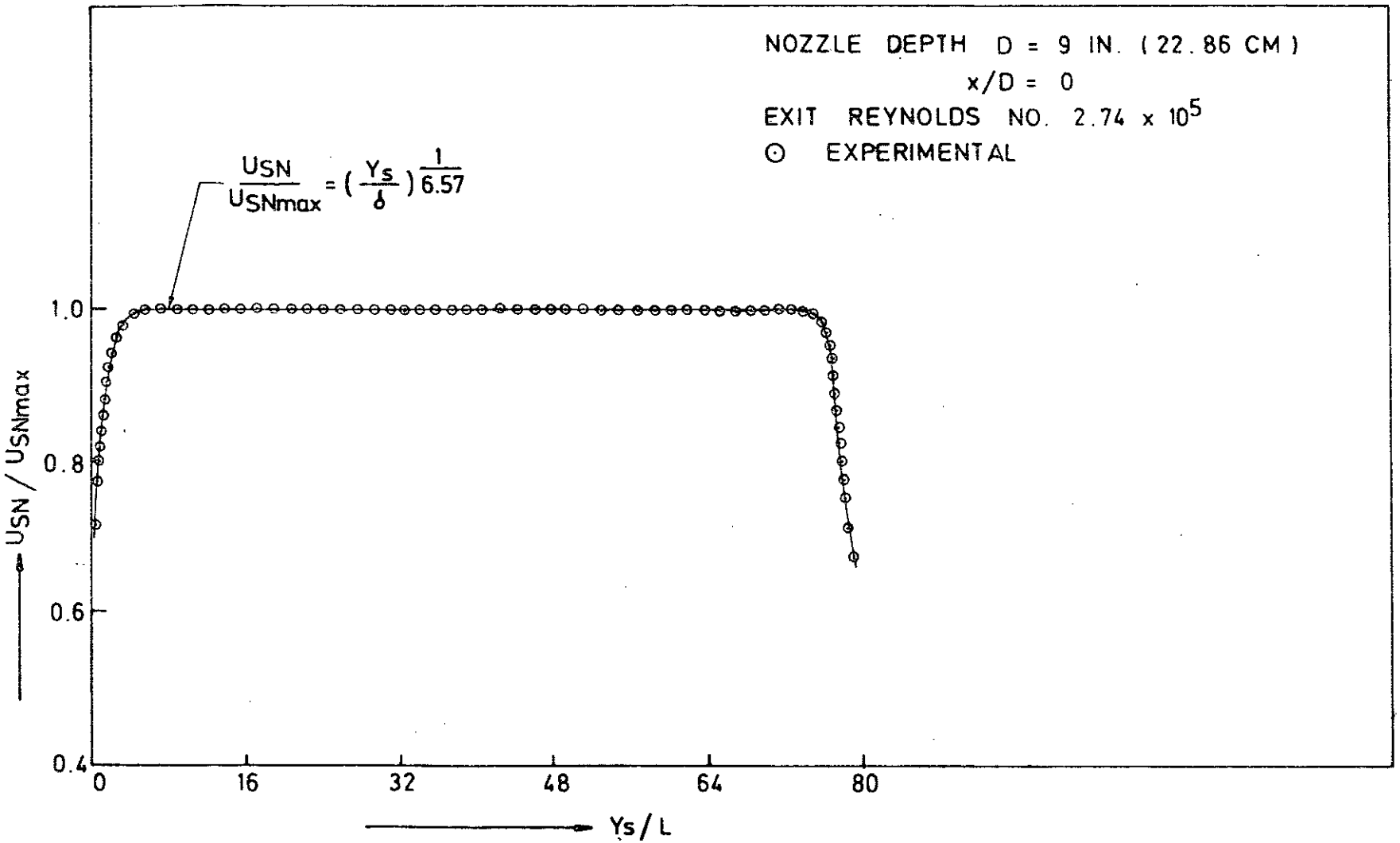

FIG. 3.26 MEASURED MEAN AXIAL VELOCITY DISTRIBUTION IN THE SUPERIMPOSING CHANNEL AT THE EXIT PLANE.

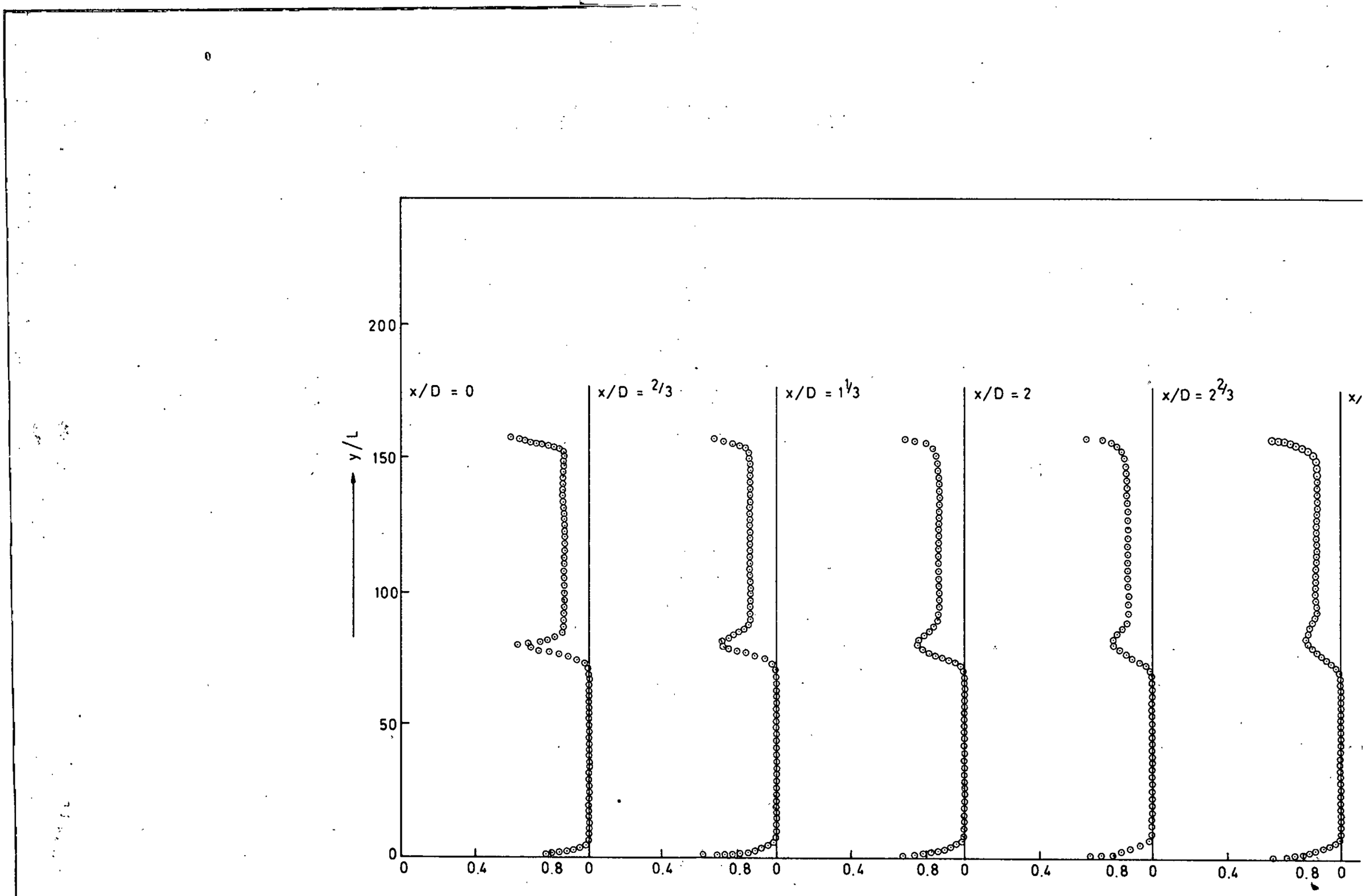

FIG. 3.27 MEASURED MEAN AXIAL VELOCITY DISTRIBUTION IN THE STREAMS AT DIFFERENT AXIAL

NOZZLE DEPTH D = 9 IN. (22.86 CM)
D_s / D_T = 0.5
EXIT REYNOLDS NO. 2.74×10^5
⊙ EXPERIMENTAL

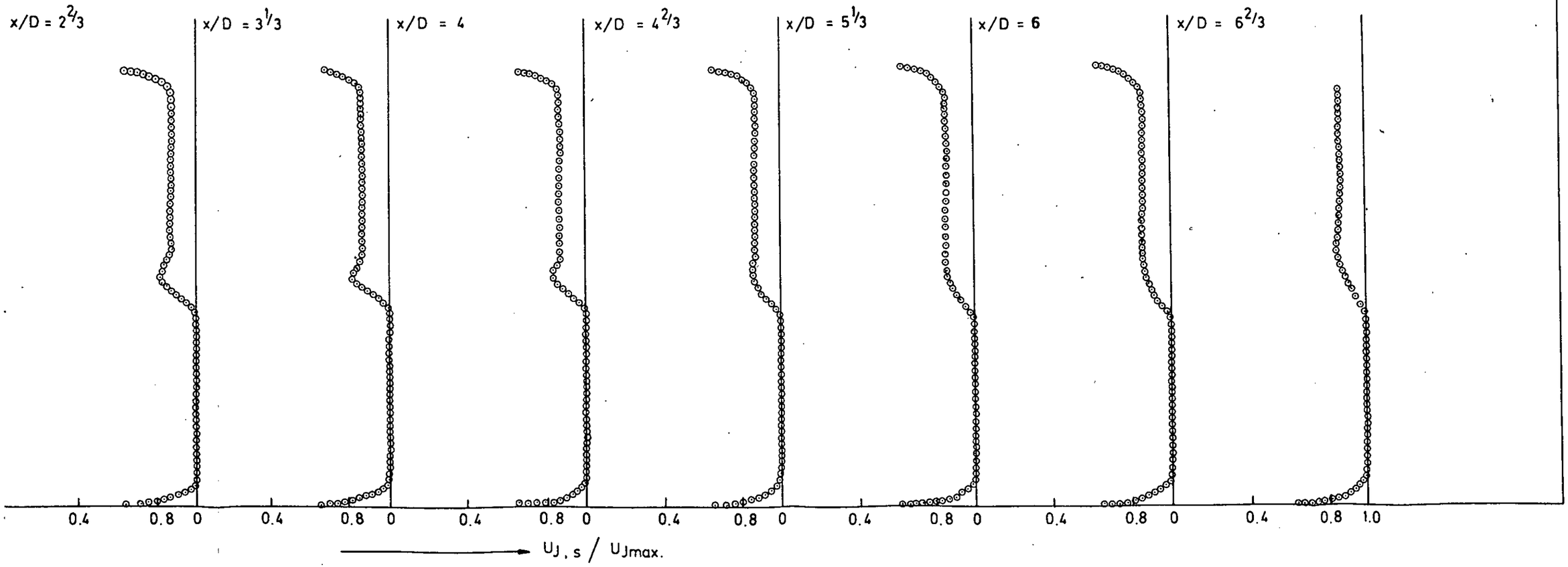

T DIFFERENT AXIAL DISTANCES.

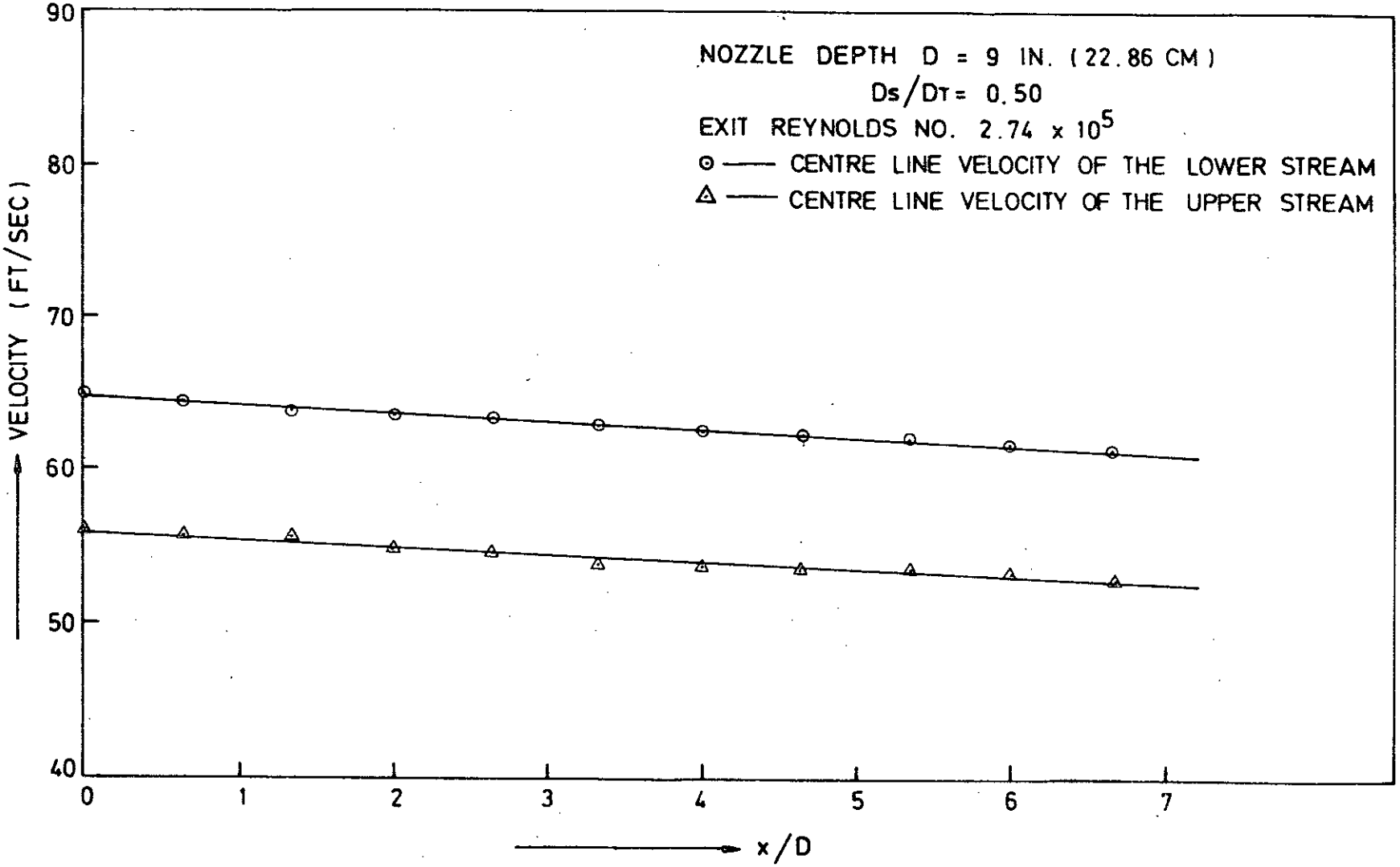

FIG. 3.28 MAXIMUM MEAN AXIAL VELOCITY DISTRIBUTION IN THE TWO STREAMS ALONG THE AXIAL DIRECTION.

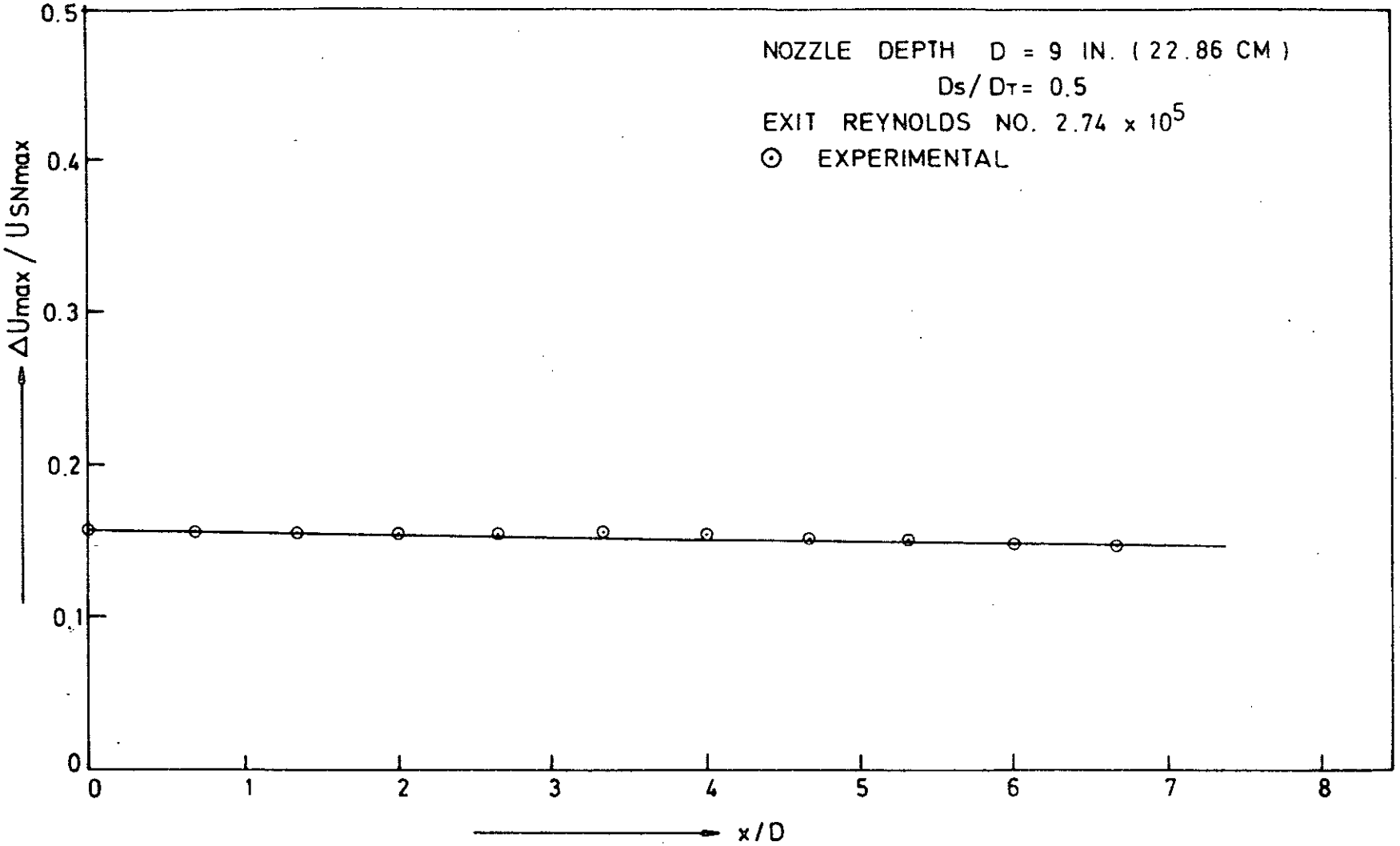

FIG. 3.29 EXCESS MEAN AXIAL VELOCITY DISTRIBUTION IN THE STREAMS ALONG THE AXIAL DIRECTION.

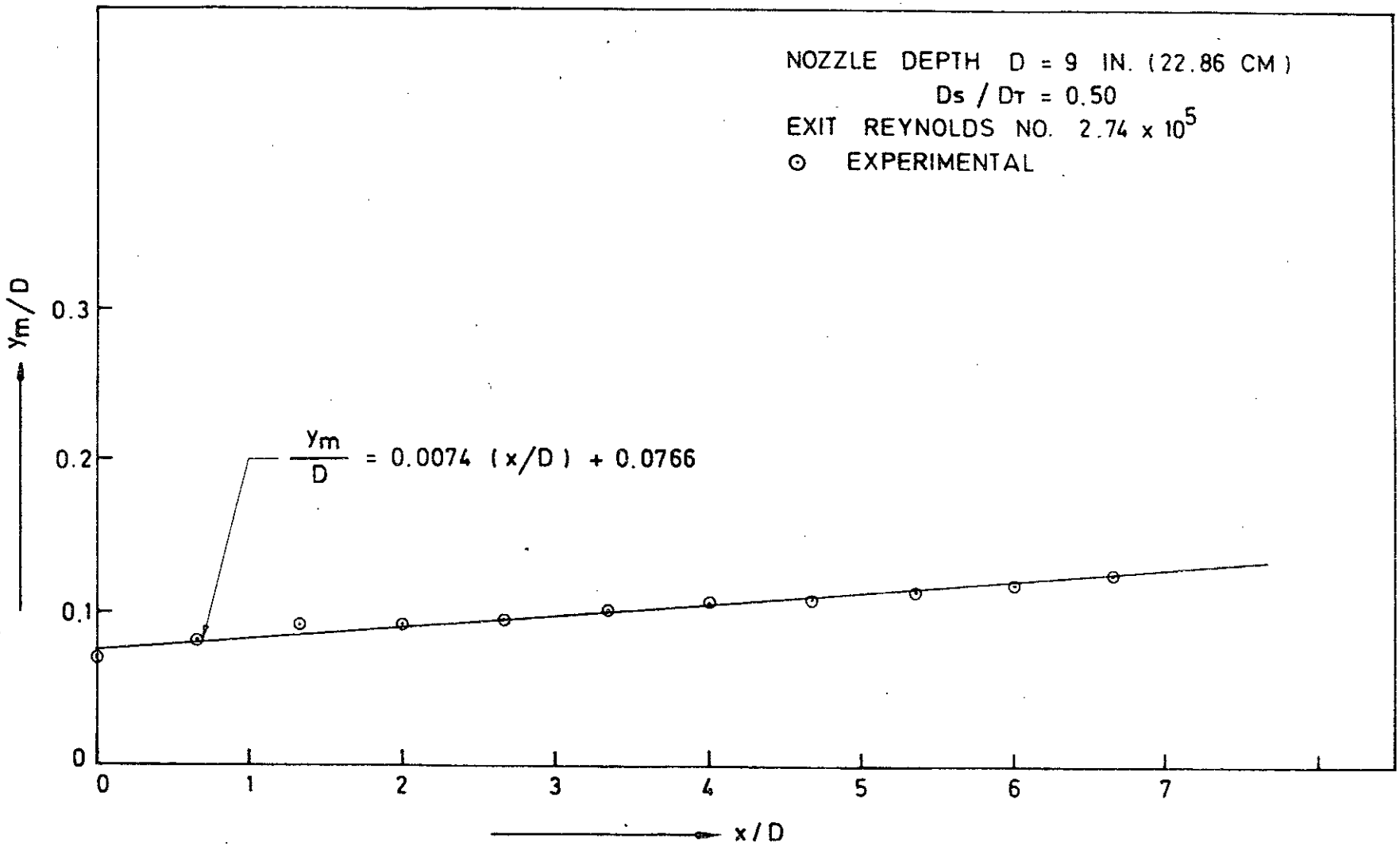

FIG. 3.30 VARIATION OF THE WIDTH FOR MAXIMUM VELOCITY ALONG THE AXIAL DIRECTION.

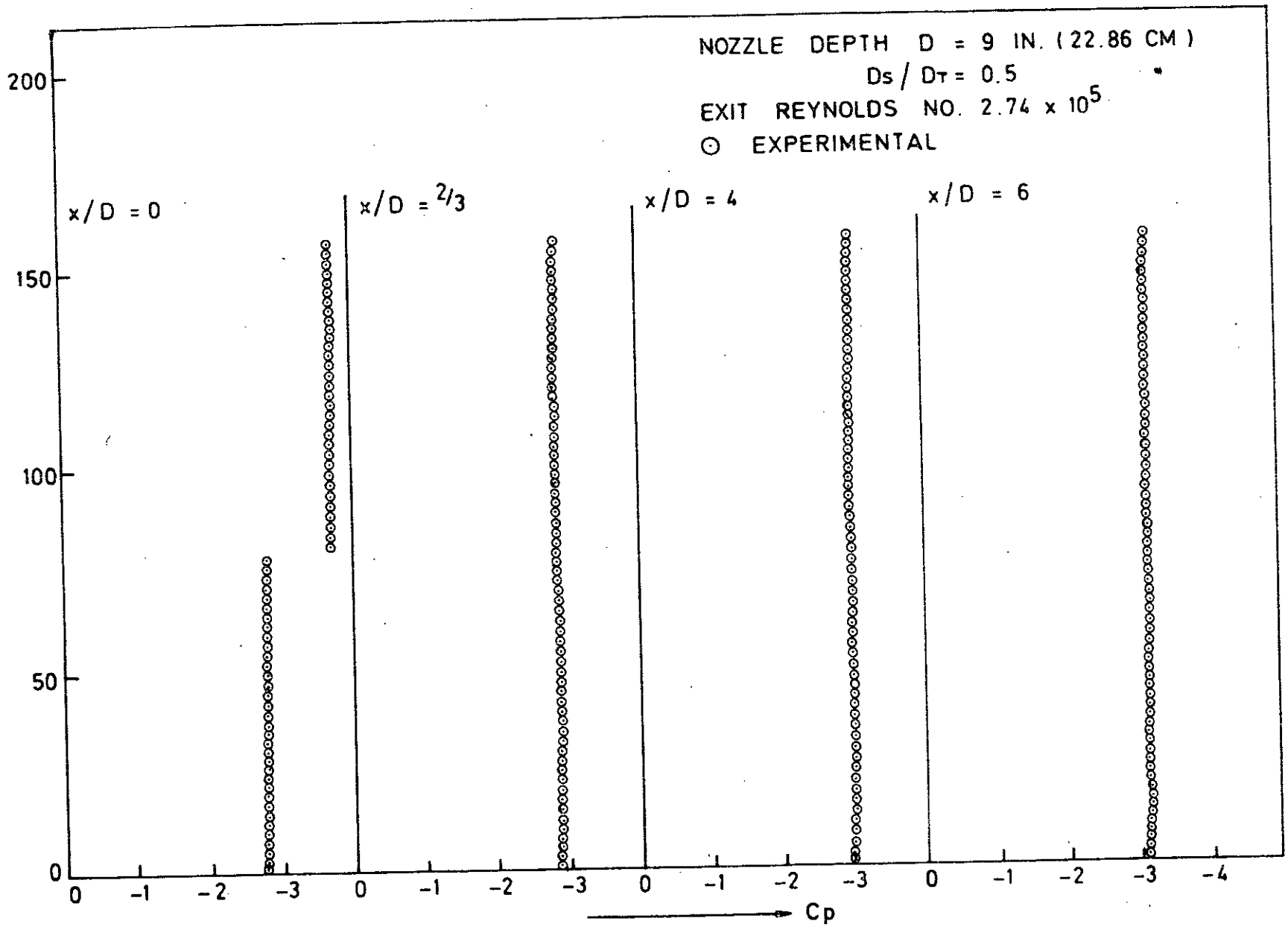

FIG. 3.31 DISTRIBUTION OF THE PRESSURE COEFFICIENT IN THE STREAMS AT DIFFERENT AXIAL DISTANCES.

A P P E N D I C E S

APPENDIX - I

THE PARTICULARS OF THE WIND TUNNEL

The Converging Section :

Length of the duct : 5 ft (152.4 cm)

Ratio of contraction : 5 : 1

Wide side dimension : 40" x 40" (101.6 cm x 101.6 cm)

Contraction side dimension : 18" x 18" (45.72 cm x 45.72 cm)

Material Used : 15 SWG - Black sheet.

The flow Straighteners :

Made of : Iron wire net

Mesh size : 16 holes / inch.

The Test Section :

Length of the duct : 10 ft 8 inches (325.12 cm)

Area of cross section : 18 in. x 18 in. (45.72 cm x 45.72 cm)

Material used : Perspex, Wood and G. I. Sheet.

The Diverging Section :

Length of the duct : 15 ft 6 inches (472.44 cm)

Angle of divergence of the duct : 6^{o}

Material used : 15 SWG - black sheet.

The Fan :

Type : Contra - rotating multistage axial flow fan

Capacity : 30,000 cfm (849.51 m^3 / minute)

Head for free delivery : 6 inches (15.24 cm) of water

Two stage L - type aerofoil fan

with pitch angle : $31 / 27^{o}$

Diameter : 38 in. (96.52 cm)

Speed of the rotor : 1475 rpm

Electric supply : 400 / 50 Hz / 3 ph.

Manufacturer : Woods of Colchester Ltd., England.

Code No. : 38J TE

Frame Size : AF 4049.

APPENDIX - II

UNCERTAINTY ANALYSIS

i) Uncertainty for Velocity Measurements

Let an air stream of density ρ_a (slug/ft^3) flow with a velocity V (ft/sec). A pitot-static tube is placed parallel to the flow, and the dynamic head is measured by a manometer reading h (ft). Let the density of the liquid used in the manometer be ρ_l (slug/ft^3).

$$\therefore \quad \tfrac{1}{2} \rho_a V^2 = h \rho_l g \tag{1}$$

$$\text{or,} \quad V^2 = 2(\rho_l / \rho_a)\, hg$$

$$\text{or,} \quad V = \sqrt{2g(\rho_l/\rho_a)\, h}$$

$$\text{or,} \quad V = \sqrt{2g(W_1/W_a)\, h} \tag{2}$$

where W_1 and W_a are the specific weights (lb/ft^3) of the liquid and air respectively. Suppose the sensing point of the pitot-static tube is deviated by an angle θ from the direction of flow due to wrong adjustment. Then the measured velocity will be given by

$$V = \sqrt{2g(W_1/W_a)\, h}\, \cos\theta \tag{3}$$

But we know that

$$Pa = W_a RT \tag{4}$$

where Pa, R and T are the pressure, the gas constant and the absolute temperature of a gas respectively.

From eqns (3) and (4) we get

$$V = \sqrt{\frac{2g \times 62.45\ sh}{(Pa/RT)}} \cos\theta \qquad (5)$$

where s is the specific gravity of the liquid.

or, $V = \sqrt{2gR \times 62.45}\ \sqrt{\frac{shT}{Pa}} \cos\theta$

or, $V = \sqrt{\frac{2gR \times 62.45}{12}}\ \sqrt{\frac{shT}{Pa}} \cos\theta$ if the manometer reading is taken in inches.

$$V = C \sqrt{\frac{shT}{Pa}} \cos\theta \qquad (6)$$

$$\text{where } C = \sqrt{\frac{2gR \times 62.45}{12}} \qquad (7)$$

Let us now differentiate both the sides of eqn (6) with respect to s, Pa, T, h and θ respectively.

$$\frac{\partial V}{\partial s} = C \cdot \tfrac{1}{2} \left(\frac{shT}{Pa}\right)^{-\frac{1}{2}} \frac{hT}{Pa} \cos\theta = \frac{C}{2} \sqrt{\frac{hT}{sPa}} \cos\theta \qquad (8)$$

$$\frac{\partial V}{\partial Pa} = C \cdot \tfrac{1}{2} \left(\frac{shT}{Pa}\right)^{-\frac{1}{2}} shT \left(-\frac{1}{Pa^2}\right) \cos\theta = -\frac{C}{2} \sqrt{\frac{shT}{Pa^3}} \cos\theta \qquad (9)$$

$$\frac{\partial V}{\partial T} = \frac{C}{2} \left(\frac{shT}{Pa}\right)^{-\frac{1}{2}} \frac{sh}{Pa} \cos\theta = \frac{C}{2} \sqrt{\frac{sh}{TPa}} \cos\theta \qquad (10)$$

$$\frac{\partial V}{\partial h} = \frac{C}{2} \left(\frac{shT}{Pa}\right)^{-\frac{1}{2}} \frac{sT}{Pa} \cos\theta = \frac{C}{2} \sqrt{\frac{sT}{hPa}} \cos\theta \qquad (11)$$

$$\frac{\partial V}{\partial \theta} = C \sqrt{\frac{shT}{Pa}} (-\sin\theta) = -C \sqrt{\frac{shT}{Pa}} \sin\theta \qquad (12)$$

Let U_V be the uncertainty in the result, and U_s, U_{Pa}, U_T, U_h and U_θ be the uncertainties in the specific gravity, pressure, temperature, manometer reading and angle of deviation respectively.

$$\therefore U_V = \left[\left(\frac{\partial V}{\partial s} U_s\right)^2 + \left(\frac{\partial V}{\partial Pa} U_{Pa}\right)^2 + \left(\frac{\partial V}{\partial T} U_T\right)^2 + \left(\frac{\partial V}{\partial h} U_h\right)^2 + \left(\frac{\partial V}{\partial \theta} U_\theta\right)^2 \right]^{\frac{1}{2}} \quad (13)$$

Combining eqns (8) to (13) we get

$$U_V = \left[\frac{C^2}{4} \frac{hT}{Pa^s} \cos^2\theta \, U_s^2 + \frac{C^2}{4} \frac{shT}{Pa^3} \cos^2\theta \, U_p^2 + \frac{C^2}{4} \frac{sh}{TPa} \cos^2\theta \, U_T^2 + \frac{C^2}{4} \frac{sT}{hPa} \cos^2\theta \, U_h^2 + C^2 \frac{shT}{Pa} \sin^2\theta U_\theta^2 \right]^{\frac{1}{2}}$$

$$\text{or, } U_V = \left[\frac{C^2}{4} \cos^2\theta \left\{ \left(\frac{hT}{Pas}\right) U_s^2 + \left(\frac{shT}{Pa^3}\right) U_{Pa}^2 + \left(\frac{sh}{TPa}\right) U_T^2 + \left(\frac{sT}{hPa}\right) U_h^2 + 4\left(\frac{shT}{Pa}\right) \tan^2\theta \, U_\theta^2 \right\} \right]^{\frac{1}{2}}$$

$$\text{or, } U_V = \frac{C.\cos\theta}{2} \left[\left(\frac{hT}{Pa^s}\right) U_s^2 + \left(\frac{shT}{Pa^3}\right) U_{Pa}^2 + \left(\frac{sh}{TPa}\right) U_T^2 + \left(\frac{sT}{hPa}\right) U_h^2 + 4\left(\frac{shT}{Pa}\right) U_\theta^2 \tan^2\theta \right]^{\frac{1}{2}} \quad (14)$$

Combining eqns (6) and (14)

$$\frac{U_V}{V} = \frac{1}{2} \left[\frac{U_s^2}{s^2} + \frac{U_{Pa}^2}{Pa^2} + \frac{U_T^2}{T^2} + \frac{U_h^2}{h^2} + 4 U_\theta^2 \tan^2\theta \right]^{\frac{1}{2}} \quad (15)$$

Putting

$s = 0.834 \pm 0.025$

$h = 1.48$ in. $\pm$ 0.01 in.

$Pa = 29.85$ in. $\pm$ 0.1 in. of Hg

$T = 28^{\circ}C \pm 2^{\circ}C$

$\theta = 0^{\circ} \pm 3^{\circ}$

$\frac{U_V}{V} = 0.0158$ i.e. 1.58%

ii) Uncertainty for Pressure Measurements

Let

Pa = atmospheric static pressure

P = static pressure in the stream

Pr = relative static pressure (= Pa - P)

Now,

$$Pr = W_1 h - \frac{W_a V^2}{2g} \cos^2 (90 - \theta)$$

or, $$Pr = W_1 h - \frac{W_a V^2}{2g} \sin^2 \theta$$

or, $$Pr = 62.4\, sh - \frac{PaV^2}{2RTg} \sin^2 \theta$$

or, $$Pr = \frac{62.4}{12} sh - \frac{PaV^2}{2RTg} \sin^2 \theta$$ if h is measured in inches.

or, $$Pr = C_1\, sh + C_2 \frac{PaV^2}{T} \sin^2 \theta \qquad (16)$$

where $C_1 = \frac{62.4}{12} = 5.2$ (17)

$$C_2 = \frac{1}{-2Rg} = -\frac{1}{2 \times 53.3 \times 32.2} = -2.913 \times 10^{-4} \quad (18)$$

Let $Pr = P_1 + P_2$ (19)

Comparing eqns (16) and (19)

$$P_1 = C_1 sh \quad (20)$$

$$P_2 = C_2 \frac{PaV^2}{T} \sin^2\theta \quad (21)$$

Let U_{P_1} and U_{P_2} be the uncertainties in P_1 and P_2 respectively.

Therefore,

$$U_{P_1} = \left[\left(\frac{\partial P_1}{\partial s} U_s\right)^2 + \left(\frac{\partial P_1}{\partial h} U_h\right)^2 \right]^{\frac{1}{2}}$$

or, $$U_{P_1} = \left[(C_1 h U_s)^2 + (C_1 s U_h)^2 \right]^{\frac{1}{2}}$$

or, $$U_{P_1} = C_1 hs \left[\left(\frac{U_s}{s}\right)^2 + \left(\frac{U_h}{h}\right)^2 \right]^{\frac{1}{2}}$$

$$\therefore \frac{U_{P_1}}{P_1} = \left[\left(\frac{U_s}{s}\right)^2 + \left(\frac{U_h}{h}\right)^2 \right]^{\frac{1}{2}} \quad (22)$$

$$U_{P_2} = \left[\left(\frac{\partial P_2}{\partial Pa} U_{Pa}\right)^2 + \left(\frac{\partial P_2}{\partial V} U_V\right)^2 + \left(\frac{\partial P_2}{\partial T} U_T\right)^2 + \left(\frac{\partial P_2}{\partial \theta} U_\theta\right)^2 \right]^{\frac{1}{2}}$$

$$\text{or,}\quad U_{P_2} = \left[\left(\frac{C_2 V^2 \sin^2\theta}{T}\, U_{Pa}\right)^2 + \left(\frac{C_2 P_a 2V \sin^2\theta}{T}\, U_V\right)^2 + \left(\frac{-C_2 P_a V^2 \sin^2\theta}{T^2}\, U_T\right)^2 + \left(\frac{C_2 P_a V^2}{T}\, 2 \sin\theta \cos\theta\, U_\theta\right)^2\right]^{\frac{1}{2}}$$

$$\text{or,}\quad U_{P_2} = \frac{C_2 P_a V^2}{T} \sin^2\theta \left[\left(\frac{U_{Pa}}{Pa}\right)^2 + \left(\frac{2U_V}{V}\right)^2 + \left(\frac{U_T}{T}\right)^2 + \left(\frac{2U_\theta}{\tan\theta}\right)^2\right]^{\frac{1}{2}}$$

$$\therefore \frac{U_{P_2}}{P_2} = \left[\left(\frac{U_{Pa}}{Pa}\right)^2 + \left(\frac{2U_V}{V}\right)^2 + \left(\frac{U_T}{T}\right)^2 + \left(\frac{2U_\theta}{\tan\theta}\right)^2\right]^{\frac{1}{2}} \qquad (23)$$

Now, $Pr = P_1 + P_2$

$$\therefore U_{Pr} = \left[\left(\frac{\partial Pr}{\partial P_1} U_{P_1}\right)^2 + \left(\frac{\partial Pr}{\partial P_2} U_{P_2}\right)^2\right]^{\frac{1}{2}}$$

$$U_{Pr} = \left[U_{P_1}^2 + U_{P_2}^2\right]^{\frac{1}{2}} \qquad (24)$$

Putting

$s = 0.834 \pm 0.025$

$h = 3.07$ in. $\pm$ 0.01 in.

$Pa = 29.9$ in. $\pm$ 0.1 in.

$T = 28^\circ C \pm 2^\circ C$

$\theta = 0^\circ \pm 3^\circ$

$V = 84.16$ ft/sec. $\pm$ 1.33 ft/sec.

Eqn.(22) gives $\frac{UP_1}{P_1} = 0.03015$

$\therefore UP_1 = 0.40145$

Eqn. (23) gives $\frac{UP_2}{P_2} = 1.4139$

$\therefore UP_2 = 4.8919 \times 10^{-4}$

Eqn. (24) gives $UPr = 0.40145$

$Pr = P_1 + P_2 = 13.31399 + 3.46 \times 10^{-4} = 13.3143$

$\therefore \frac{UPr}{Pr} = 0.03015$ i.e. 3.01%

APPENDIX III

COMPUTER PROGRAMS USED FOR THE CALCULATION OF EXPERIMENTAL RESULTS.

```
C*************************************************************************
C       MAIN PROGRAM                                                     *
C       THIS PROGRAM CALCULATES THE MEAN AXIAL VELOCITY AND THE PRESSURE *
C       COEFFICIENT AT A POINT IN A WALL JET.IT USES SIMPSON'S RULE FOR  *
C       NUMERICAL INTEGRATION TO FIND THE AREA-AVERAGE AXIAL VELOCITY.THE*
C       REYNOLDS NUMBER OF THE FLOW IS CALCULATED ON THE BASIS OF AVERAGE*
C       AXIAL VELOCITY AND THE NOZZLE DEPTH.IT ALSO FINDS THE LOCATION AND*
C       MAGNITUDE OF THE MAXIMUM VELOCITY. THE EXCESS VELOCITY BETWEEN THE*
C       JET AND THE UPPER STREAM IS ALSO CALCULATED.THE TITLE,THE STATION*
C       NUMBER,THE PRESSURE,THE TEMPERATURE,THE DYNAMIC HEAD,THE STATIC  *
C       PRESSURE HEAD AND THE ORDINATE OF THE POINT MUST BE SUPPLIED AS  *
C       INPUT TO THE PROGRAM.                                            *
C       THE PROGRAM IS WRITTEN BY GAZI A. KHALIL AND EXECUTED ON THE     *
C       IBM 370-115/2 COMPUTER OF BANGLADESH UNIVERSITY OF ENGG.& TECHNOLOGY*
C*************************************************************************
0001        DIMENSION DATE(20),NUMBER(300),HEIGHT(300),HEAD(300),AIRVEL(300),
          1RATIO(300),STATIC(300),DISTAN(300),FRACTN(300),COEFCN(300),SPSELF(
          2300),SPBYSP(300),SPLAIT(300),REYIT(300),RSELF(300)
0002        NOTEST=12
0003        DO 85 LOOK=1,NOTEST
0004        READ(1,40) NTIME
0005     40 FORMAT(I3)
0006        READ(1,41) DATE
0007     41 FORMAT(20A4)
0008        WRITE(3,42) DATE
0009     42 FORMAT(/////2X,20A4)
0010        READ(1,43) NRULE
0011     43 FORMAT(I5)
CCCCCCCCCCCCCCCCCCCCCCCCCCCCCCCCCCCCCCCCCCCCCCCCCCCCCCCCCCCCCCCCCCCCCCCCC
```

```
0012              C
0013                   WRITE(3,44) NHOLE
0014                44 FORMAT(2X,' THE PITOT STATIC TUBE IS PLACED IN STATION NO.',I3)
0015                   READ(1,45) NREAD
0016                45 FORMAT(I3)
0017                   READ(1,46) PRESSR,TEMPER
0018                46 FORMAT(2F10.2)
0019                   WRITE(3,47) PRESSR
                    47 FORMAT(2X,' THE ATMOSPHERIC PRESSURE (IN INCHES OF MERCURY) IS = '
                   1,F6.2)
0020                   WRITE(3,48) TEMPER
0021                48 FORMAT(2X,' THE ATMOSPHERIC TEMPERATURE (IN DEGREES CENTIGRADE )
                   1IS = ',F6.2///)
                  CCCC   BASIC INFORMATION SUPPLY ZONE. CCCCCCCCCCCCCCCCCCCCCCCCCCCCCCC
0022                   BAKFLO=0.30
0023                   EXITMX=33.156
0024                   SPGOIL=0.834
0025                   SPWATR=62.43
0026                   NREAD1=21
0027                   COFLOW=54.13
0028                   IF(LUCK.EQ.1) COFLOL=COFLOW
0029                   IF(LUCK.EQ.2) COFLOL=0.0
0030                   IF(LUCK.EQ.3) COFLOL=50.06
0031                   IF(LUCK.EQ.4) COFLOL=47.66
0032                   IF(LUCK.EQ.5) COFLOL=46.10
0033                   IF(LUCK.EQ.6) COFLOL=45.33
0034                   IF(LUCK.EQ.7) COFLOL=44.41
0035                   IF(LUCK.EQ.8) COFLOL=43.09
0036                   IF(LUCK.EQ.9) COFLOL=41.35
0037                   IF(LUCK.EQ.10) COFLOL=40.00
0038                   IF(LUCK.EQ.11) COFLOL=38.04
0039                   IF(LUCK.EQ.12) COFLOL=35.97
                  CCCCCCCCCCCCCCCCCCCCCCCCCCCCCCCCCCCCCCCCCCCCCCCCCCCCCCCCCCCCCCCCCCCCCC
0040                   NREAD2=NREAD-(NREAD1-1)
0041                   GAMOIL=SPGOIL*SPWATR
0042                   IF(NFIVE.EQ.1) GO TO 52
0043                   WRITE(3,49)
0044                49 FORMAT(1X,'  NUMBER OF      HEIGHT OF      MANOMETER    STATIC   AIR
                   1-SPEED     RATIO     FRACTION ')
```

```
      WRITE(3,50)
   50 FORMAT(1X,'  OBSERVATION   PITOT TUBE   READING H    PRESSURE
     2 V              OF      OF HEIGHT')
      WRITE(3,51)
   51 FORMAT(1X,'                          (IN INCHES)   (IN INCH)   (IN INCH)  (FT
     3/SEC)       V/VC     (IN./IN.)')
      GO TO 57
   52 CONTINUE
      WRITE(3,53)
   53 FORMAT(1X,'  NO. OF     TIME OF     LENGTH     MANOMETER    STATIC    A
     1IR-SPLE)   RATIO ')
      WRITE(3,54)
   54 FORMAT(1X,'  OBSERV-    OBSERV-    OF TIME      READING      HEAD
     2    V              OF')
      WRITE(3,55)
   55 FORMAT(1X,'  ATION.     ATION.    (MINUTE )     (INCH)       (INCH)
     3(FT/SEC)      V/VC ')
      WRITE(3,56)
   56 FORMAT(1X,'                      (MINUTE)')
   57 CONTINUE
      READ(1,58)(NUMBER(I),HEIGHT(I),HEAD(I),STATIC(I),I=1,NREAD)
   58 FORMAT(I1,3F10.2)
      FULLH=HEIGHT(NREAD)-HEIGHT(1)
      IF(NHOLE.EQ.2) FULLH=17.90
      IF(NHOLE.EQ.11) FULLH=17.90
      HALFH=FULLH/2.
      HALFHT=HALFH+HEIGHT(1)
      IF(NHOLE.EQ.2) HALFHT=HALFH+HEIGHT(1)-BAKFLO
      DO 60 I=1,NREAD
      TOLERN=1.0E-4
      ERRORC=HEIGHT(I)-HALFHT
      IF(ABS(ERRORC)-TOLERN)59,59,60
   59 NCENTR=NUMBER(I)
      GO TO 61
   60 CONTINUE
   61 HEADCR=HEAD(NCENTR)
      CALL AIRDEN(TEMPER,PRESSR,SPGAIR,DENAIR)
      VELSQ=(2.*GAMOIL*HEADCR/12.)/DENAIR
```

```
C
      VCENTR=SQRT(VELSQ)
      IF(NTIME.EQ.1) VCENTR=40.66
      IF(NTIME.EQ.0) GO TO 62
      DEPTH=HEIGHT(NREAD)-HEIGHT(1)
      GO TO 63
   62 CONTINUE
      DEPTH=HEIGHT(NREAD)-HEIGHT(1)+(1./16.)
      IF(NHOLE.EQ.2) DEPTH=17.90+1./16.
      IF(NHOLE.EQ.11) DEPTH=17.90+1./16.
   63 CONTINUE
      DO 65 I=1,NREAD
      IF(NTIME.EQ.0) GO TO 64
      DISTAN(I)=HEIGHT(I)-HEIGHT(1)
      GO TO 65
   64 CONTINUE
      DISTAN(I)=HEIGHT(I)-HEIGHT(1)+(1./32.)
      IF(NHOLE.EQ.2) DISTAN(I)=DISTAN(I)+BAKFLO
   65 CONTINUE
      FRACTN(I)=DISTAN(I)/DEPTH
      VELSQR=(2.*GAMOIL*HEAD(I)/12.)/DENAIR
      AIRVEL(I)=SQRT(VELSQR)
      RATIO(I)=AIRVEL(I)/VCENTR
      IF(NTIME.EQ.1) GO TO 67
      WRITE(3,66) NUMBER(I),HEIGHT(I),HEAD(I),STATIC(I),AIRVEL(I),RATIO(
     1I),FRACTN(I)
   66 FORMAT(4X,I8,2X,F10.3,2X,F10.2,3(,F10.2,2X,F10.2,F10.2,F10.2/)
      GO TO 69
   67 CONTINUE
      WRITE(3,68) NUMBER(I),HEIGHT(I),DISTAN(I),HEAD(I),STATIC(I),AIRVEL
     1(I),RATIO(I)
   68 FORMAT(2X,I4,2X,F10.3,2X,F10.2,1X,F10.2,1X,F10.2,1X,3F10.2/)
   69 CONTINUE
      IF(NTIME.EQ.1) GO TO 62
      IF(NHOLE.GT.1) GO TO 72
      AGAP1=0.05
      AGAP2=0.10
      AGAP3=AGAP1
      AINTER=AGAP1
C
```

```
C
0114        NSTART=1
0115        NEND=NREAD1
0116        CALL SIMSUN(DISTAN,AIRVEL,AINTER,NSTART,NEND,AREA1)
0117        AINTER=AGAP2
0118        NSTART=NREAD1
0119        NEND=NREAD2
0120        CALL SIMSUN(DISTAN,AIRVEL,AINTER,NSTART,NEND,AREA2)
0121        AINTER=AGAP3
0122        NSTART=NREAD2
0123        NEND=NREAD
0124        CALL SIMSUN(DISTAN,AIRVEL,AINTER,NSTART,NEND,AREA3)
0125        TOTALA=AREA1+AREA2+AREA3
0126        WRITE(3,70) TOTALA
0127     70 FORMAT(2X,'THE TOTAL AREA COMPUTED BY THE SIMPSONS RULE IS=',F8.2)
0128        VMEAN=TOTALA/DEPTH
0129        WRITE(3,71)VMEAN
0130     71 FORMAT(2X,'THE MEAN VELOCITY (IN FT/SEC) IS=',F6.2)
0131     72 CONTINUE
0132        WRITE(3,73) NCENTR
0133     73 FORMAT(1X,' THE   CENTRAL   OBSERVATION NUMBER IS =',I3)
0134        WRITE(3,74) VCENTR
0135     74 FORMAT(1X,' THE   CENTRAL   VELOCITY (IN FT/SEC) IS=',F7.2)
C
0136        IF(NHOLE.GT.1) GO TO 76
0137        WRITE(3,97)DENAIR
0138     97 FORMAT(2X,'THE DENSITY OF AIR(IN SLUGS/CUBIC FEET)=',E12.6)
0139        CALL AREU(TEMPER,VISCOS)
0140        WRITE(3,98) VISCOS
0141     98 FORMAT(2X,'THE COEFFICIENT OF VISCOSITY (IN SLUGS/FT-SEC)=',E12.6)
0142        RENOLD=(DENAIR*VMEAN*DEPTH)/(12.*VISCOS)
0143        WRITE(3,75) RENOLD
0144     75 FORMAT(1X,' REYNOLDS NO.(BASED ON MEAN VELOCITY AND DEPTH OF NOZZL
          1E)=',E12.6)
0145     76 CONTINUE
0146        KOUNTV=1
0147        SELFMX=AIRVEL(1)
C
```

```
0148                C
                        DO 77 I=2,NREAD
0149                    IF(AIRVEL(I).LE.SELFMX) GO TO 77
0150                    SELFMX=AIRVEL(I)
0151                    KOUNTV=I
0152                77  CONTINUE
0153                    WRITE(3,78) KOUNTV,FRACTN(KOUNTV),SELFMX,RATIO(KOUNTV)
0154                78  FORMAT(2X,'THE LOCATION & MAGNITUDE OF MAXIMUM VELOCITY ARE',//I10
                      1,3(5X,F8.3))
0155                    WRITE(3,79)
0156                79  FORMAT(//////2X,'NUMBER    DISTANCE    FRACTION     V/SELFMAX    V/EXI
                      1TMAX          CP          EXIT-CC     SELF-CC     DISTANCE')
0157                    IF(LOCK.EQ.1) EXITMX=SELFMX
0158                    DO 81 I=1,NREAD
0159                    CALL EULER(STATIC,SELFMX,GAMOIL,DENAIR,I,CCEFCN)
0160                    SPSELF(I)=AIRVEL(I)/SELFMX
0161                    SPEXIT(I)=AIRVEL(I)/EXITMX
0162                    REXIT(I)=(AIRVEL(I)-COFLOW)/(EXITMX-COFLOW)
0163                    RSELF(I)=(AIRVEL(I)-COFLOL)/(SELFMX-COFLOL)
0164                    WRITE(3,80) NUMBER(I),DISTAN(I),FRACTN(I),SPSELF(I),SPEXIT(I),CCEF
                      9CN(I),REXIT(I),RSELF(I),DISTAN(I)
0165                80  FORMAT(I5,8(2X,F10.3)/)
0166                81  CONTINUE
0167                82  CONTINUE
                C
0168                    WRITE(3,84)COFLOL
0169                84  FORMAT(1X,'THE LOCAL COFLOW (IN FT/SEC)=',F10.3)
                C
0170                85  CONTINUE
0171                    STOP
0172                    END
```

```
0001            SUBROUTINE SIMSON(XCORD,YCORD,AINTER,NSTART,NEND,AREA)
              C*** ********************************************************
              C       THIS SUBROUTINE USES SIMPSON'S FIRST RULE FOR NUMERICAL INTEGRATION *
              C       TO COMPUTE THE AREA UNDER THE MEAN AXIAL VELOCITY PROFILE. THE AREA  *
              C       IS THEN DIVIDED BY THE NOZZLE DEPTH TO OBTAIN THE AREA-AVERAGE AXIAL *
              C       VELOCITY OF THE WALL JET.                                           *
              C*** ********************************************************
0002            DIMENSION XCORD(300),YCORD(300)
0003            ODD=0.0
0004            EVEN=0.0
0005            M1=NEND-1
0006            KOUNT1=NSTART+1
0007            DO 47 I=KOUNT1,M1,2
0008            EVEN=EVEN+YCORD(I)
0009         47 CONTINUE
0010            M2=NEND-2
0011            KOUNT2=NSTART+2
0012            DO 48 I=KOUNT2,M2,2
0013            ODD=ODD+YCORD(I)
0014         48 CONTINUE
0015            AREA=(AINTER/3.)*(YCORD(NSTART)+4.0*EVEN+2.0*ODD+YCORD(NEND))
0016            RETURN
0017            END


0001            SUBROUTINE MEEU(TEMPER,VISCOS)
              C*** ********************************************************
              C       THIS SUBROUTINE COMPUTES THE COEFFICIENT OF VISCOSITY OF AIR IF THE *
              C       ATMOSPHERIC TEMPERATURE (IN DEGREES CENTIGRADE) IS SUPPLIED BY THE  *
              C       MAIN PROGRAM.                                                       *
              C*** ********************************************************
0002            TEMP1=TEMPER*9./5.
0003            FAREN=TEMP1+32.
0004            RANKIN=FAREN+459.6
0005            FACTOR=1.0E-8
0006            VISCO=2.27*(RANKIN**1.5)/(RANKIN+198.6)
0007            VISCOS=VISCO*FACTOR
              C
0008            RETURN
0009            END
```

```
DOS FORTRAN IV 360N-FO-479 3-8          EULER                    DATE    10/02/83      TIME      12.51.58      PAGE 00

0001                  SUBROUTINE EULER(STATIC,VELOCT,GAMGIL,DENAIR,I,COEFCN)
                C*** ********************************************************************
                C     THIS SUBROUTINE COMPUTES THE PRESSURE COEFFICIENT IF THE STATIC HEAD *
                C     THE VELOCITY AND THE DENSITY OF AIR ARE SUPPLIED BY THE MAIN PROGRAM *
                C*** ********************************************************************
0002                  DIMENSION STATIC(300),CLEECN(300)
0003                  STATPR=(STATIC(I)/12.)*GAMGIL
0004                  DYNAPR=.5*DENAIR*VELOCT**2
0005                  COEFCN(I)=STATPR/DYNAPR*(-1.)
0006                  RETURN
0007                  END
```

```
DOS FORTRAN IV 360N-FO-479 3-8          AIRDEN                   DATE    10/02/83      TIME      12.51.47      PAGE 000

0001                  SUBROUTINE AIRDEN(TEMPER,PRESSR,SPWATR,DENAIR)
                C*** ********************************************************************
                C     THIS SUBROUTINE COMPUTES THE DENSITY OF AIR IF THE MAIN PROGRAM     *
                C     SUPPLIES THE ATMOSPHERIC PRESSURE AND TEMPERATURE.                  *
                C*** ********************************************************************
0002                  ABSTEM=273.+TEMPER
0003                  RCONST=96.
0004                  PRESS=PRESSR*13.6/12.
0005                  P=SPWATR*PRESS
0006                  GAMAIR=P/(RCONST*ABSTEM)
0007                  DENAIR=GAMAIR/32.2
0008                  RETURN
0009                  END
```

```
DOS FORTRAN IV 360N-FO-479 3-8          MAINPGM          DATE    13/02/83      TIME      13.16.24      PAGE 00

                C
                C*********************************************************************
                C      SECOND PROGRAM.                                                *
                C      THIS PROGRAM COMPUTES THE POWER OF THE VELOCITY PROFILE WITHIN THE  *
                C      BOUNDARY LAYER AT THE NOZZLE EXIT.THE VELOCITY  PROFILE IS  OF THE  *
                C      FORM  U/V=(Y/DELTA)**N . THE METHOD OF LEAST SQUARES IS  USED  FOR  *
                C      FITTING THE EXPERIMENTAL VALUES TO A NONLINEAR CURVE. THE MEASURED  *
                C      VALUES OF MEAN AXIAL VELOCITY AT DIFFERENT HEIGHTS ARE SUPPLIED AS  *
                C      INPUT TO THE PROGRAM.                                          *
                C*********************************************************************
0001                   DIMENSION YBYHT(99),UBYMAX(99),UBYV(99),Y(99),YBYDEL(99),X(99)
0002                   READ(1,3)NPOINT
0003                 3 FORMAT(I5)
0004                   WRITE(3,9)NPOINT
0005                 9 FORMAT(1X,'THE TOTAL NO. OF POINTS IS',I5)
0006                   READ(1,10)(I,YBYHT(I),UBYMAX(I),I=1,NPOINT)
0007                10 FORMAT(I10,2F10.3)
0008                   WRITE(3,11)
0009                11 FORMAT(1X,'NUMBER    HEIGHT     U/UMAX    ')
0010                   WRITE(3,12)(I,YBYHT(I),UBYMAX(I),I=1,NPOINT)
0011                12 FORMAT(I7,2F10.3)
0012                   WRITE(3,16)
0013                16 FORMAT(1X,'THE BOUNDARY LAYER THICKNESS AT THE NOZZLE EXIT IS CALL
                      1ED DELTA.')
0014                   READ(1,17)DELFRA
0015                17 FORMAT(F10.3)
0016                   WRITE(3,18)DELFRA
0017                18 FORMAT(1X,'THE RATIO OF DELTA TO THE NOZZLE DEPTH IS=',F6.3)
0018                   DO 19 I=1,NPOINT
0019                   UBYV(I)=UBYMAX(I)/0.99
0020                   Y(I)=UBYV(I)
0021                   YBYDEL(I)=YBYHT(I)/DELFRA
0022                   X(I)=YBYDEL(I)
0023                19 CONTINUE
0024                   SUMXX=0.0
0025                   SUMXY=0.0
0026                   DO 20 I=2,NPOINT
0027                   SUMXX=SUMXX+ALOG(X(I))*ALOG(X(I))
0028                   SUMXY=SUMXY+ALOG(X(I))*ALOG(Y(I))
0029                20 CONTINUE
0030                   AN=SUMXY/SUMXX
0031                   POWER=1./AN
0032                   WRITE(3,21) POWER
0033                21 FORMAT(1X,'POWER OF THE VELOCITY PROFILE IS 1 DIVIDED BY',F7.3)
0034                   STOP
0035                   END
```

```
OCS FORTRAN IV 360N-FO-475 3.8          MAINPGM          DATE    20/02/83      TIME     13.44.44
C*********************************************************************
C       THIRD PROGRAM.                                                *
C       THIS PROGRAM FITS THE EXPERIMENTAL VALUES OF MEAN AXIAL VELOCITY *
C       (WITHIN THE BOUNDARY LAYER AT THE NOZZLE EXIT) TO THE  UNIVERSAL *
C       VELOCITY PROFILE AT THE WALL GIVEN BY  THE  FOLLOWING  EQUATION. *
C       UPLUS=1/K.LOG(YPLUS)+A ,WHERE UPLUS=U/USTAR,YPLUS=(Y.USTAR)/NEEU, *
C       K AND A ARE CONSTANTS.USTAR IS THE SHEAR VELOCITY.IN THE PROCEDURE *
C       OF FITTING BY THE METHOD OF LEAST SQUARES THE VALUES OF K AND A  *
C       ARE OBTAINED FOR VARIOUS VALUES OF USTAR STARTING FROM 0.5 FT/SEC *
C       TO 10 FT/SEC,AND THE CORRESPONDING RMS ERRORS OF THE  MEAN AXIAL *
C       VELOCITIES ARE COMPUTED.THE OPTIMUM VALUES OF A ,K  AND USTAR ARE *
C       SELECTED ON THE BASIS OF THE LEAST RMS ERROR.                 *
C       THE PROGRAM IS WRITTEN BY GAZI MQ. KHALIL, AND  EXECUTED  ON THE *
C       IBM 370-115/2 COMPUTER OF BUET,DHAKA.                         *
C*********************************************************************
00 01           DIMENSION TITLE(20),NUMBER(100),YINPUT(100),UINPUT(100),YBIG(100),
               1UCOMP(100),UPLUS(100),YPLUS(100)
00 02           NCYCLE=4
00 03           DO 10 LOOK=1,NCYCLE
00 04           IF(LOOK.EQ.1) USTAR=3.0
00 05           IF(LOOK.EQ.2) USTAR=0.70
00 06           IF(LOOK.EQ.3) USTAR=4.0
00 07           IF(LOOK.EQ.4) USTAR=2.0
0008            K=0
0009            BBEBB=USTAR
0010            READ(1,1)TITLE
0011          1 FORMAT(20A4)
0012            WRITE(3,2)TITLE
0013          2 FORMAT(///3X,20A4)
0014            READ(1,11)TEMPER,PRESSR
0015         11 FORMAT(2F10.2)
0016            WRITE(3,12)TEMPER,PRESSR
0017         12 FORMAT(2X,'THE TEMPERATURE AND PRESSURE ARE=',2F10.2)
0018            SPWAIR=62.45
0019            CALL AIRDEN(TEMPER,PRESSR,SPWAIR,DENAIR)
0020            WRITE(3,13)DENAIR
0021         13 FORMAT(2X,'THE AIR DENSITY (IN SLUG/CUBIC FEET)=',E12.6)
0022            CALL VEEU(TEMPER,VISCOS)
0023            WRITE(3,14)VISCOS
0024         14 FORMAT(2X,'THE COEFFICIENT OF VISCOSITY (IN SLUG/FT-SEC)=',E12.6)
0025            ANEEU=VISCOS/DENAIR
0026            WRITE(3,15)ANEEU
0027         15 FORMAT(2X,'KINEMATIC COEFFICIENT OF VISCOSITY IS=',E12.6)
CCCCCCCCCCCCCCCCCCCCCCCCCCCCCCCCCCCCCCCCCCCCCCCCCCCCCCCCCCCCCCCCCCCCCCC
```

```
C
      READ(1,21)NPOINT
   21 FORMAT(I3)
      WRITE(3,22)NPOINT
   22 FORMAT(2X,'THE NUMBER OF POINTS=',I5)
      READ(1,23)((NUMBER(I),YINPUT(I),UINPUT(I)),I=1,NPOINT)
   23 FORMAT(I3,2F10.3)
      WRITE(3,24)
   24 FORMAT(2X,'        SERIAL   DISTANCE   VELOCITY ')
      WRITE(3,25)((NUMBER(I),YINPUT(I),UINPUT(I)),I=1,NPOINT)
   25 FORMAT(2X,I10,2F10.3)
  101 DO 26 I=1,NPOINT
      YPLUS(I)=YINPUT(I)*USTAR/(12.0*ANEEU)
      YBIG(I)=ALOG(YINPUT(I)*USTAR/(12.0*ANEEU))
      UPLUS(I)=UINPUT(I)/USTAR
   26 CONTINUE
      CALL FITTER(YBIG,UPLUS,NPOINT,A1,A0)
      D=A1
      B=A0
      WRITE(3,27)
   27 FORMAT(1X,'  USTAR              RMS                D                B   ')
      SUMSQ=0.0
      DO 28 I=1,NPOINT
      UCOMP(I)=(D*YBIG(I)+B)*USTAR
      DIFFER=(UINPUT(I)-UCOMP(I))**2
      WRITE(3,200)UCOMP(I),UINPUT(I),DIFFER,YPLUS(I),UPLUS(I)
  200 FORMAT(5(E12.5,3X))
      SUMSQ=SUMSQ+DIFFER
   28 CONTINUE
      SMS=SQRT(SUMSQ)
      WRITE(3,30)USTAR,SMS,D,B
   30 FORMAT(4(E12.5,2X))
      K=K+1
      BB=K
      USTAR=BB*0.0+0.1*BB
      IF(K.LE.1) GO TO 101
  100 CONTINUE
      STOP
      END
```

```
DOS FORTRAN IV 360N-FO-479 3-8          FITTER          DATE    20/02/83      TIME     13.45.08

0001                  SUBROUTINE FITTER(X,Y,N,A1,A0)
                C*************************************************************************
                C     THIS SUBROUTINE USES THE METHOD OF LEAST SQUARES TO FIT N NUMBER    *
                C     OF POINTS TO A STRAIGHT LINE OF THE FORM   Y=A1.X + A0. THE MAIN    *
                C     PROGRAM SUPPLIES THE VALUES OF N,X AND Y. THIS SUBROUTINE COMPUTES  *
                C     THE VALUES OF A1 AND A0.                                            *
                C*************************************************************************
0002                  DIMENSION X(100),Y(100)
0003                  WRITE(3,12)
0004               12 FORMAT(///1X,' X-COORDINATE      Y-COORDINATE')
0005                  WRITE(3,13)(X(I),Y(I),I=1,N)
0006               13 FORMAT(/2(F10.3,5X))
0007                  SUMX=0.0
0008                  SUMY=0.0
0009                  SUMXX=0.0
0010                  SUMXY=0.0
0011                  DO 15 I=1,N
0012                  SUMX=SUMX+X(I)
0013                  SUMY=SUMY+Y(I)
0014                  SUMXX=SUMXX+X(I)*X(I)
0015                  SUMXY=SUMXY+X(I)*Y(I)
0016               15 CONTINUE
0017                  AN=N
0018                  DENOM=AN*SUMXX-SUMX**2
0019                  A0=(SUMY*SUMXX-SUMX*SUMXY)/DENOM
0020                  A1=(AN*SUMXY-SUMX*SUMY)/DENOM
0021                  WRITE(3,16)
0022               16 FORMAT(1X,'THE EQUATION TO THE STRAIGHT LINE IS Y=A1.X+A0')
0023                  WRITE(3,17)
0024               17 FORMAT(1X,'THE VALUES OF A1 AND A0 ARE RESPECTIVELY')
0025                  WRITE(3,18)A1,A0
0026               18 FORMAT(/2F10.3)
0027                  RETURN
0028                  END
```